Automated Sequence Design of 3D Polyhedral Wireframe DNA Origami with Honeycomb Edges

Supporting Information

Hyungmin Jun,[†,‡] Tyson R. Shepherd,[†,‡] Kaiming Zhang,[†,§] William P. Bricker,[‡] Shanshan Li,[§] Wah Chiu,[§,∥] Mark Bathe[*,‡]*

[‡]Department of Biological Engineering, Massachusetts Institute of Technology, Cambridge, MA 02139, USA

[§]Department of Bioengineering, Microbiology and Immunology, and James H. Clark Center, Stanford University, Stanford, CA 94305, USA

[∥]SLAC National Accelerator Laboratory, Stanford University, Menlo Park, CA 94025 USA

S1 Design algorithm

S1.1 Top-down sequence design software

The fully automatic inverse design procedure TALOS (Three-dimensional, Algorithmically-generated Library of DNA Origami Shapes) is available for use as open source software (http://github.com/lcbb/talos) and online at http://talos-dna-origami.org. Details for compiling the source code can be found in the documentation provided with the software.

S1.2 User-specified geometric input

The goal of this work is to design and synthesize wireframe polyhedral scaffolded DNA origami structures with edges composed of six-helix bundles (6HB),[1] which is a molecular complex consisting of a cyclic configuration of six duplexes on a honeycomb lattice covalently attached using antiparallel double crossovers. Given a target 3D polyhedral structure of specified size and geometry (Figure S19), the algorithm will route a single-stranded scaffold throughout the entire geometry with 6HB edges and generate the required staple strands needed to experimentally fold the structure (Figures S20-S27 and Tables S8-S16). 3D geometries are specified using a closed surface that is discretized using a polyhedral mesh (Figure S1a). In order to specify the geometry for scaffold routing, the spatial coordinates of all vertices and faces to which these vertices belong must be provided (Figure S1b). These may be provided manually or through an ASCII file format that defines the polygonal geometry, such as the Polygon File Format (PLY), STereoLithography (STL), or Virtual Reality Modeling Language (WRL). As explained in more detail below, any closed, 3D surface geometry can serve as input to the algorithm.

S1.3 Generating 6HB duplex segments from the wireframe model

To generate six line segments per each wireframe edge, representative of the six duplexes in the 6HB, each wireframe edge is detached from the wireframe vertices and its length is shortened (Figure S1c) with the offset-distance (between the vertex and the end point of the adjusted line segment) calculated with respect to the minimum angle between any two adjacent edges at a vertex and according to that vertex's degree to eliminate steric hindrance in the final structure. Then, at the center of every separated line, three basis vectors $\mathbf{t_1}$-$\mathbf{t_2}$-$\mathbf{t_3}$ of the local coordinate system are introduced to determine the orientation of the 6HB along the wireframe edge. The local vector $\mathbf{t_1}$ (red arrow in Figure S1) is defined by position vectors of two endpoints of each line segment. The direction of the vector $\mathbf{t_3}$ (olive arrow in Figure S1) is determined by the centers of the two intersecting faces of the wireframe edge and oriented such that the vector starts in the face with the direction of the curl of the face oriented in the same direction as $\mathbf{t_1}$ and ends in the face with the direction of the curl of the face oriented in the opposite direction as $\mathbf{t_1}$ (Figure S1d). The local vector $\mathbf{t_2}$ (blue arrow) is obtained by the cross product of two vectors $\mathbf{t_3}$ and $\mathbf{t_1}$.

Based on the $\mathbf{t_3}$-$\mathbf{t_2}$ plane, the cross-section of a honeycomb lattice shape has six circles representative of the six DNA duplexes and each circle has a diameter of 2.25 nm, as assumed previously.[2–4] The integer number (hereafter called a section ID) on each circle is assigned to model the asymmetric ends of DNA strands: even section IDs have 5′-terminal phosphate groups and odd section IDs have 3′-terminal hydroxyl groups orientations of the scaffold strand.

Then, according to the section ID, each separated line is replaced (Figure S1e) with six scaffold segments (blue line) with endpoints. For even number circles, the scaffold segment points from 5′ to 3′ in the same direction to local vector $\mathbf{t_1}$. For odd-numbered circles, the scaffold segment points from 5′ to 3′ in the opposite direction of $\mathbf{t_1}$. The desired minimum edge length is assigned to the shortened line and the other lines are subsequently scaled likewise. The minimum edge length should be a multiple of 21 base pairs (bp) and greater than or equal to 42 bp to have at least two double-crossovers per every edge.

To avoid clashing between neighboring duplexes, which occurs depending on the dihedral angle between two adjacent faces of the structure, two vertex designs are suggested; the inner connection layer (Figure S3a) in which the origin of two local vectors is located at the center of two inner circles (hereafter called reference circles) and the middle connection layer (Figure S3f) in which two middle circles are used as reference circles.

S1.4 Building the loop-crossover structure and two vertex designs

The next step is to generate the loop-crossover structure as an intermediate process of the scaffold routing. The endpoints of multiple scaffold segments are joined such that every segment becomes part of a loop (Figure S1f). In the flat vertex (FV) case, the endpoint of the scaffold segment located on the reference circle is connected (red line) to the closest endpoint of the neighboring scaffold segment from reference circle by crossing the vertex. Four remaining endpoints are interconnected (blue line) with each other according to the following rule; two endpoints are diagonally connected (Figure S4a) in the inner connection layer and horizontally connected (Figure S4b) in the middle connection layer. Thus, the initial geometry consisting of N_F faces and N_E edges introduce $N_F+2\times N_E$ closed loops, where the N_F loops are generated by the connection through the red line

shown in Figure S4 and the $2 \times N_E$ loops are generated by the connection of the endpoints by the blue line shown in Figure S4. In the mitered vertex (MV) case, all scaffold segments are covalently connected to segments on the adjacent edge across the vertex, with the algorithm computing the precise length of dsDNA required to extend the duplex without inducing steric hindrance (Figure S2a,b). Thus, joining all scaffold segments with neighboring segments across the vertex results in two more scaffold crossings per 6HB wireframe edge than the FV case. In the MV case, $4N_F$ closed loops are generated.

To find all scaffold double crossovers between every two neighboring loops, a DNA model to define the position of each nucleotide is introduced. First, the length of scaffold segments that are the part of the scaffold loop is discretized as a multiple of base pair lengths, 0.34 nm that is the length of base-pair rise in the double-helical B-form DNA model. By adopting the conventions of caDNAno, for the inner connection layer, the initial angles pointing the nucleotide of the scaffold (block ID = 0, where the block ID is the base pair position along the length of the 6HB) are set as 270° and 90° (Figure S3b) for the even and odd section IDs, respectively. For the middle connection layer, the initial angles are set as 30° and 210° (Figure S3g) for the even and odd section IDs, respectively. Given the helical periodicity with 21 bp every two turns, there are two possible starting blocks: the prior and posterior block, where the directions of two nucleotides from the reference circles are opposite to each other and nearly the same to the local vector $\mathbf{t_3}$. The prior and posterior block are located in the block ID of 3 and 1 for the inner connection layer (Figure S3c), 1 and 11 for the middle connection layer (Figure S3h), respectively, where the nucleotide at the end of the scaffold segment can be connected without any unpaired nucleotides one of the ends of the scaffold if the scaffold segment length is a multiple of 10.5 bp.

Possible staple crossovers are restricted to intersections between the block and every third layer of a stack of planes orthogonal to the helical axes, spaced apart in intervals of 7 bp or two-thirds of a turn[5]. Then, possible scaffold crossovers (red line) are permitted (Figure S3d,i) at positions displaced upstream or downstream of the corresponding possible staple crossover points by 5 bp or a half-turn. For the FV design, because scaffold segments that are not located in reference circle are connected each other without crossing the vertex, all segments are adjusted to where the next single crossover position exists. For the inner connection layer, discretized segments originated from a section ID of 2 or 3 are moved 3 bp on the 3′-end direction and those from a section ID of

4 or 5 are moved 1 bp on the direction of the 5′-end (Figure S3c,d), which is to connect diagonally each other at the permitted position of the scaffold single crossover. For the middle connection layer, all discretized segments except for those from a section ID of 3 are shifted by 1 bp on the 3′-end direction (Figure S3h,i), resulting in each pair of duplexes to be connection through allowable crossover locations based on the dsDNA helix. For the MV design, the connections between two scaffold segments crossing the vertex are accomplished by introducing unpaired nucleotides of the scaffold strand at vertices in order to accommodate 5′- and 3′-end misalignment. The number of unpaired nucleotides is calculated by dividing the distance between two nucleotides by the ssDNA length which is used as the value of 0.42nm to release the tensional stresses for their connections.[6]

To build the loop-crossover structures, possible scaffold crossovers that are 7 bp away from both ends of the discretized segments (faint red line in Figure S3) and the double-crossovers (faint red line in Figure S3) connecting its loop are eliminated (Figure S3d,i). Then, only one double-crossovers (yellow and red line lines in Figure S3) per section 0 to 5 in a zig-zag pattern with respect to the center edge are selected (Figure S3e,j), creating the loop-crossover structure. The scaffold loops with initial scaffold double-crossovers (Figure S1g and Figure S2c) can be projected in 2D as a Schlegel diagram (Figure S1h and Figure S2e), in which N_F+2×N_E–1 (for the FV) or 4N_F-1 (for the MV) double-crossovers among them are selected through the following scaffold route process.

The use of different starting blocks results in the different patterns of scaffold and staple crossovers, which affect the processes, especially, final staple route and sequence design. We adapted and used the posterior block as the starting block in both the inner and middle connection layers since it has more the 14-nt seed dsDNA domains whose presence enhances folding yield (Tables S1 and S2).[7,8]

S1.5 Generating the spanning tree of the dual graph

In routing the single-stranded scaffold through the entire DNA origami structure, the first requirement is to ensure an Eulerian circuit exists.[9] An Eulerian circuit, which is stricter than an Eulerian path, is required because the ends of the scaffold should be adjacent to create a single

scaffold nick. An Eulerian circuit is guaranteed when the degree of every vertex is even. This can be achieved by using an even number of duplexes per edge in the structure; in this work, we have chosen to use six duplexes per edge, each a 6HB. Because the degree of every corner connected by the crossover and loop always remains two (even), it becomes an Eulerian circuit by choosing the proper number of double-crossovers of the loop-crossover structure. Thus, the scaffold routing problem can be solved by computing a spanning tree of the dual graph of the loop-crossover structure, which determines the proper number of double-crossovers without any cycle that is a path of edges and nodes wherein a node is reachable from itself.

For the FV design, N_f+2N_e closed loops should be connected to each other with N_f+2N_e-1 double-crossovers, implying that the edge is constructed by six duplexes with two or three scaffold double-crossovers which are determined by the spanning tree calculation. In order to consistently select two or three double-crossovers for each edge, the weight factor is assigned (Figure S4a for the inner connection layer and Figure S4b for the middle connection layer) to each double-crossover with the value of 1 for two mandatory double-crossovers (red), the value of 2 for the occasional double-crossover (orange), and the value of 3 for the unwanted double-crossover. Despite having twelve ways to impose the weight factor of the double-crossover connecting two adjacent loops (Figure S4), we chose to adapt pattern #1 for the inner connection layer and pattern #13 for the middle connection layer since the final staples with this pattern include more 14-nt seed dsDNA domains (Tables S1 and S2). These patterns are also applied in the MV design.

Then, the dual graph of the loop-crossover structure is generated (Figure S1i and Figure S2e), in which each loop becomes represented by a node (black circle in Figure S1 and Figure S2) and each double-crossover becomes represented as an edge (red line in Figure S1 and Figure S2) joining the associated nodes and transferring the assigned weight factor of the double-crossover. Given the dual graph network, Prim's algorithm can be used to find the minimum weight spanning tree (Figure S1j, Figure S2f, Figure S20 and Figure S21) in which N_F+2×N_E–1 edges or 4N_F–1 edges (cyan line in Figure S1 and Figure S2) are determined with the priority of small weight factor of the edge. The edges that are members of the spanning tree corresponding to the subset of double-crossovers required to complete the Eulerian circuit.

S1.6 Inverting the spanning tree and completing scaffold route

Once the spanning tree of the dual graph network has been determined, the graph is inverted back to the loop-crossover structure only using members of the spanning tree. By choosing a particular subset of double-crossovers in the loop-crossover structure, these discrete loops can be connected to form one continuous circular scaffold through the entire structure. The direction of the circular scaffold is set to have the same direction defined by the corresponding section ID, and the scaffold nick position is chosen to be placed on the duplex far from crossovers and staple nicks, which reveals the final scaffold routing (Figures S1k, Figure S1i, Figure S2g, Figure S2h, Figure S22 and Figure S23).

S1.7 Adding staple strands and sequences

In this step, the staple strands wind in an antiparallel direction around the scaffold can assemble B-form double helices, and the staple sequences can be computed based on complementary Watson-Crick base pairing with the scaffold sequence. First, initial staple paths complementary to the scaffold are assigned (Figure S5a-c) by placing and connecting all permitted staple double-crossovers except for those (dotted orange line) that would be not 5 bp away from a scaffold crossover between the same two helices and not 7 bp away from the both ends of discretized lines in the base pair model. The staples crossing the vertex are connected with a certain number of nucleotides with poly-T bulges where the staple paths do not bind to the scaffold, which serves as to prevent blunt-end stacking. Because a phosphate-phosphate distance of roughly 0.55 nm is known as B-form DNA[10,11], the number of unpaired nucleotides in the poly-T bulge is calculated by dividing the spatial distance between two nucleotides to be joined by 0.42 nm (a value slightly smaller than 0.55 nm is used to reduce the tension between the connection).[6] Second, the initial staple paths are linearized by placing a nick in the staple at the center of the longest dsDNA domain (green circle of the initial staple #1 shown in Figure S5c) and where it is non-coincident with staple and scaffold crossovers. Lastly, the non-circular staple paths are broken into the user-define staple length (20 to 60 nucleotides long as a default, resulting in usually a mean length of about 40 nucleotides). With design criteria of including at least one 14-nt seed domain per each staple, we suggested and investigated two alternative staple-break rules, one to maximize staple length

(hereafter “maximized length”) and the other to maximize the number of seed domains (hereafter “maximized seed)” (Figure S5d and Figure S6).

Before applying the “maximized length” staple-break rule, the algorithm first determines the size of dsDNA domains of each initial staple from the 5′-end to 3′-end. From the 5′, the algorithm moves in the 3′ direction to the next dsDNA domain until the distance traveled exceeds the user-defined maximum staple length (60 nt as a default). The algorithm then moves back to the center of the dsDNA domain in the 3′ direction until the domain located is longer than or equal to 14-bp length. If the above conditions are satisfied, the backbone nick is placed at the center of the domain to divide the staple into two. The above steps are repeated until the length of the remaining staple is smaller than the user-defined maximum staple length (see Figures S5-S7) The algorithm does not consider the inclusion of the 14-nt seed domain for the staple when breaking it but guarantees the 7 bp length as the minimum length of the dsDNA domain for the segmented staple (Figures S8-S18, Table S3 and Table S4).

For the “maximized seed” staple-break rule, the algorithm is based on the previously suggested staple-break rule[7,8] where backbone nicks are never placed in dsDNA domain longer than 7 bp and nicks are positioned 3 or 4 bp away from crossovers in the 7-bp domain. To apply the above staple-break rule to our staple route design procedure automatically, the searching bar that is initially placed at the 5′ end and scans in the 3′ direction to the next dsDNA domain until finding the domain that is longer than or equal to the 14-bp length and the distance traveled exceeds the user-defined minimum staple length (20 nt as a default). Then the backbone nick is placed at the center position of the next dsDNA domain regardless its size (Figures S5-S7). In the above rule, the initial staples are broken by considering the presence of the 14-nt seed domain of the staple to be cut, so it is most likely to contain more than one 14-nt seed domain per each staple. However, each broken staple has the potential to include the dsDNA domains with the small size since it does not consider the size of the domain to be broken.

Note that each staple broken by the “maximized length” rule contains the 14-nt seed domain with more than 80% of total staples, which is a slight decrease in percentage than when applying the “maximized seed” rule (Figure S13, Table S3 and Table S4). However, since it does not contain

the weak, small-size domain, we adapted and used the "maximized length" staple-break rule in the staple design process.

With introducing weight factors to choose two or three scaffold crossovers in a consistent way, for the FV design, each edge is rendered (Figure S1m and Figures S8-S12) with one of two possible scaffold and staple routing patterns for every structure. After all staples are segmented (Figure S1m, Figure S2i and Figures S24-S27), each staple is denoted by a vector of numbers, with each value corresponding to the scaffold nucleotide to which it is base-paired. The input or generated scaffold sequence is then used to match base identities (A, T, G, or C) to the corresponding scaffold number assuming Watson-Crick base-pairing. If no sequence is provided, a segment of M13mp18 is used by default if the required scaffold length is less than or equal to 7,249-nt, and a sequence is randomly generated of the required length is greater. Finally, this list of staple sequences is output for synthesis (Tables S8-S16).

S1.8 Predicting atomic-level 3D structure and editing staples

Each base pair is modeled with 0.34 nm axial rise per bp, whose center and three orientations are defined using 3DNA convention.[4] The three orientation vectors point to the major groove, the preferred nucleotide, and along the duplex axis towards the 3′ direction of the strand with the preferred nucleotide, respectively. Based on the position and orientation vectors, the atomic-level 3D structure is obtained by four standard reference atomic structures of base pairs A-T, T-A, G-C, and C-G. Each standard reference atomic structure consists of two phosphates, two deoxyriboses, and two paired bases. Thus, an all-atom model is calculated by placing the standard reference atomic structures, using rigid-body translation and rotation, to the positions and orientations of the base pairs (Figures S28-S36).

With the *JSON* file as one of the outputs from the algorithm, the user can edit the staple crossover positions and sequences using the caDNAno software.[5] We provide the guide model which can be loaded in USCF Chimera,[12] which gives the information which edges of the target structure is associated with the which cross-sections of caDNAno representation (Figures S37-S45).

In conclusion, we have demonstrated here an algorithm that automatically generates scaffold routing and staple sequence design of 6HB DNA-NPs from a polyhedral mesh. The algorithm provides advantageous features such as two alternative vertex designs, editing capability for the staple routing and sequences, no use of unpaired scaffold nucleotides for the FV design, at least one continuous dsDNA domain of 14 nt per staple if possible, no less than 4 nt for any dsDNA domains, and vertex staples (connecting two neighboring edges) containing unpaired stretches with poly-T bulges whose length depend on the distance between two nucleotides to be joined. In addition, the automated sequence design includes the following constraints such as edge lengths as multiples of 21 bp, at least two scaffold double-crossovers per edge.

S2 Experimental Methods

S2.1 Assembly of 6HB DNA-NPs

To maximize DNA-NP yield, we varied several conditions important for assembly, including staple-to-scaffold ratio, magnesium and sodium chloride concentration, and time of folding. Folding conditions for the DNA-NPs were tested on tetrahedra of 42-bp and 63-bp edge lengths and an octahedron of 84-bp edge length. To test salt conditions, solutions containing 10 nM full-length M13 scaffold and 400 nM staples in 1× TAE were combined with 0, 2.5, 5, 7.5, 10, 12, or 14 mM MgCl2 or 0, 25, 50, 100, 150, 200, or 500 mM NaCl and brought up to 50 µL (Figure S46). Structures were annealed in a T100 thermocycler (Bio-Rad) over a 24-hour annealing time (5 min at 95ºC, 5 min at 90ºC, 5 min at each 0.5ºC temperature interval between 85ºC and 70ºC, and 13.75 min at each 0.5ºC intervals between 70ºC and 29ºC, and 10 min at each 1ºC between 29ºC and 25ºC). To test the staple ratio, in a solution containing 10 nM full-length M13 scaffold in 1× TAE with 100 mM NaCl and 14 mM MgCl2, staples were added to final concentrations of 50, 100, 200, 400, 600, and 800 nM individually final concentration, and brought up to 50 µL. Annealing was done as above. To test optimal annealing time, with 50 µL solutions containing 1× TAE with 100 mM NaCl and 14 mM MgCl2, 10 nM M13 scaffold and 400 nM staples, annealing times of 12, 18, 24, and 48 hours were tested by increasing the length of time for each 0.5ºC step (7.5 min/ºC, 11 min/ºC, 15 min/ºC, and 35 min/ºC).

In all cases, folding was initially checked by agarose gel electrophoretic mobility shift assays (EMSA). 20 μL of folded sample was combined with 4 μL 6× loading buffer (NEB), and loaded to a 2% agarose gel with 1× TAE and 12.5 mM $MgCl_2$ and 1× SybrSafe (ThermoFisher). Each gel was run at 90V for 5 minutes followed by 65V for 2-4 hours in 1× TAE with 12.5 mM $MgCl_2$. Gels were run in an ice-chilled water bath. Gels were then visualized under blue light (Figure S48).

Folded DNA-NPs used for subsequent structural studies were folded in a solution of 20 nM scaffold, 600 nM staples, 1× TAE, 100 mM NaCl, and 14 mM $MgCl_2$ and annealed over the course of 24 hours.

Folded DNA-NPs were purified from staples and folding buffer by the use of buffer exchange via spin filter concentrator columns with size 100 kDa MWCO first cleaned with nuclease free water. DNA-NPs were exchanged into buffer composed of 30 mM Tris-HCl pH 8.1 with 100 mM NaCl and 12 mM $MgCl_2$ by centrifugation at 3000 RPMs for 40 minutes at 20ºC and diluted approximately 10-fold and re-concentrated a total of 6 times. PEG-8000 precipitation and size exclusion spin purification (Illustra S300, GE) was also successfully used to purify the folded DNA-NPs.

Dynamic light scattering (DLS) was used to assay the monodispersity of the folded DNA-NPs. A Wyatt DynaPro NanoStar M3300 was used to collect light-scattering data (Figure S49a,b). DNA-NPs were folded and purified as described. Additionally, purified particle solution was filtered by a 0.22μm to remove any large aggregates. DNA-NP concentration was determined by a ThermoFisher NanoDrop 2000, and a final concentration of 10 nM was used to collect the light scattering data. Data was collected at multiple temperatures to assay global particle thermal stability. A Malvern NanoSight NS300 was additionally used to collect light-scattering data on the folded nanoparticles. Folded, purified, and filtered MV tetrahedron of 84-bp edge length and MV octahedron of 84-bp edge length DNA-NPs were diluted to approximately 10 pM concentration and individual particle tracking was used to obtain particle sizes (Figure S49c,d). Movie captures of the light scattering from individual particles are shown in Movies S1 and S2.

Melting curves were generated to assay the thermal stability of the folded DNA-NPs. 20 μl of 1 or 5 nM folded and purified DNA-NPs in 30 mM Tris-HCl pH 8.1 with 100 mM NaCl and 12 mM $MgCl_2$ were incubated with 1× SybrGreen I and a QuantStudio 6 (ThermoFisher) was used to

assay thermal stability by observing fluorescence as temperature increased stepwise from 25-90°C in 5-minute increments per 1°C (Figure S50).

S2.2 Transmission electron microscopy (TEM)

The final DNA-NP concentration was approximately 10 nM. Samples were floated to the formvar surface for 1 minute, blotted with ashless Whatman paper #45, stained by 2% uranyl formate with 50mM NaOH for 30 seconds, and blotted dry. Negative stained TEM images were captured using a FEI Tecnai Spirit Transmission Electron Microscope set to 120kV potential (Figure 2g, Figures S51–S54, Figure S58 and Figure S59).

S2.3 Cryogenic Electron Microscopy (cryo-EM) and Single particle images processing

Three microliter of the freshly concentrated DNA nanostructure solution was applied onto the glow-discharged 200-mesh Quantifoil 2/1 grid, blotted for three secs and rapidly frozen in liquid ethane using a Vitrobot Mark IV (FEI). All grids were screened on a JEM2200FS cryo-electron microscope (JEOL) or a Talos Arctica cryo-electron microscope (FEI) operated at 200 kV. And then imaged in the JEOL 3200 cryo-electron microscope (JEOL) or in a Titan Krios cryo-electron microscope (FEI). Micrographs were recorded with a Gatan K2 Summit direct electron detector in counting mode, where each image is composed of 32 individual frames with an exposure time of 8 s and a total dose ~40 electrons per $Å^2$. A total of 96 images for the FV tetrahedron of 84-bp edge length, 119 images for the MV tetrahedron of 84-bp edge length, 724 images for the FV octahedron of 84-bp edge length, 657 images for the MV octahedron of 84-bp edge length and 662 images for the MV tetrahedron of 63-bp edge length were collected (Figures S55–S57 and Figures S60–S64) with a defocus range of ~1.5–4 μm. All the images were motion-corrected using MotionCor2.[13] Single-particle image processing and 3D reconstruction was performed (Figures S65–S70 and Movies S3–S6) using the image processing software package EMAN2.[14] All particles were picked manually by *e2boxer.py* in EMAN2. The initial models generated by TALOS software were low pass filtered to 60Å to avoid model bias. The following steps were performed as previously described.[15] A total of 1,669 particles for the FV tetrahedron of 84-bp edge length,

1,092 particles for the MV tetrahedron of 84-bp edge length, 3,308 particles for the FV octahedron of 84-bp edge length, 5,705 particles for the MV octahedron of 84-bp edge length and 2,511 particles for the MV tetrahedron of 63-bp edge length were used for final refinement, applying tetrahedral, tetrahedral, octahedral, octahedral and tetrahedral symmetries, respectively. Resolutions for the final maps were estimated using the 0.143 criterion of the Fourier shell correlation (FSC) curve without any mask. A Gaussian low-pass filter was applied to the final 3D maps displayed in the UCSF Chimera software package.[12] Correlation of each map with its corresponding atomic model is calculated by the UCSF Chimera fitmap function.

S3 Edge and vertex analysis of 6HB and DX MD trajectories

A geometric approach for analyzing each frame in the MD trajectory of a DX DNA-NP was extended to 6HB DNA-NPs here.[16] In this approach, the 6HB edges are split into sets of two duplexes which are connected at the inner (FV and MV) and outer (MV) vertices. At each inner and outer vertex, two M-bp DNA duplexes of each edge are connected with a 1-bp offset along the edge direction, resulting in a protruding base pair at each end of the edge. The protruding base pairs are excluded from downstream analysis, and the remaining base pairs of the two-duplex edge are indexed as $\mathrm{bp}_{1,1}$, $\mathrm{bp}_{1,2}$, …, $\mathrm{bp}_{1,M-1}$, $\mathrm{bp}_{2,1}$, $\mathrm{bp}_{2,2}$, …, $\mathrm{bp}_{2,M-1}$. The Python package ProDy[17] then computes the geometric center of atoms in each base pair, denoted $\mathbf{x}_{1,1}$, …, $\mathbf{x}_{2,M-1}$, and the geometric center of atoms in each pair of base pairs $(\mathrm{bp}_{1,i}, \mathrm{bp}_{2,i})$, $i = 1, 2, ..., M-1$, denoted $\mathbf{c}_i$. A right-handed orthonormal basis $(\mathbf{b}_1, \mathbf{b}_2, \mathbf{b}_3)$ is defined using the three principal axes of the point cloud $\{\mathbf{x}_{1,1}, \ldots, \mathbf{x}_{1,M-1}, \mathbf{x}_{2,1}, \ldots, \mathbf{x}_{2,M-1}\}$, in which $\mathbf{b}_1$ is coincident with the first principal axis and points from $\mathbf{c}_1$ to $\mathbf{c}_{M-1}$, $\mathbf{b}_2$ is coincident with the second principal axis and points from $\mathrm{bp}_{1,1}$ to $\mathrm{bp}_{2,1}$, and $\mathbf{b}_3$ is coincident with the third principal axis and points outwards of the NP. Next, a L-bp-long region at the starting end of the edge is selected to define a vector $\mathbf{a}_1$, which is coincident with the first principal axis of the point clouds $\{\mathbf{c}_1, \ldots, \mathbf{c}_L\}$, and points from $\mathbf{c}_1$ to $\mathbf{c}_L$. The bow- and twist-angles associated with the left half-edge are computed by projecting $\mathbf{a}_1$ onto the $\mathbf{b}_3$-$\mathbf{b}_1$ plane and the $\mathbf{b}_1$-$\mathbf{b}_2$ plane as $\mathbf{a}_{1,\mathrm{bow}}$ and $\mathbf{a}_{1,\mathrm{twist}}$, respectively. The bow-angle is defined as the right-handed rotation angle from $\mathbf{a}_{1,\mathrm{bow}}$ to $\mathbf{b}_1$ about $\mathbf{b}_2$, and the twist-angle as the right-handed rotation angle from $\mathbf{b}_1$ to $\mathbf{a}_{1,\mathrm{twist}}$ about $\mathbf{b}_3$. This geometric approach allows calculation of two properties of

an *N*-arm vertex in each frame: average bow-angle, Ψ, and average twist-angle, Θ. Finally, the bow- and twist-angles are averaged over the *N* half-edges that are directly connected to the vertex. Edge and vertex properties are shown in detail for the FV 6HB tetrahedron (Figure S72), the MV 6HB tetrahedron (Figure S73 and Figure S74), and the DX tetrahedron (Figure S75), all with 42-bp edge lengths and simulated using all-atom MD (Movies S7-S9).

Reference

(1) Mathieu, F.; Liao, S.; Kopatsch, J.; Wang, T.; Mao, C.; Seeman, N. C. Six-Helix Bundles Designed from DNA. *Nano Lett.* **2005**, *5*, 661–665.

(2) Dietz, H.; Douglas, S. M.; Shih, W. M. Folding DNA into Twisted and Curved Nanoscale Shapes. *Science* **2009**, *325*, 725–730.

(3) Castro, C. E.; Kilchherr, F.; Kim, D.-N.; Shiao, E. L.; Wauer, T.; Wortmann, P.; Bathe, M.; Dietz, H. A Primer to Scaffolded DNA Origami. *Nat. Methods* **2011**, *8*, 221–229.

(4) Pan, K.; Kim, D.-N.; Zhang, F.; Adendorff, M. R.; Yan, H.; Bathe, M. Lattice-Free Prediction of Three-Dimensional Structure of Programmed DNA Assemblies. *Nat. Commun.* **2014**, *5*, 5578.

(5) Douglas, S. M.; Marblestone, A. H.; Teerapittayanon, S.; Vazquez, A.; Church, G. M.; Shih, W. M. Rapid Prototyping of 3D DNA-Origami Shapes with CaDNAno. *Nucleic Acids Res.* **2009**, *37*, 5001–5006.

(6) Jun, H.; Zhang, F.; Shepherd, T.; Ratanalert, S.; Qi, X.; Yan, H.; Bathe, M. Autonomously Designed Free-Form 2D DNA Origami. *Sci. Adv.* **2019,** 5, eaav0655.

(7) Ke, Y.; Bellot, G.; Voigt, N. V.; Fradkov, E.; Shih, W. M. Two Design Strategies for Enhancement of Multilayer–DNA-Origami Folding: Underwinding for Specific Intercalator Rescue and Staple-Break Positioning. *Chem. Sci.* **2012**, *3*, 2587–2597.

(8) Martin, T. G.; Dietz, H. Magnesium-Free Self-Assembly of Multi-Layer DNA Objects. *Nat. Commun.* **2012**, *3*, 1103.

(9) Ellis-Monaghan, J. A.; McDowell, A.; Moffatt, I.; Pangborn, G. DNA Origami and the Complexity of Eulerian Circuits with Turning Costs. *Nat. Comput.* **2015**, *14*, 491–503.

(10) Rich, A. The Rise of Single-Molecule DNA Biochemistry. *Proc. Natl. Acad. Sci.* **1998**, *95*, 13999–14000.

(11) Murphy, M. C.; Rasnik, I.; Cheng, W.; Lohman, T. M.; Ha, T. Probing Single-Stranded DNA Conformational Flexibility Using Fluorescence Spectroscopy. *Biophys. J.* **2004**, *86*, 2530–2537.

(12) Pettersen, E. F.; Goddard, T. D.; Huang, C. C.; Couch, G. S.; Greenblatt, D. M.; Meng, E. C.; Ferrin, T. E. UCSF Chimera—A Visualization System for Exploratory Research and Analysis. *J. Comput. Chem.* **2004**, *25*, 1605–1612.

(13) Zheng, S. Q.; Palovcak, E.; Armache, J.-P.; Verba, K. A.; Cheng, Y.; Agard, D. A. MotionCor2: Anisotropic Correction of Beam-Induced Motion for Improved Cryo-Electron Microscopy. *Nat. Methods* **2017**, *14*, 331–332.

(14) Tang, G.; Peng, L.; Baldwin, P. R.; Mann, D. S.; Jiang, W.; Rees, I.; Ludtke, S. J. EMAN2: An Extensible Image Processing Suite for Electron Microscopy. *J. Struct. Biol.* **2007**, *157*, 38–46.

(15) Veneziano, R.; Ratanalert, S.; Zhang, K.; Zhang, F.; Yan, H.; Chiu, W.; Bathe, M. Designer Nanoscale DNA Assemblies Programmed from the Top Down. *Science* **2016**, *352*, 1534–1534.

(16) Pan, K.; Bricker, W. P.; Ratanalert, S.; Bathe, M. Structure and Conformational Dynamics of Scaffolded DNA Origami Nanoparticles. *Nucleic Acids Res.* **2017**, *45*, 6284–6298.

(17) Bakan, A.; Meireles, L. M.; Bahar, I. ProDy: Protein Dynamics Inferred from Theory and Experiments. *Bioinformatics* **2011**, *27*, 1575–1577.

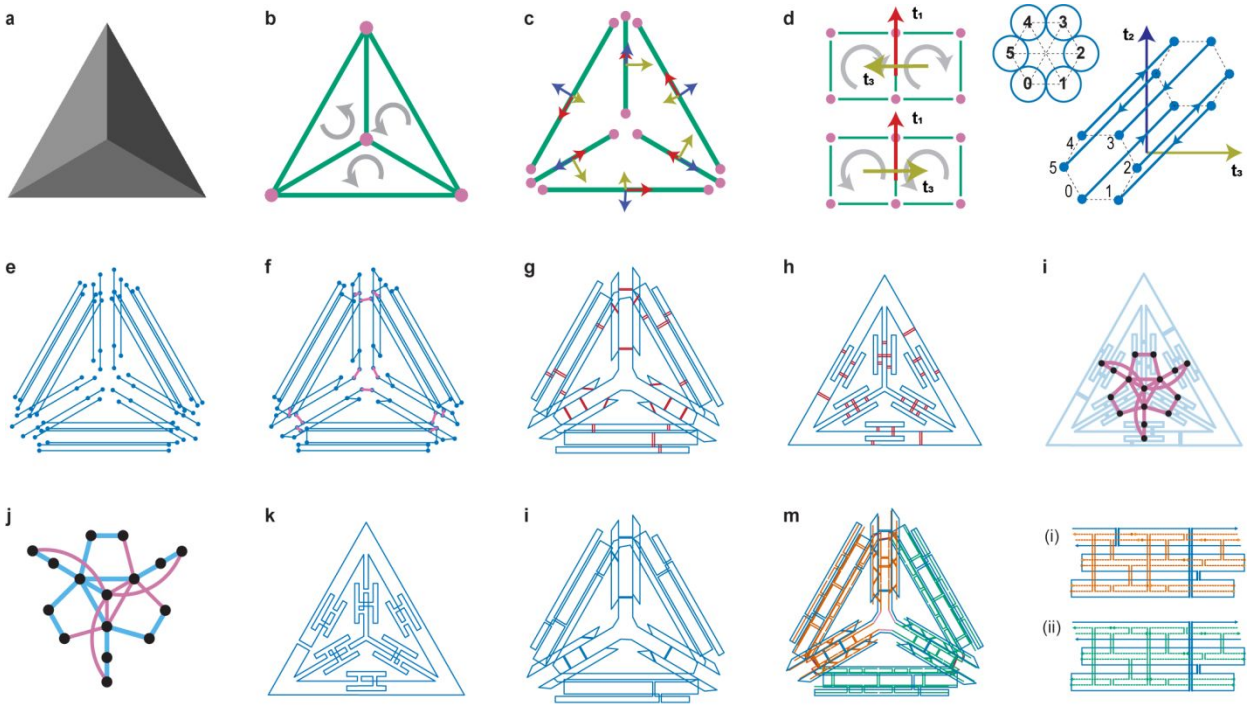

Figure S1. Schematic illustrating design algorithm for a FV tetrahedron. (**a-b**) The polygon mesh file contains information for positions of points and the face connectivity, for this example it consists of the triangular mesh (**b**) with the consistent orientation. (**c**) All edges are separated from the vertex associated and the local coordinate system, $\mathbf{t_1}$-$\mathbf{t_2}$-$\mathbf{t_3}$ is introduced at the center of each separated edge. (**d**) The three vectors are calculated by the direction of two neighboring faces and the interfacing line. Then, the cross-section of the six-helix bundle is defined on the local vectors, $\mathbf{t_3}$-$\mathbf{t_2}$ and the six lines whose direction depends on the cross-section ID (number in circle) are introduced. (**e-f**) Each separated line is substituted with six scaffold segments and closed loops are generated (**f**) by connecting endpoints of multiple lines at the vertex. (**g**) The multiple lines are discretized to represent the base pair, in which the scaffold double-crossovers (red double line) for each two closed loops are introduced. (**h-j**) The loop-crossover structure is projected in 2D as a Schlegel diagram and converted (**i**) into the dual graph that is used to compute (**j**) the spanning tree. (**k-i**) By inverting (**k**) the spanning tree to the Schlegel diagram, the scaffold routing is completed (**i**). (**m**) Staples are added and sequences are assigned, resulting in two edge routing patterns.

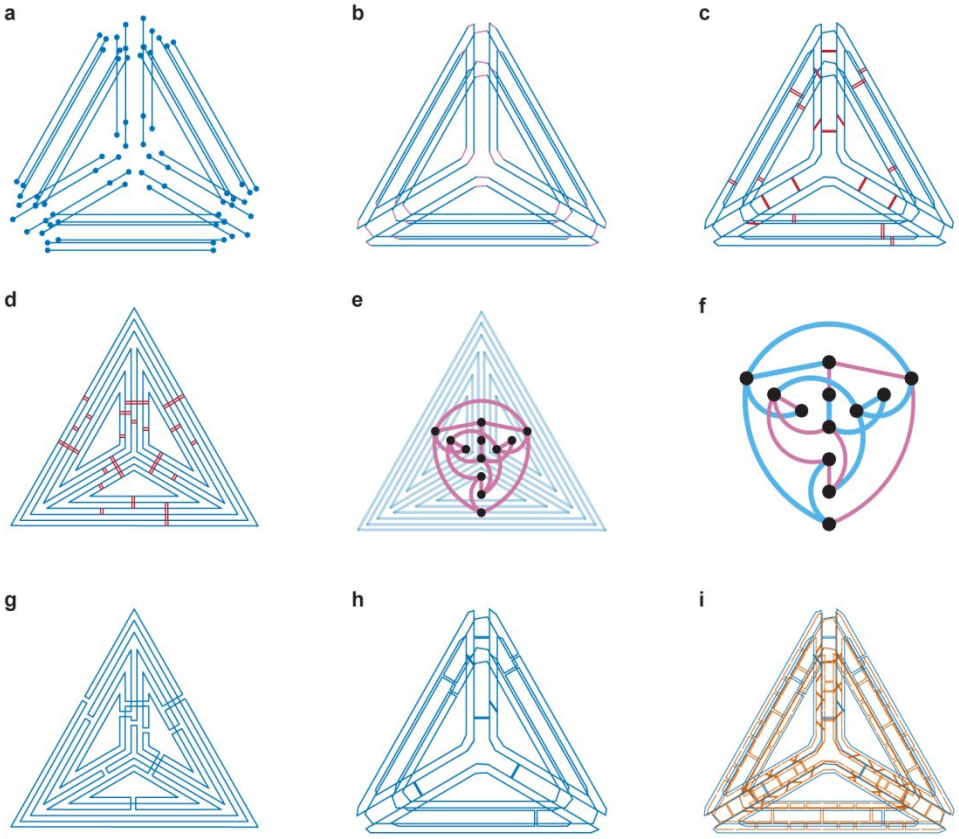

Figure S2. Schematic illustrating design algorithm for a MV tetrahedron. (**a**-**b**) Line segments are extended to connect their neighboring lines crossing at the vertex and closed loops are formed by connecting endpoints of the each line at the vertex. (**c**) The multiple lines are discretized to represent the base pair, in which the scaffold double-crossovers (red double line) for each two closed loops are introduced. (**d**-**f**) The loop-crossover structure is projected in 2D as a Schlegel diagram and converted (**e**) into the dual graph that is used to compute (**f**) the spanning tree. (**g**-**h**) By inverting the spanning tree to the Schlegel diagram, the scaffold routing is completed. **i**, Staples are added and sequences are assigned.

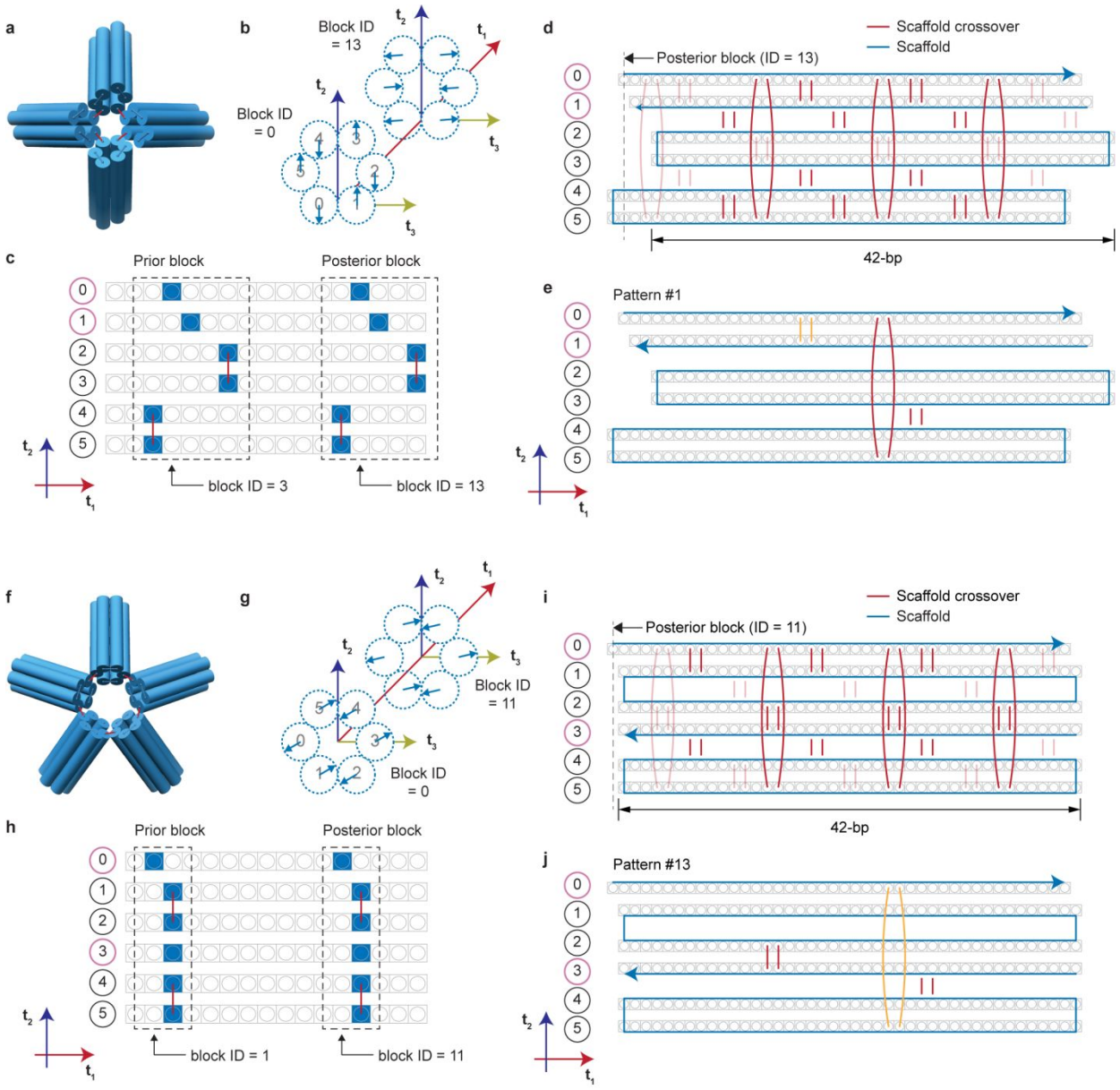

Figure S3. Initial scaffold crossovers according to the inner and middle connection layer. (**a-b**) In the inner connection layer, the nucleotide at the 5'-end is initially located in the 270° direction for even numbers and 90° direction for odd numbers. The positions of nucleotides are rotated by 34.28° counterclockwise per base pair mean twist (21 base pairs every two turns). (**c-d**) There are two possible positions to define the 5'-end of the scaffold, prior and posterior block, resulting in different patterns (**d**) of scaffold possible crossovers (red line) on the edge. The crossover is removed (faint red line) when it is 7-bp away from the end of the line. (**e**) The only double-crossover between two loops is assigned by a zigzag pattern sequentially from section 1 to

6 and imposed a weight factor (1 for red, 2 for yellow, and 3 for black crossovers) according to weight patterns shown in Figure S4. (**f-g**) For the middle connection layer, the nucleotide of the scaffold is initially located in the 30° direction for even numbers and 210° direction for odd numbers. (**h-j**) Two different block positions also results in the different patterns of scaffold possible crossovers on the edge.

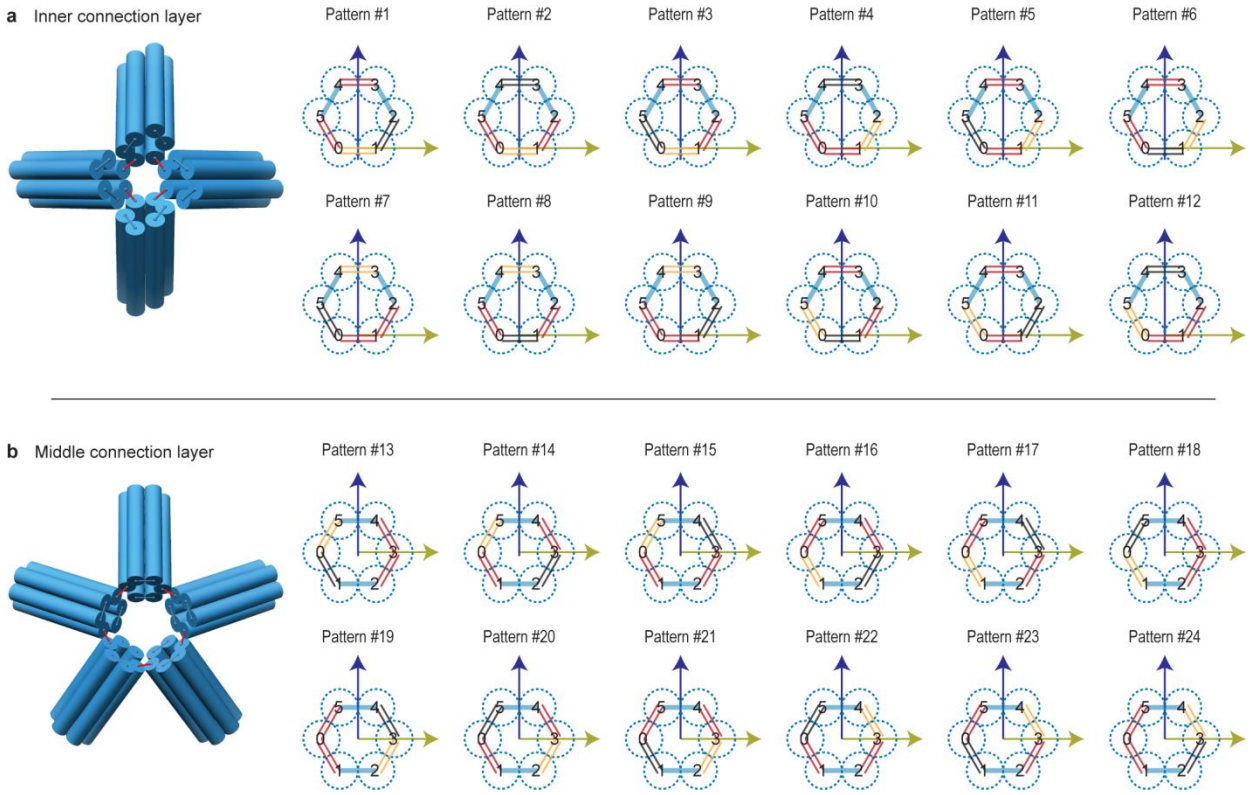

Figure S4. 12 possible patterns to define the weight factor of the scaffold crossovers for the FV design. (**a**-**b**) The six-circles show the cross-section of the six-helix bundle. Two circles that are located on the $\mathbf{t_3}$ axis are connected to the neighboring circles crossing the vertex. Four possible double-crossovers can be constructed with three different weight factors, resulting in 12 possible patterns for each connection layer. Each edge has at least two double crossovers of scaffold, which is assigned as weight factor of 1 (red double line). The others are assigned as the weight factor of 2 (yellow) or 3 (black), which is algorithmically selected.

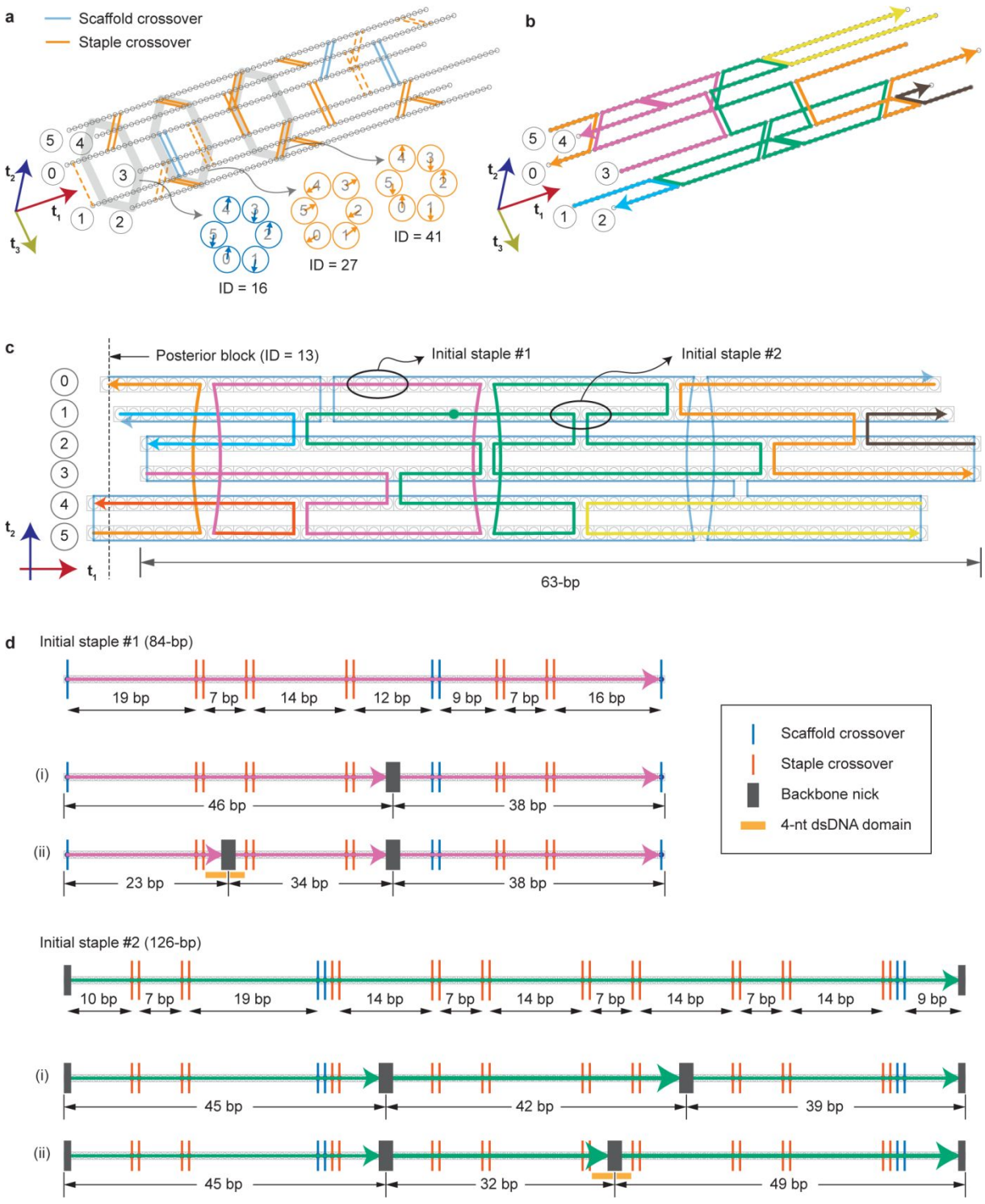

Figure S5. Schematic illustration of staple routing procedure and two staple-break rules. (**a**) Possible staple crossovers (orange line) are assigned in the permitted position except for those (orange dotted line) that would be 5 bp away from a scaffold crossover between the same helices

and 7 bp away from the both ends of discretized lines. The six-circles show the cross-section of the 6HB and the arrow indicates the position of the nucleotide of the scaffold (blue) or staple (orange) according to the block ID. (**b**) Initial staple paths (multiple colored lines) are constructed by connecting assigned possible staple crossovers, which have the orientation (arrow) that is opposite to one of the complementary scaffold. (**c**) In the planar representation of six-helix bundle shown in panel (**b**), the initial staple #1 (red) and staple #2 (green) have lengths of 84-bp and 126-bp, respectively, which is complementary to scaffold strand (blue). The staple #2 is non-circular, which is broken by the backbone nick (green circle) at the center of the longest dsDNA domain. (**d**) Two staple-break rules of the "maximized staple length" and "maximized the number of seed domains" are applied into the initial staple #1 and #2 to make short staples ranging from 20 bp to 60 bp.

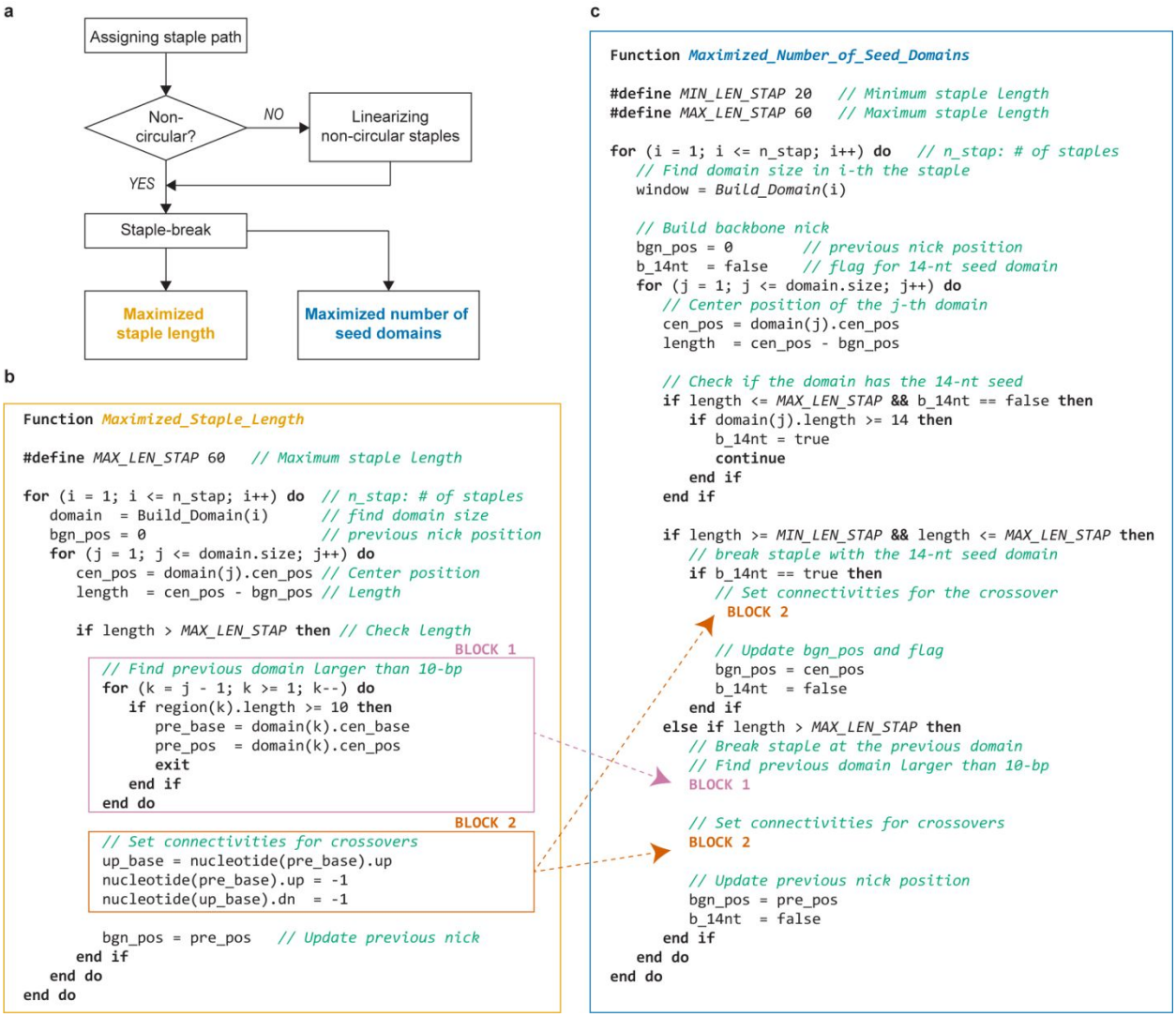

Figure S6. Procedure to design the staple routing and two algorithms to break the staples ranged from 20 bp to 60 bp. (**a**)The staple routing consists of three steps; assigning initial staple path, making non-circular and breaking the initial staple. (**b-c**) Pseudo codes for two staple-break rules, "maximized staple length" (**b**) and "maximized the number of seed domains" (**c**). Data structures used in algorithms: *domain* – the linked list to save the information on the dsDNA domain of each initial staple; *window(i).length* – the return value of the length of the *i*-th dsDNA domain; *window(i).cen_pos* – the return value of the center position at *i*-th dsDNA domain; *nucleotides* – vector array to save information on the connectivity of nucleotides; *nucleotide(i).up* – the return value indicating the upper nucleotide ID; *nucleotide(i).dn* – the return value indicating the downward nucleotide ID. Pseudocode does not include exception handling.

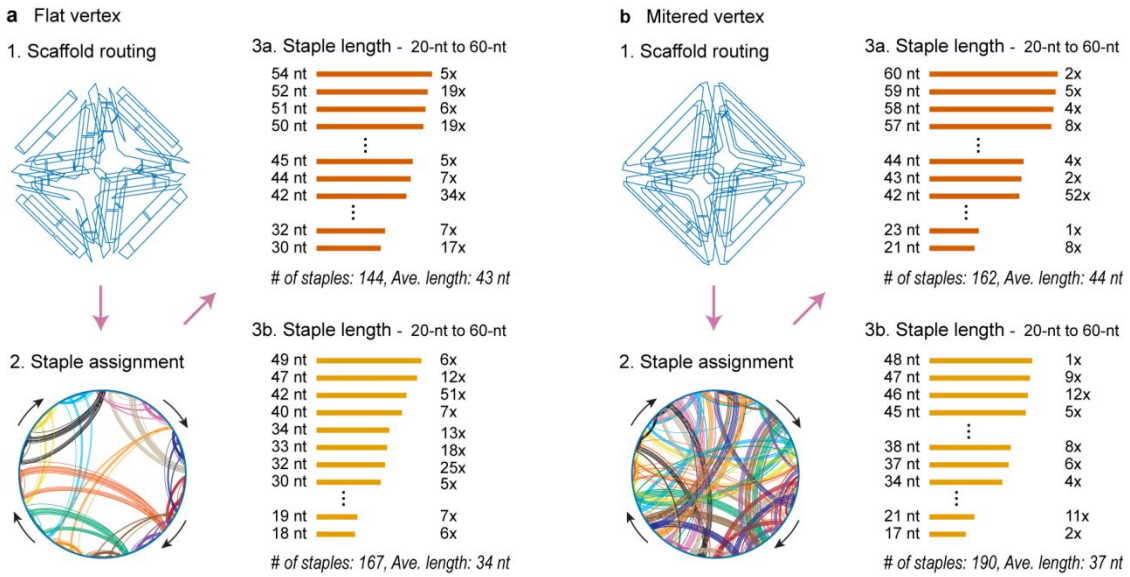

Figure S7. User defined staple length design.

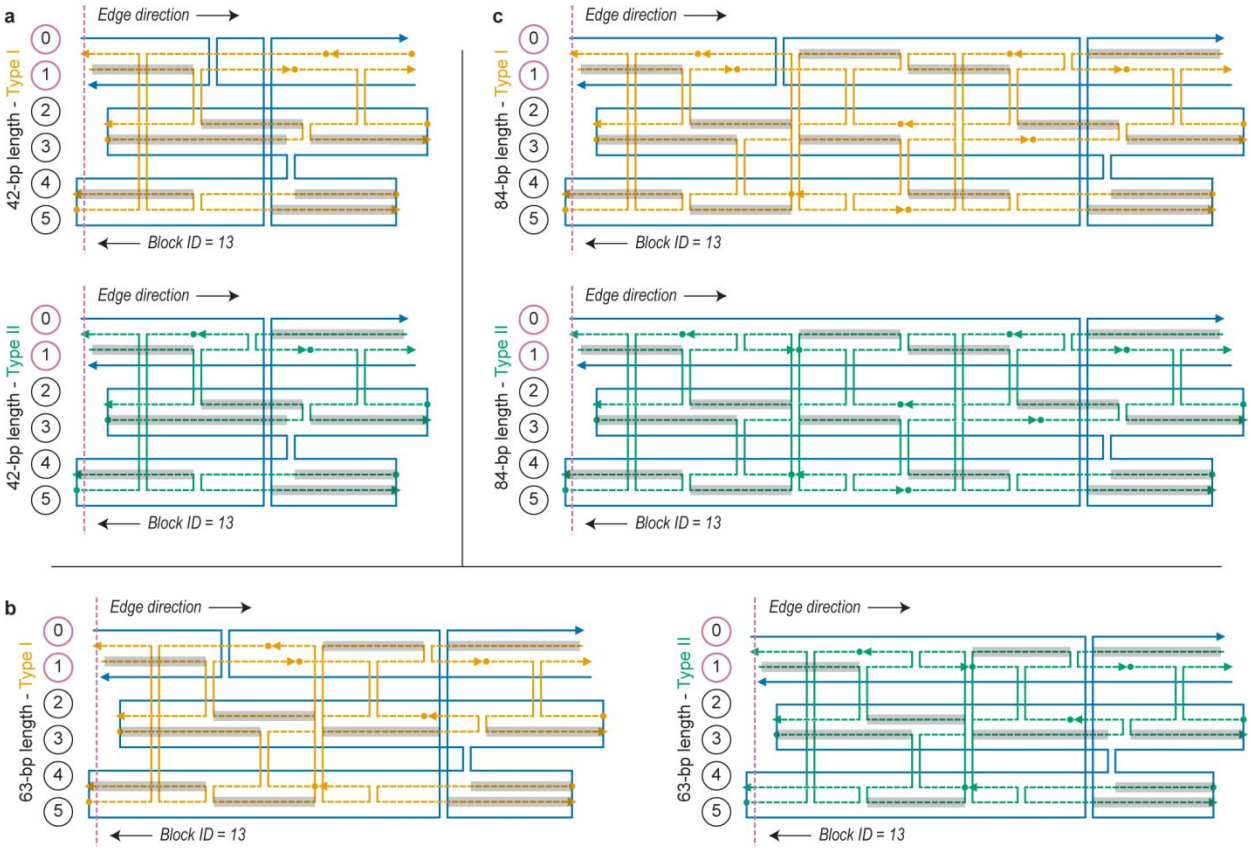

Figure S8. Edge staple-design for the inner connection layer when the "maximized staple length" breaking rule is used. (**a**-**c**) All FV DNA-NPs have only two edge staple-design patterns; type I (orange edge staples with three scaffold double-crossovers) and type II (green edge staples with two scaffold double-crossovers) for 42-bp (**a**), 63-bp (**b**) and 84-bp (**c**) edge length. The blue strand is the part of the M13mp18 scaffold strand. The gray-shaded region represents the 14-nt seed dsDNA domain and arrowheads indicate the 3′-ends of strands.

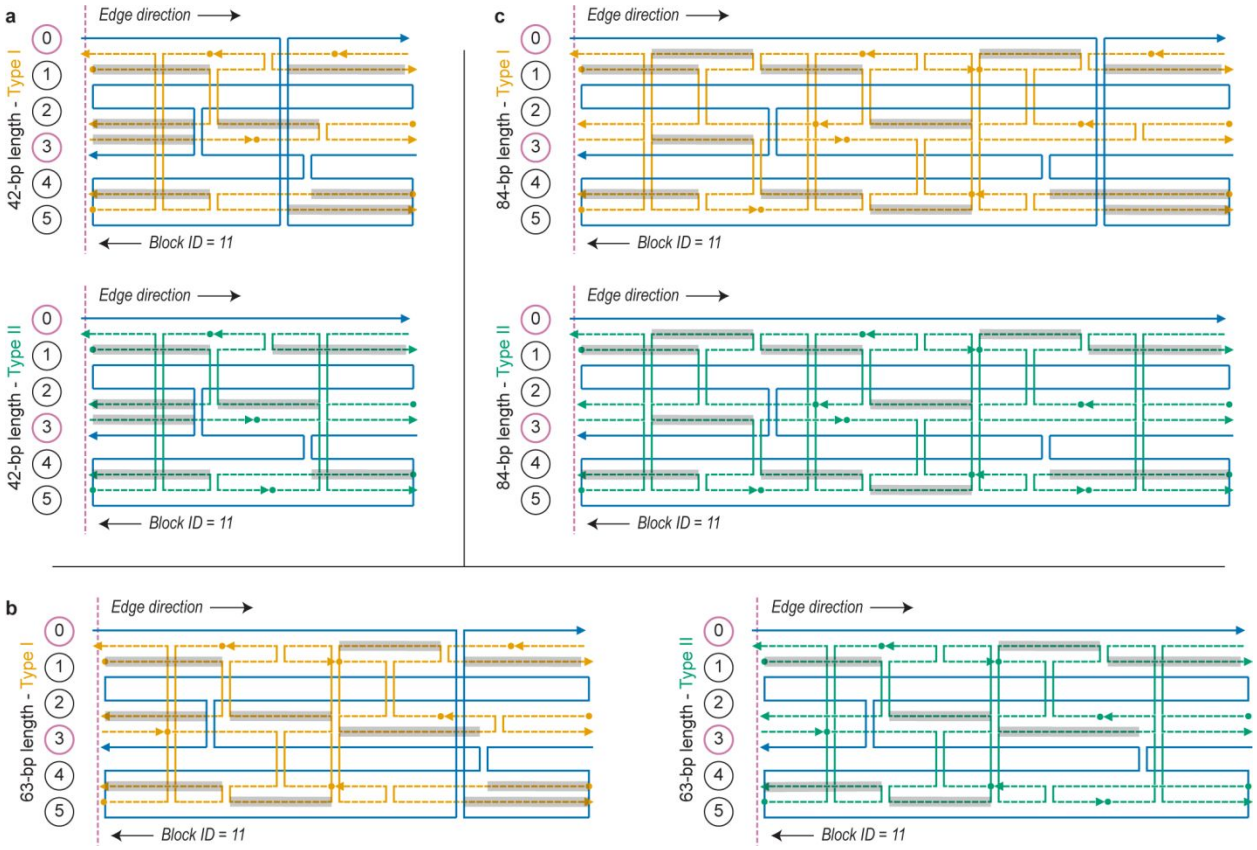

Figure S9. Edge staple-design for the middle connection layer when the "maximized staple length" breaking rule is used. (**a**-**c**) All FV DNA-NPs have only two edge staple-design patterns; type I (orange edge staples with three scaffold double-crossovers) and type II (green edge staples with two scaffold double-crossovers) for 42-bp (**a**), 63-bp (**b**) and 84-bp (**c**) edge length. The blue strand is the part of the M13mp18 scaffold strand. The gray-shaded region represents the 14-nt seed dsDNA domain and arrowheads indicate the 3′-ends of strands.

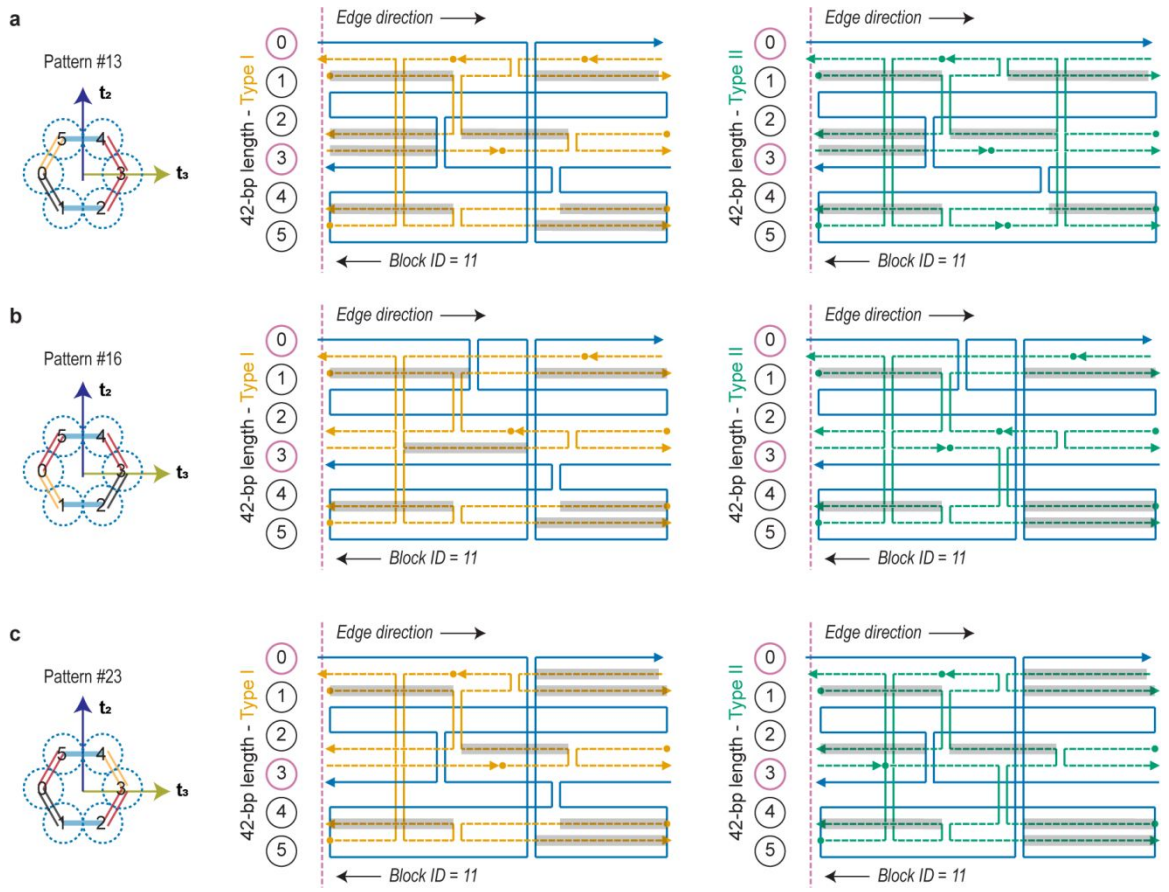

Figure S10. Edge staple-design for the middle connection layer with the "maximized staple length" breaking rule when three different scaffold crossovers are used. All FV DNA-NPs have only two edge staple-design patterns; type I (orange edge staples with three scaffold double-crossovers) and type II (green edge staples with two scaffold double-crossovers) for the 42-bp edge length. (**a**-**c**) The pattern of the edge staple-design is depending on how to assign the weight factors of initial scaffold crossovers, for example, pattern #13 (**a**), pattern #16 (**b**), and pattern #23 (**c**). The blue strand is the part of the M13mp18 scaffold strand. The gray-shaded region represents the 14-nt seed dsDNA domain and arrowheads indicate the 3′-ends of strands.

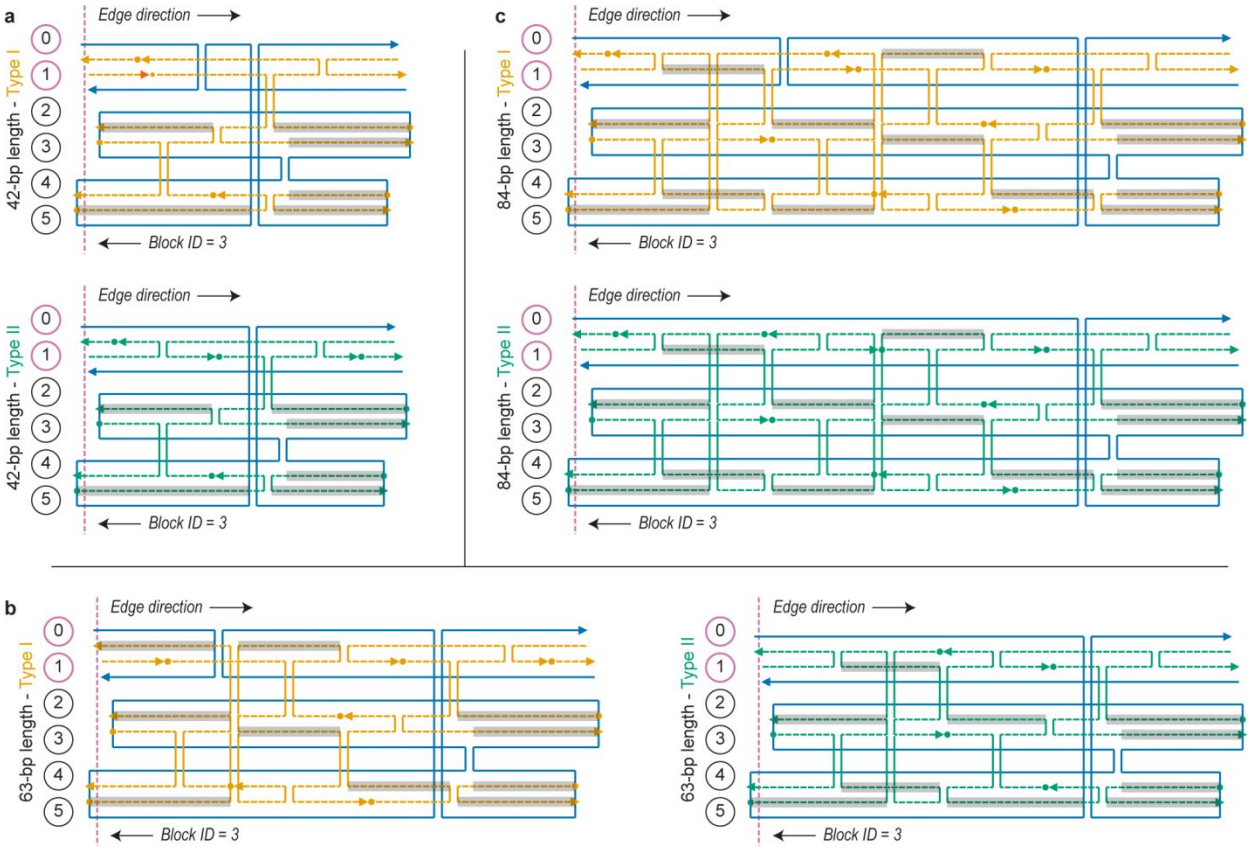

Figure S11. Edge staple-design for the inner connection layer with the "maximized staple length" breaking rule when the prior block (ID = 3) is used. (**a**-**c**) All FV DNA-NPs have only two edge staple-design patterns; type I (orange edge staples with three scaffold double-crossovers) and type II (green edge staples with two scaffold double-crossovers) for 42-bp (**a**), 63-bp (**b**) and 84-bp (**c**) edge length. The blue strand is the part of the M13mp18 scaffold strand. The gray-shaded region represents the 14-nt seed dsDNA domain and arrowheads indicate the 3′-ends of strands.

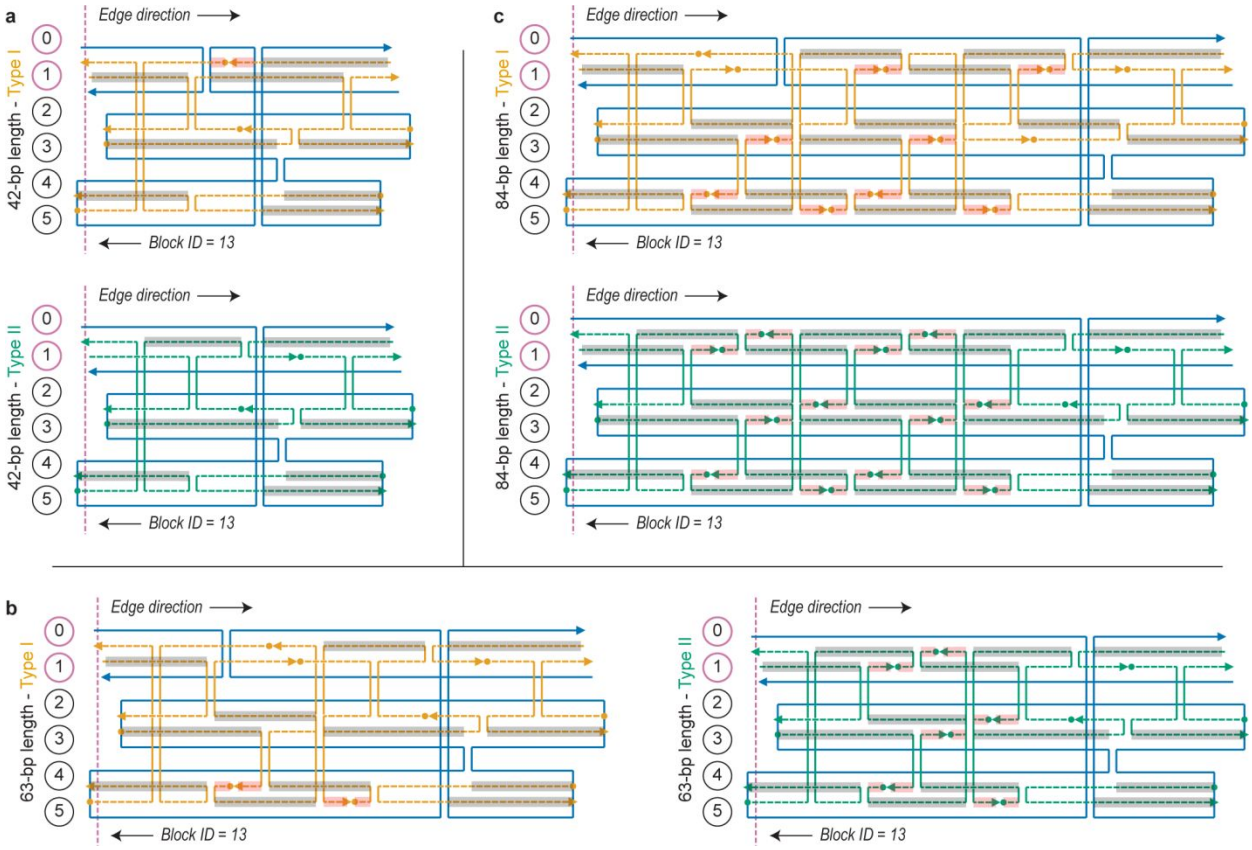

Figure S12. Edge staple-design for the inner connection layer when the "Maximized number of seeds" breaking rule is used. (**a-c**) All FV DNA-NPs have only two edge staple-design patterns; type I (orange edge staples with three scaffold double-crossovers) and type II (green edge staples with two scaffold double-crossovers) for 42-bp (**a**), 63-bp (**b**) and 84-bp (**c**) edge length. The blue strand is the part of the M13mp18 scaffold strand. The gray-shaded region represents the 14-nt seed dsDNA domain and arrowheads indicate the 3′-ends of strands.

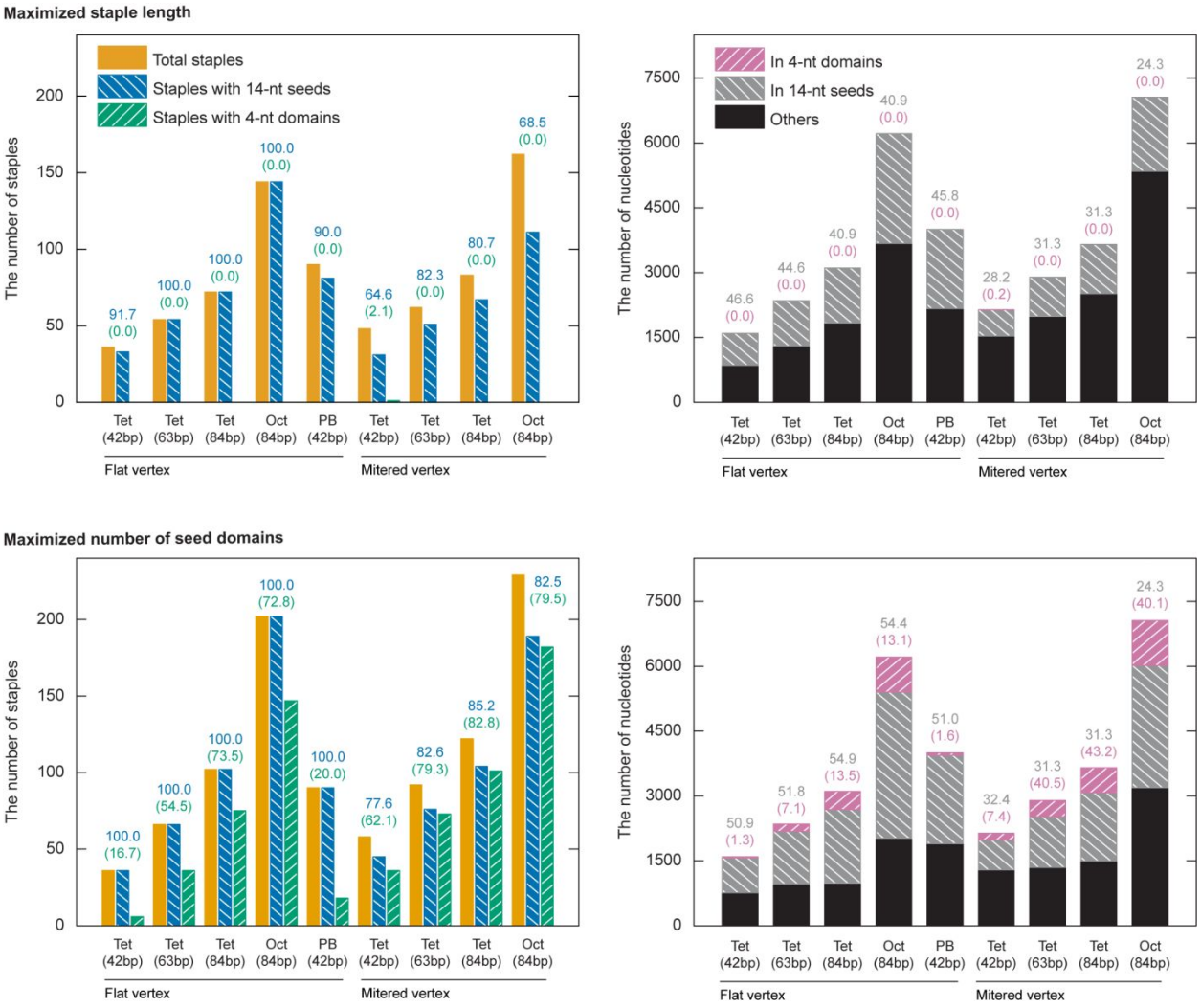

Figure S13. A comparison of the number of dsDNA domains with two different staple-break rules; "maximized staple length" and "maximized number of seed domains" in the folded DNA 6HB DNA-NPs. The values indicate the fraction of staples with 14-nt seed dsDNA domains (left) and basepairs that reside on strands with 14-nt seeds (right). The values in parenthesis denote the fraction of strands with 4-nt dsDNA domains (left) and base pairs that reside on strands with 4-nt domains (right).

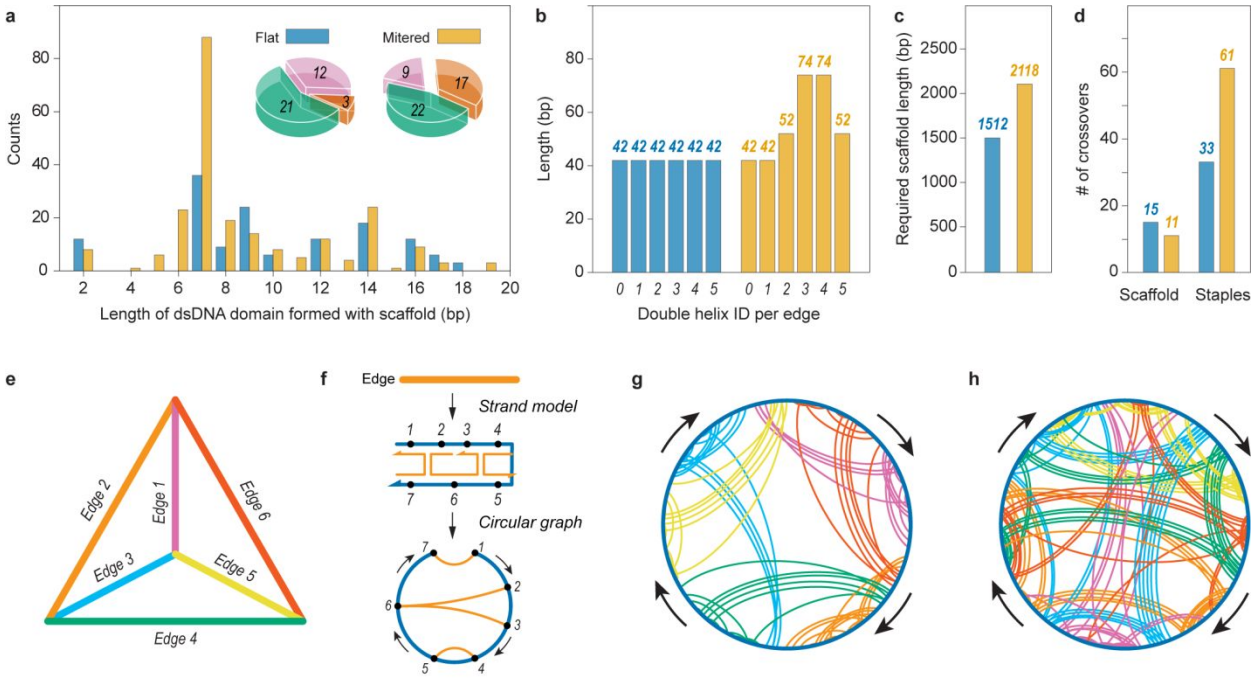

Figure S14. Quantitative analysis of the computed sequence design of the 42-bp tetrahedron DNA origami structure between the FV and MV designs. (**a-d**) The distribution of lengths of dsDNA domains (**a**), of edge lengths (**b**) of base pairs according to the cross-section ID, of required scaffold lengths (**c**) and the total number of crossovers (**d**) for the FV (blue) and MV (orange) tetrahedron of 42-bp edge length. Two pie charts (right in panel (**a**)) depict the ratio of staple distributions with the number of staples with one 14-nt seed (green), two 14-nt seeds (pink) and without the 14-nt seed (orange). (**e**) Schematic diagram of the initial geometry of the tetrahedron, which has edge ID with the specific color. (**f**) Schematic illustration of how to render a circular graph in which the outer circle representing the scaffold has points assigned in the middle of dsDNA domain. Two points can be connected when they are lined up in the same staple. A nick of the scaffold is positioned at the top and arrows indicates the 5′ to 3′-end direction of the scaffold. (**g-h**) Two circular maps for the FV (**g**) and MV (**h**) tetrahedron.

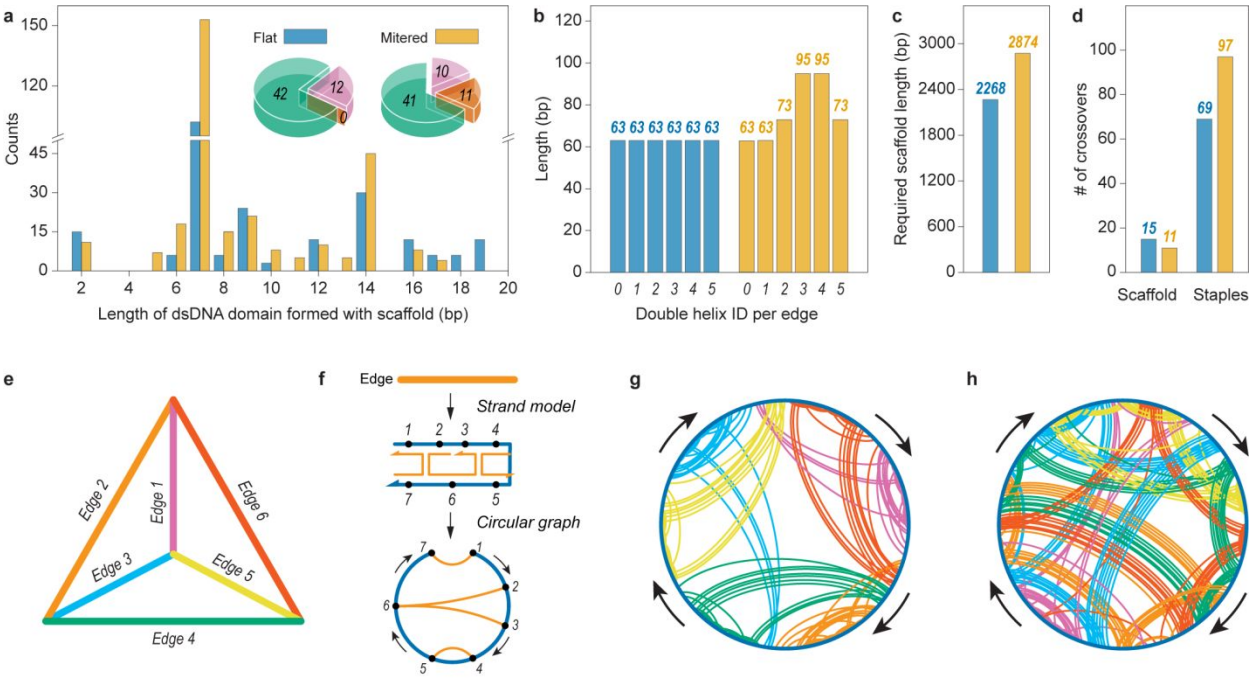

Figure S15. Quantitative analysis of the computed sequence design of the tetrahedron of 63-bp edge length between the FV and MV designs. (**a-d**) The distribution of lengths of dsDNA domains (**a**), of edge lengths (**b**) of base pairs according to the cross-section ID, of required scaffold lengths (**c**) and the total number of crossovers (**d**) for the FV (blue) and MV (orange) tetrahedron of 63-bp edge length. Two pie charts (right in panel (**a**)) depict the ratio of staple distributions with the number of staples with one 14-nt seed (green), two 14-nt seeds (pink) and without the 14-nt seed (orange). (**e**) Schematic diagram of the initial geometry of the tetrahedron, which has edge ID with the specific color. (**f**) Schematic illustration of how to render a circular graph in which the outer circle representing the scaffold has points assigned in the middle of dsDNA domain. Two points can be connected when they are lined up in the same staple. A nick of the scaffold is positioned at the top and arrows indicates the 5′ to 3′-end direction of the scaffold. (**g-h**) Two circular maps for the FV (**g**) and MV (**h**) tetrahedron.

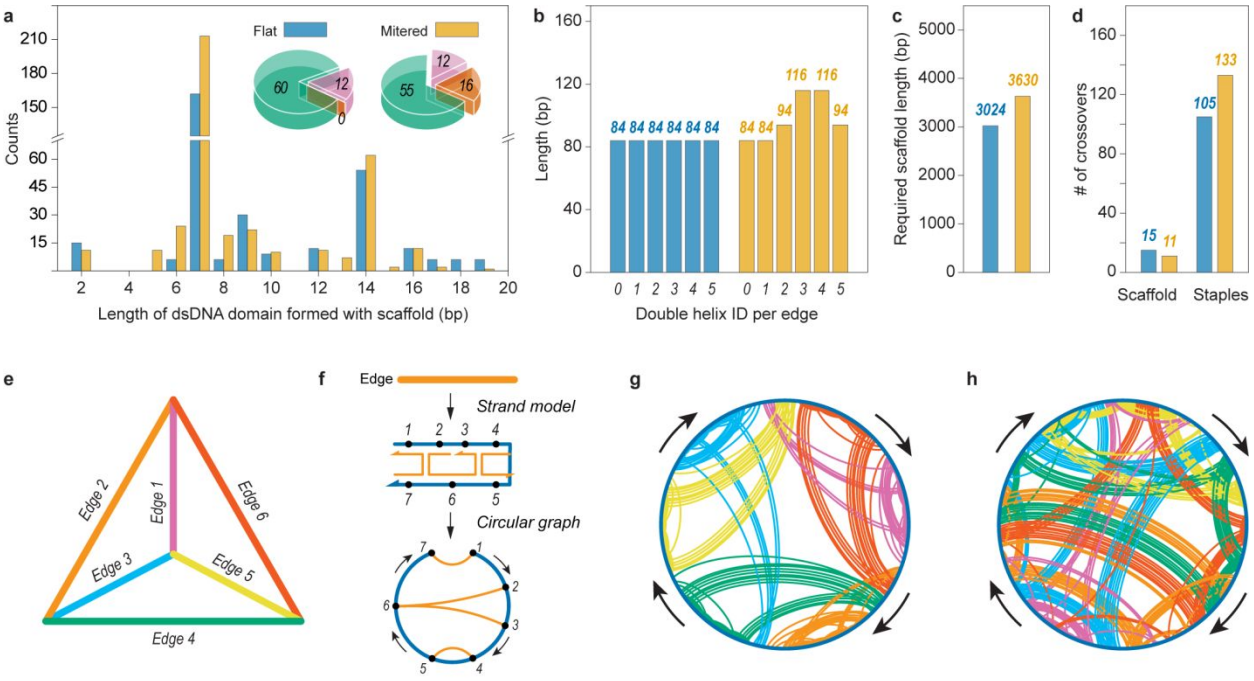

Figure S16. Quantitative analysis of the computed sequence design of the tetrahedron of 84-bp edge length between the FV and MV. (**a-d**) The distribution of lengths of dsDNA domains (**a**), of edge lengths (**b**) of base pairs according to the cross-section ID, of required scaffold lengths (**c**) and the total number of crossovers (**d**) for the FV (blue) and MV (orange) tetrahedron of 84-bp edge length. Two pie charts (right in panel (**a**)) depict the ratio of staple distributions with the number of staples with one 14-nt seed (green), two 14-nt seeds (pink) and without the 14-nt seed (orange). (**e**) Schematic diagram of the initial geometry of the tetrahedron, which has edge ID with the specific color. (**f**) Schematic illustration of how to render a circular graph in which the outer circle representing the scaffold has points assigned in the middle of dsDNA domain. Two points can be connected when they are lined up in the same staple. A nick of the scaffold is positioned at the top and arrows indicates the 5′ to 3′-end direction of the scaffold. (**g-h**) Two circular maps for the FV (**g**) and MV (**h**) tetrahedron.

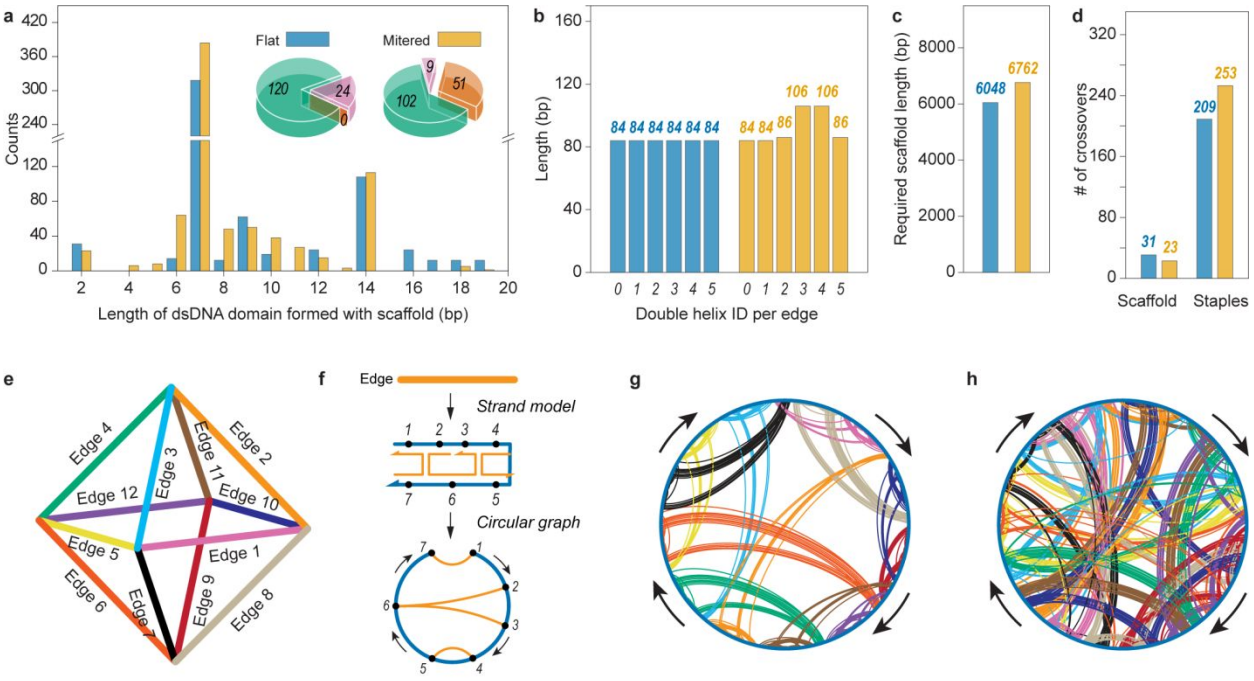

Figure S17. Quantitative analysis of the computed sequence design of the octahedron of 84-bp edge length between the FV and MV designs. (**a-d**) The distribution of lengths of dsDNA domains (**a**), of edge lengths (**b**) of base pairs according to the cross-section ID, of required scaffold lengths (**c**) and the total number of crossovers (**d**) for the FV (blue) and MV (orange) octahedron of 84-bp edge length. Two pie charts (right in panel (**a**)) depict the ratio of staple distributions with the number of staples with one 14-nt seed (green), two 14-nt seeds (pink) and without the 14-nt seed (orange). (**e**) Schematic diagram of the initial geometry of the tetrahedron, which has edge ID with the specific color. (**f**) Schematic illustration of how to render a circular graph in which the outer circle representing the scaffold has points assigned in the middle of dsDNA domain. Two points can be connected when they are lined up in the same staple. A nick of the scaffold is positioned at the top and arrows indicates the 5′ to 3′-end direction of the scaffold. (**g-h**) Two circular maps for the FV (**g**) and MV (**h**) octahedron.

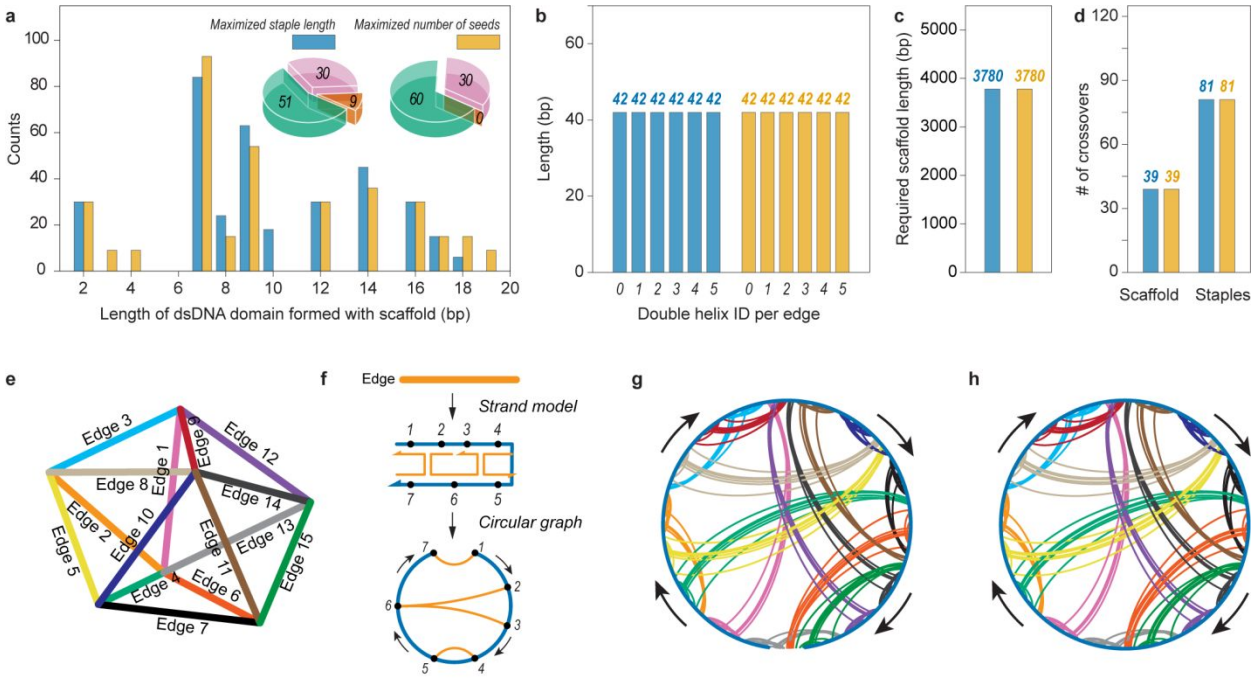

Figure S18. Quantitative analysis of the computed sequence design of the 42-bp pentagonal bipyramid DNA origami structure with the FV design when using either "maximized staple length" or "maximized number of seeds" staple breaking rule. (**a-d**) The distribution of lengths of dsDNA domains (**a**), of edge lengths (**b**) of base pairs according to the cross-section ID, of required scaffold lengths (**c**) and the total number of crossovers (**d**) for the 42-bp pentagonal bipyramid using the "maximized staple length" (blue) and "maximized number for seeds" (orange) staple breaking. Two pie charts (right in panel (**a**)) depict the ratio of staple distributions with the number of staples with one 14-nt seed (green), two 14-nt seeds (pink) and without the 14-nt seed (orange). (**e**) Schematic diagram of the initial geometry of the tetrahedron, which has edge ID with the specific color. (**f**) Schematic illustration of how to render a circular graph in which the outer circle representing the scaffold has points assigned in the middle of dsDNA domain. Two points can be connected when they are lined up in the same staple. A nick of the scaffold is positioned at the top and arrows indicates the 5′ to 3′-end direction of the scaffold. (**g-h**) Two circular maps for the 42-pentagonal pyramid using the "maximized staple length" (**g**) and "maximized number of seeds" (**h**) staple breaking.

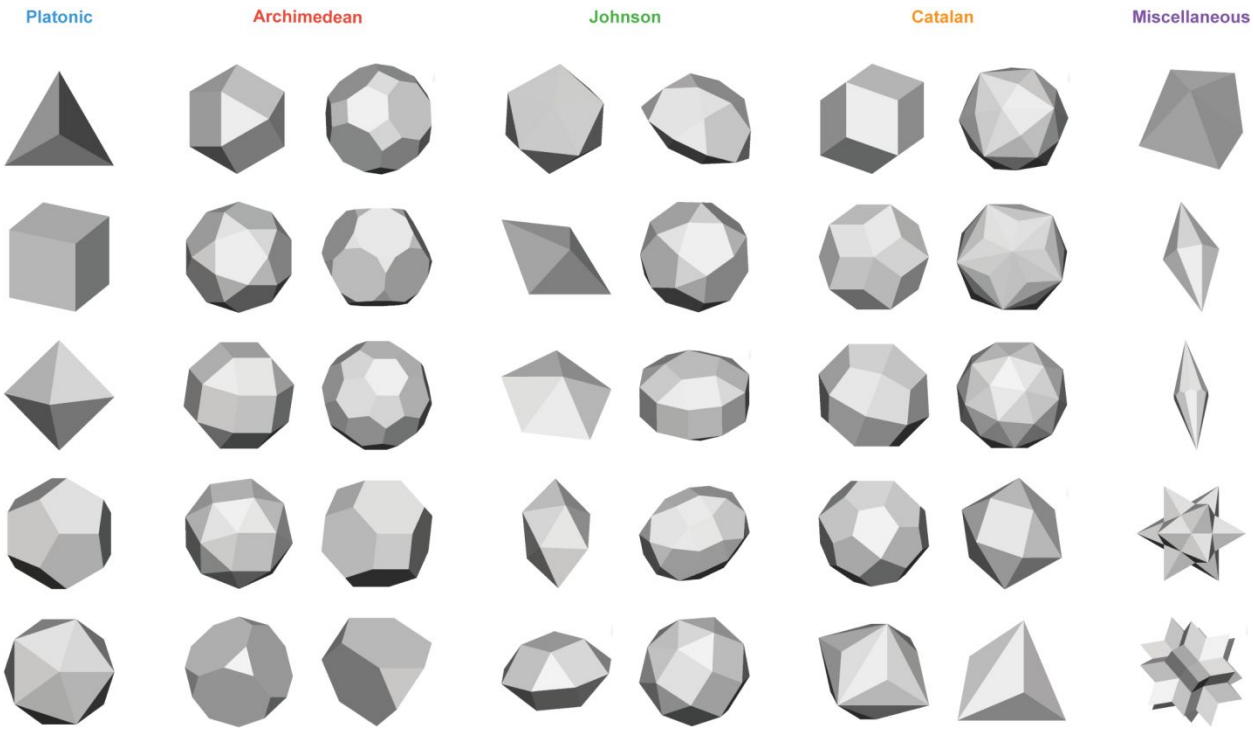

Figure S19. 40 target geometries.

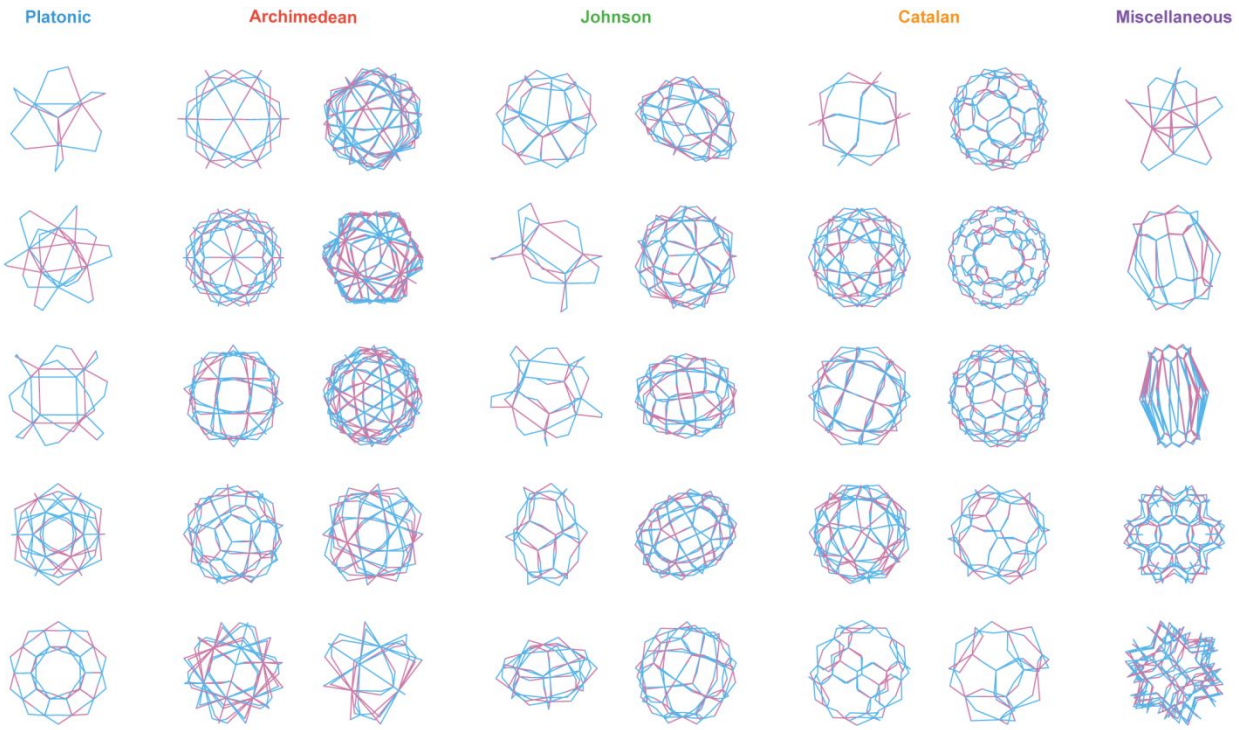

Figure S20. Spanning trees of the dual graph of the loop-crossover structure generated by the algorithm when the FV design is used. The spanning tree (sky blue) of each dual graph (reddish purple) of the loop-crossover structure defines the double crossovers to be retained by inverting into the loop-crossover structure. The double-crossovers associated with the remaining edges are deleted by the inverting procedure. The nodes in the dual graph network are not shown.

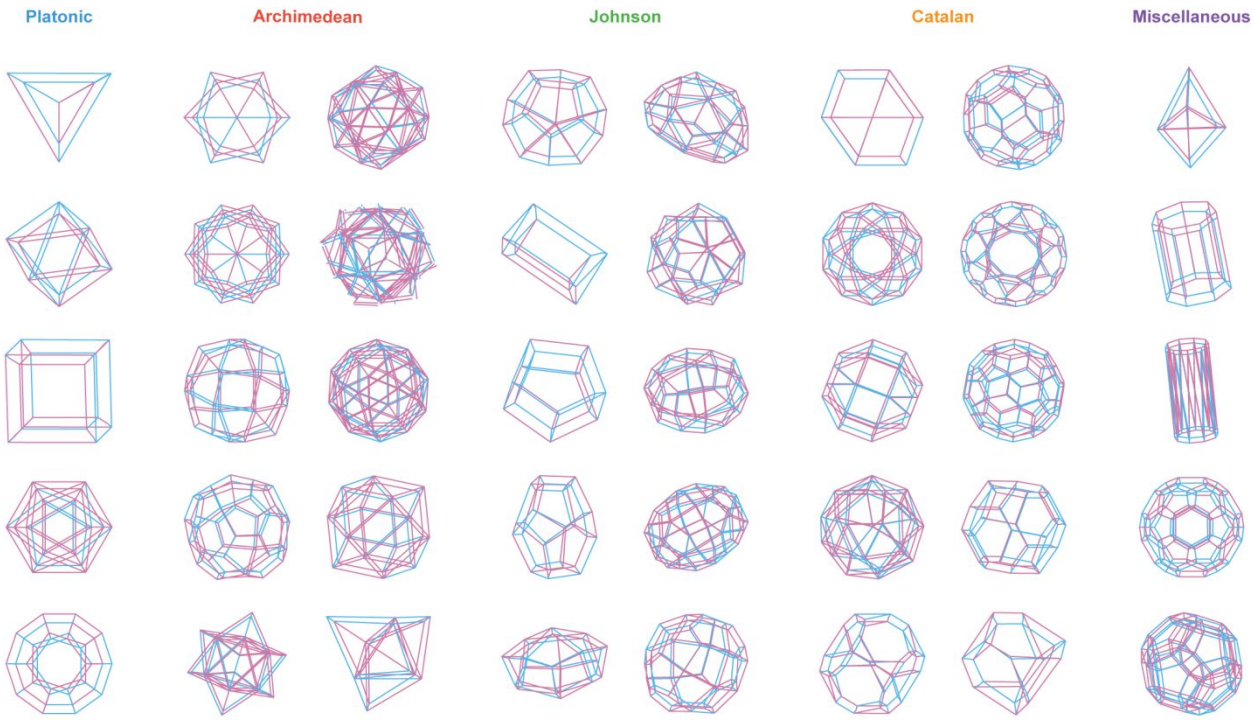

Figure S21. Spanning trees of the dual graph of the loop-crossover structure generated by the algorithm when the MV design is used. The spanning tree (sky blue) of each dual graph (reddish purple) of the loop-crossover structure defines the double crossovers to be retained by inverting into the loop-crossover structure. The double-crossovers associated with the remaining edges are deleted by the inverting procedure. The nodes in the dual graph network are not shown.

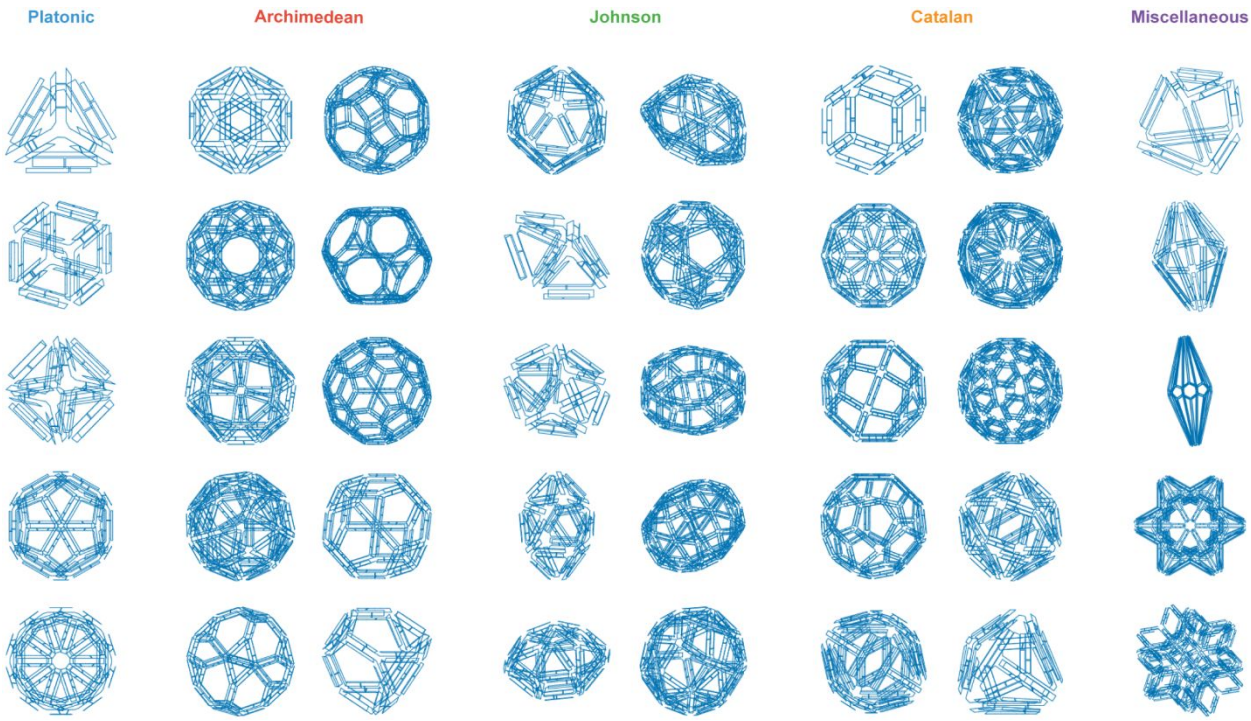

Figure S22. Scaffold-folding path of 40 diverse DNA-NPs generated by the algorithm when the FV design is used. The continuous blue loop is the single-stranded DNA scaffold routed throughout the entire DNA-NP of arbitrary shape.

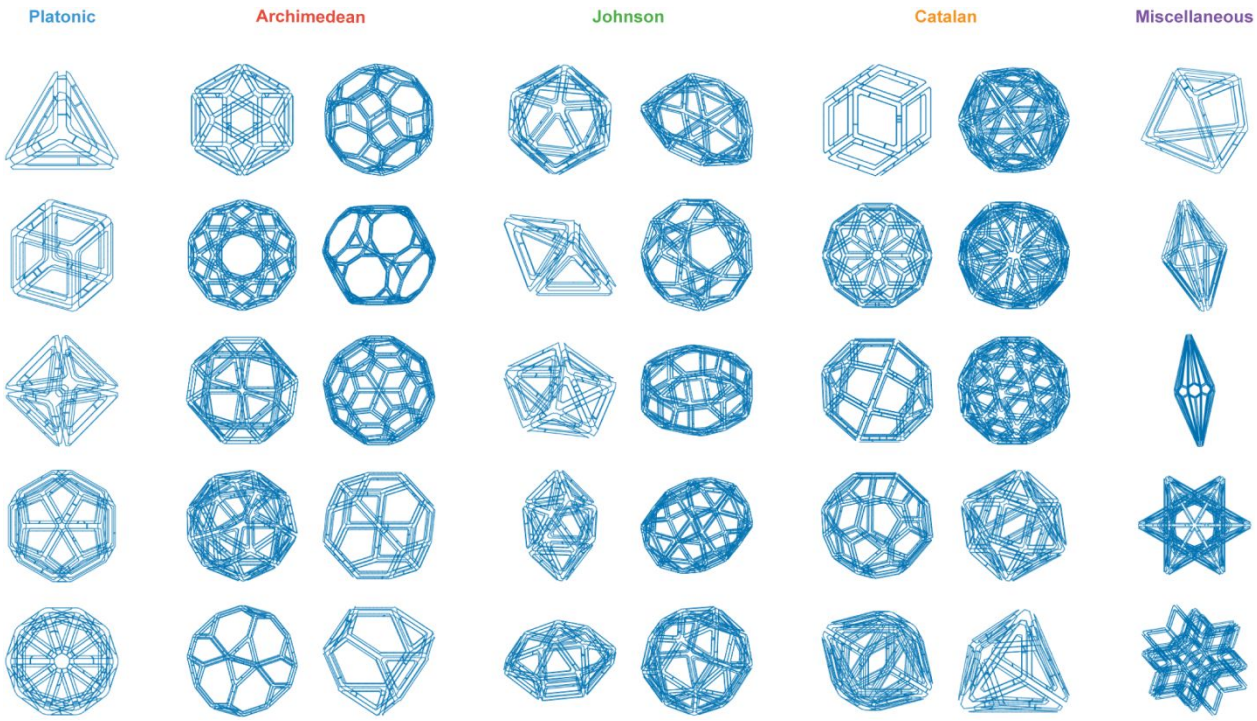

Figure S23. Scaffold-folding path of 40 diverse DNA-NPs generated by the algorithm when the MV design is used. The continuous blue loop is the single-stranded DNA scaffold routed throughout the entire DNA-NP of arbitrary shape.

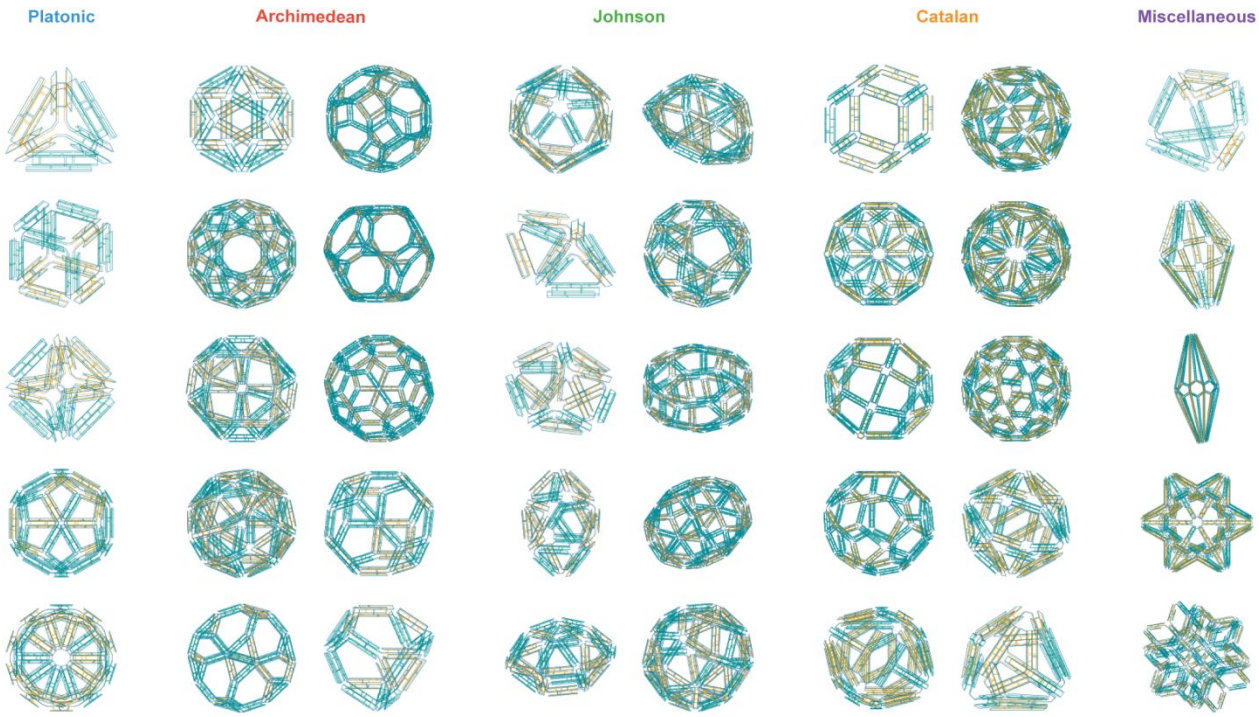

Figure S24. Staple and scaffold design path of 40 diverse DNA-NPs generated by the algorithm when the FV design is used. Complementary staples (green or orange) are wound in an antiparallel direction around the scaffold strand (blue) to assemble B-from double helices.

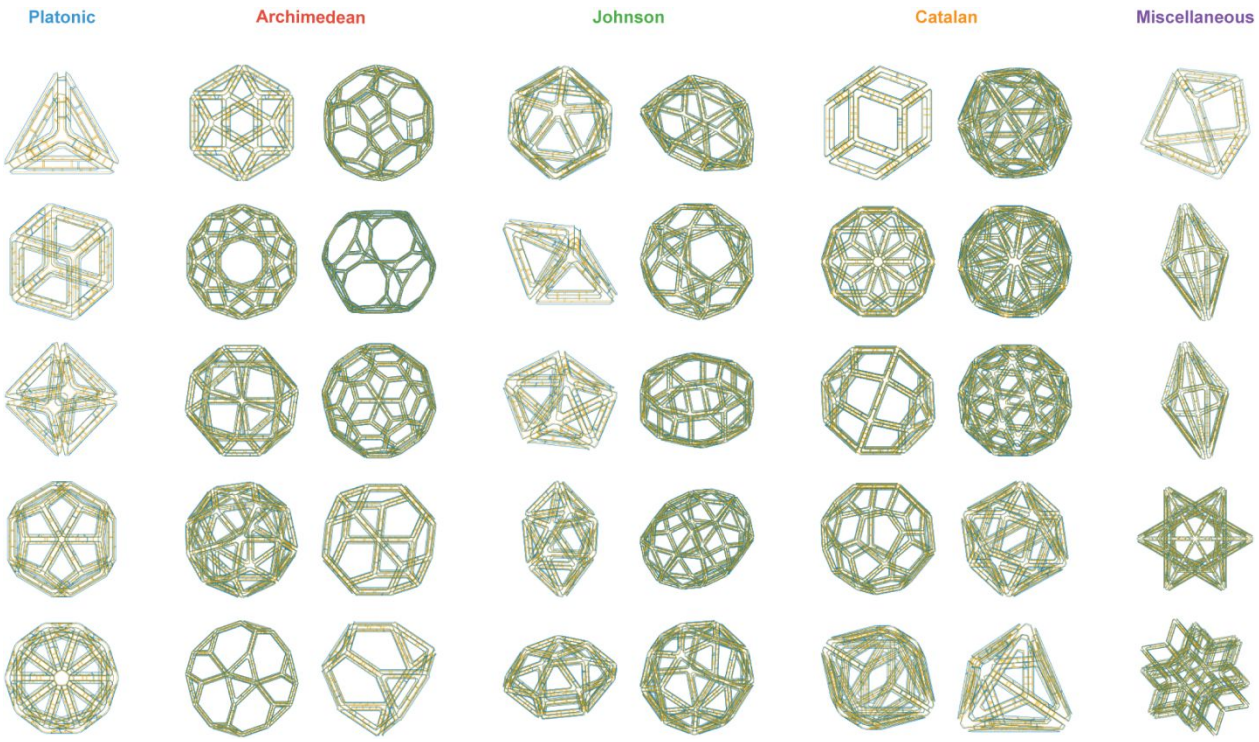

Figure S25. Staple and scaffold design path of 40 diverse DNA-NPs generated by the algorithm when the MV design is used. Complementary staples (orange) are wound in an antiparallel direction around the scaffold strand (blue) to assemble B-from double helices.

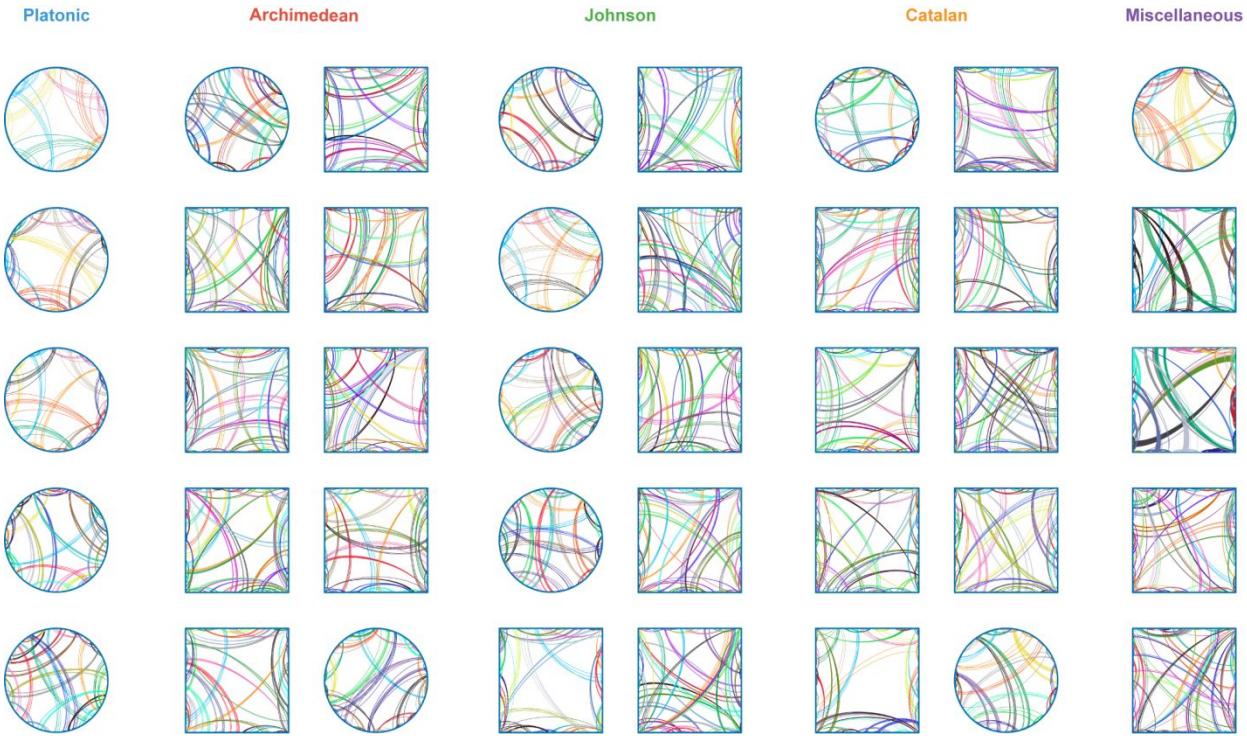

Figure S26. Circular maps of 40 diverse DNA-NPs generated by the algorithm when the FV design is used. DNA-NPs requiring scaffolds longer than 7,249-nt M13mp18 are represented by square maps.

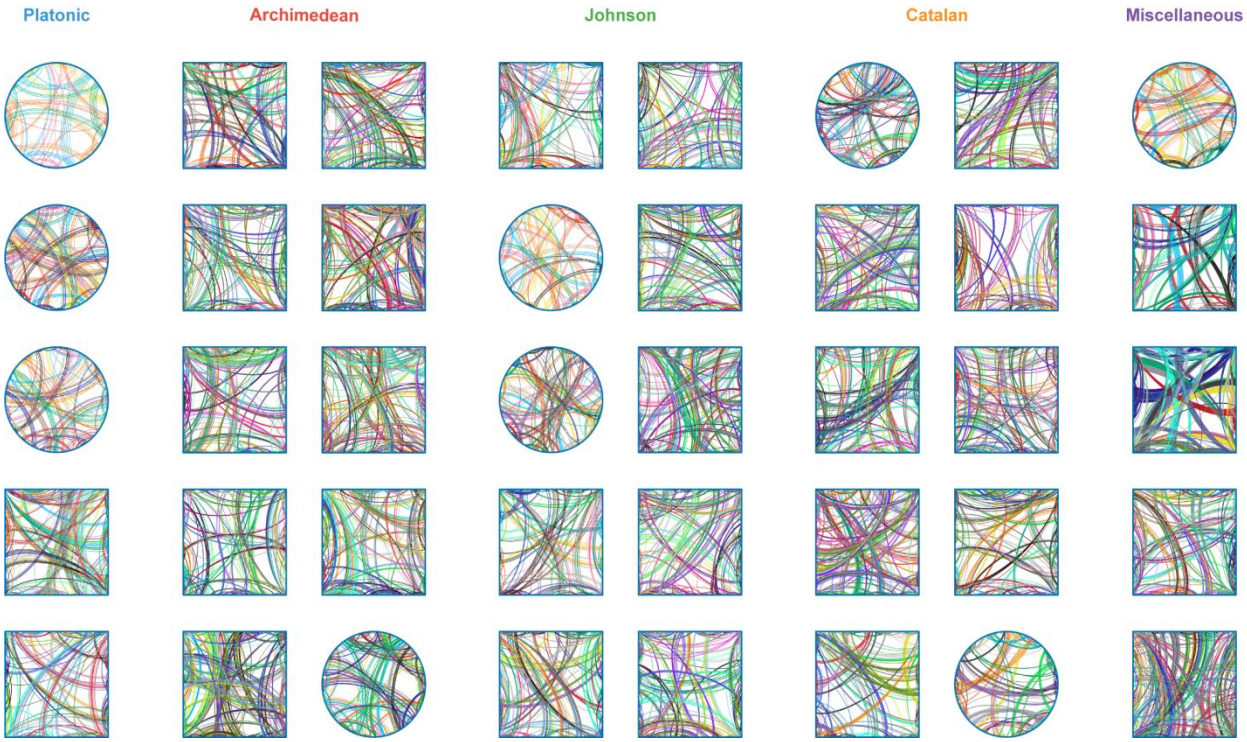

Figure S27. Circular maps of 40 diverse DNA-NPs generated by the algorithm when the MV design is used. DNA-NPs requiring scaffolds longer than 7,249-nt M13mp18 are represented by square maps.

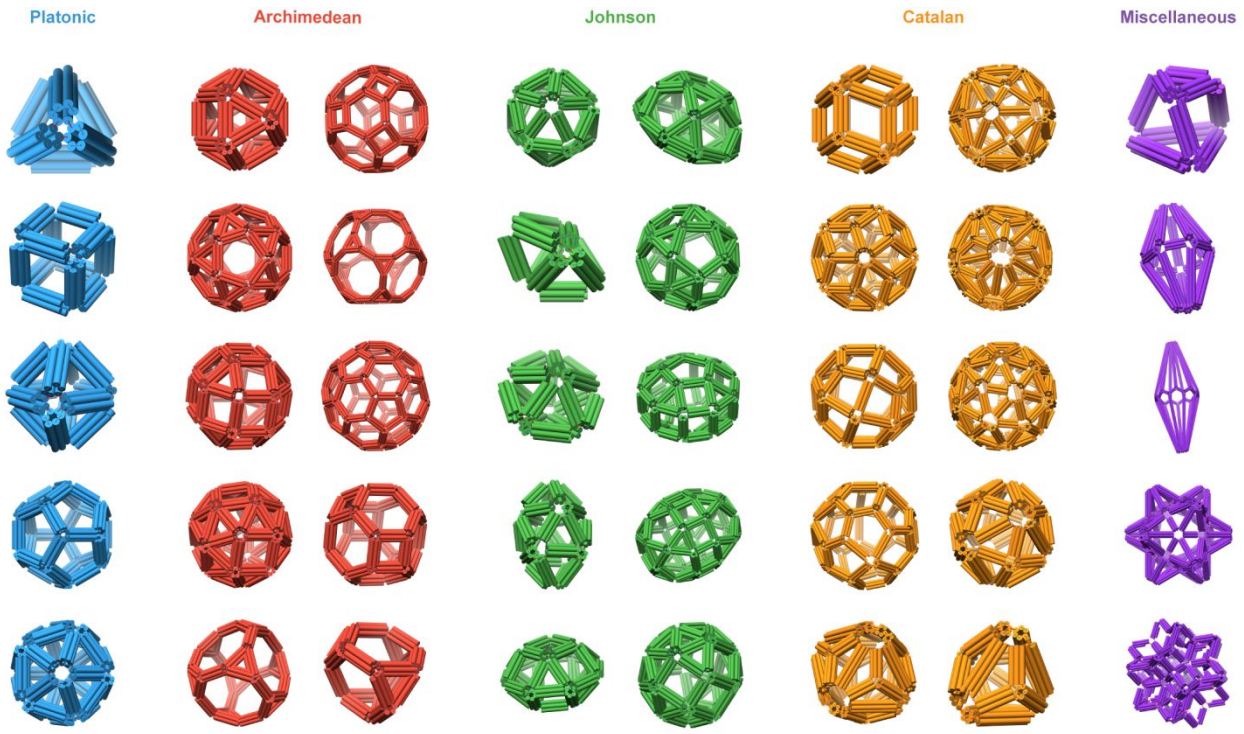

Figure S28. Cylindrical representation of 40 diverse FV DNA-NPs generated by the algorithm. Each cylinder whose diameter is 2 nm represents a DNA double helix.

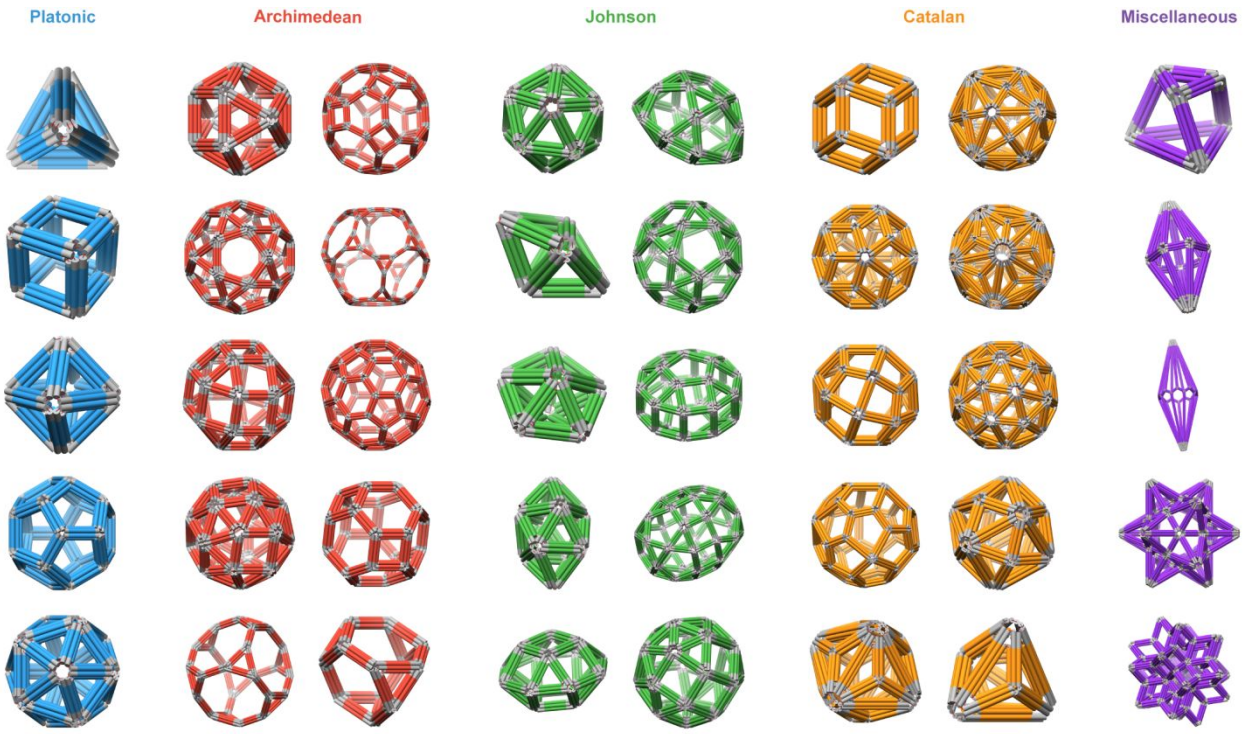

Figure S29. Cylindrical representation of 40 diverse MV DNA-NPs generated by the algorithm. Each cylinder whose diameter is 2 nm represents a DNA double helix.

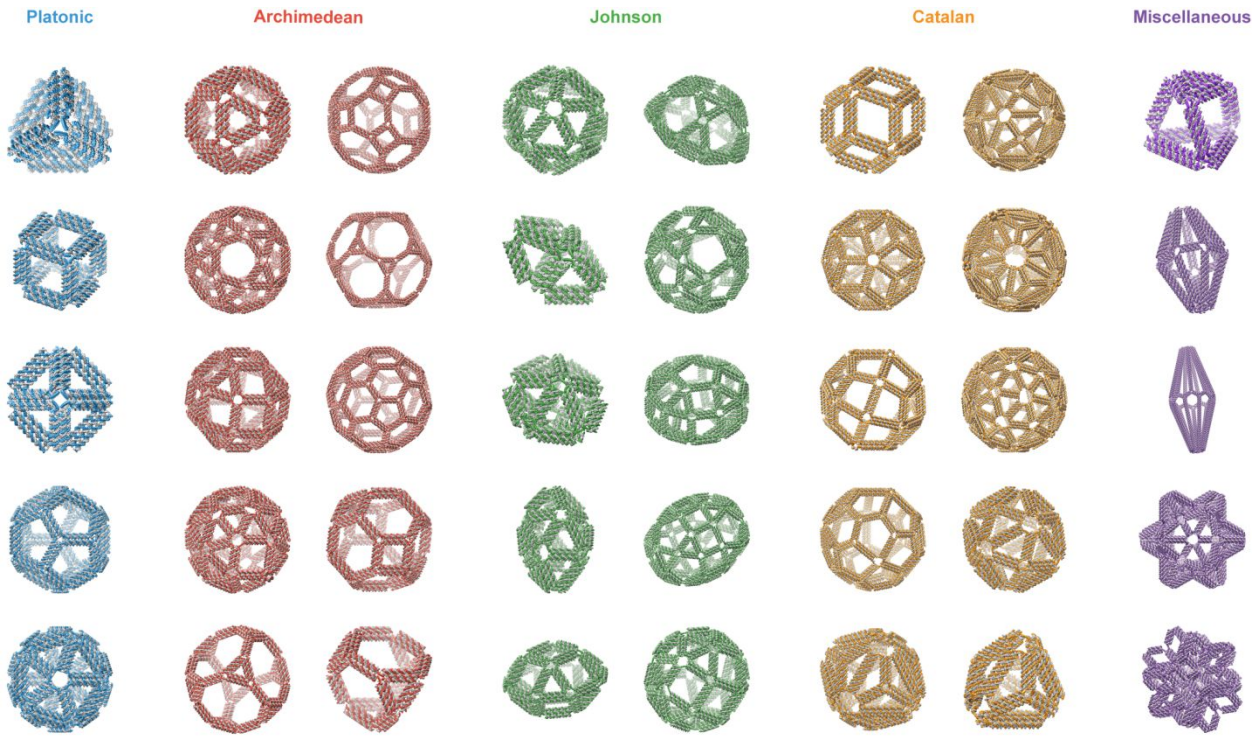

Figure S30. Atomic model of 40 diverse FV DNA-NPs generated by the algorithm.

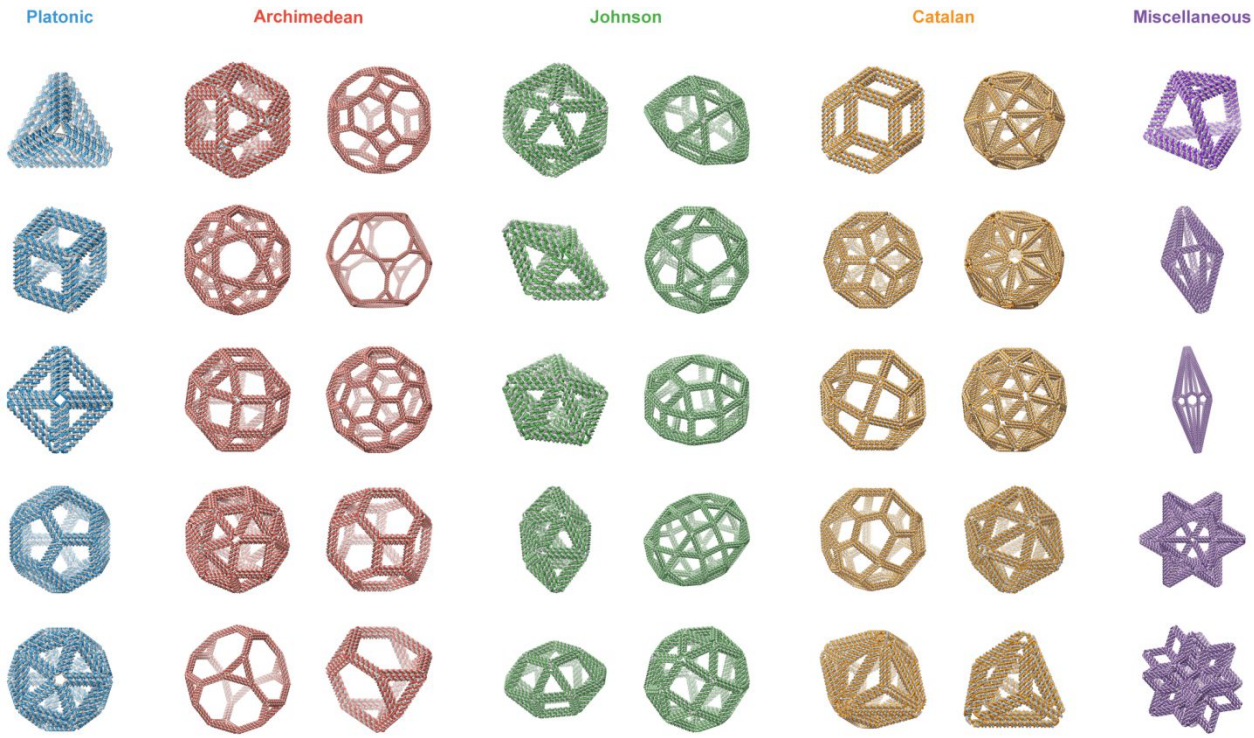

Figure S31. Atomic model of 40 diverse MV DNA-NPs generated by the algorithm.

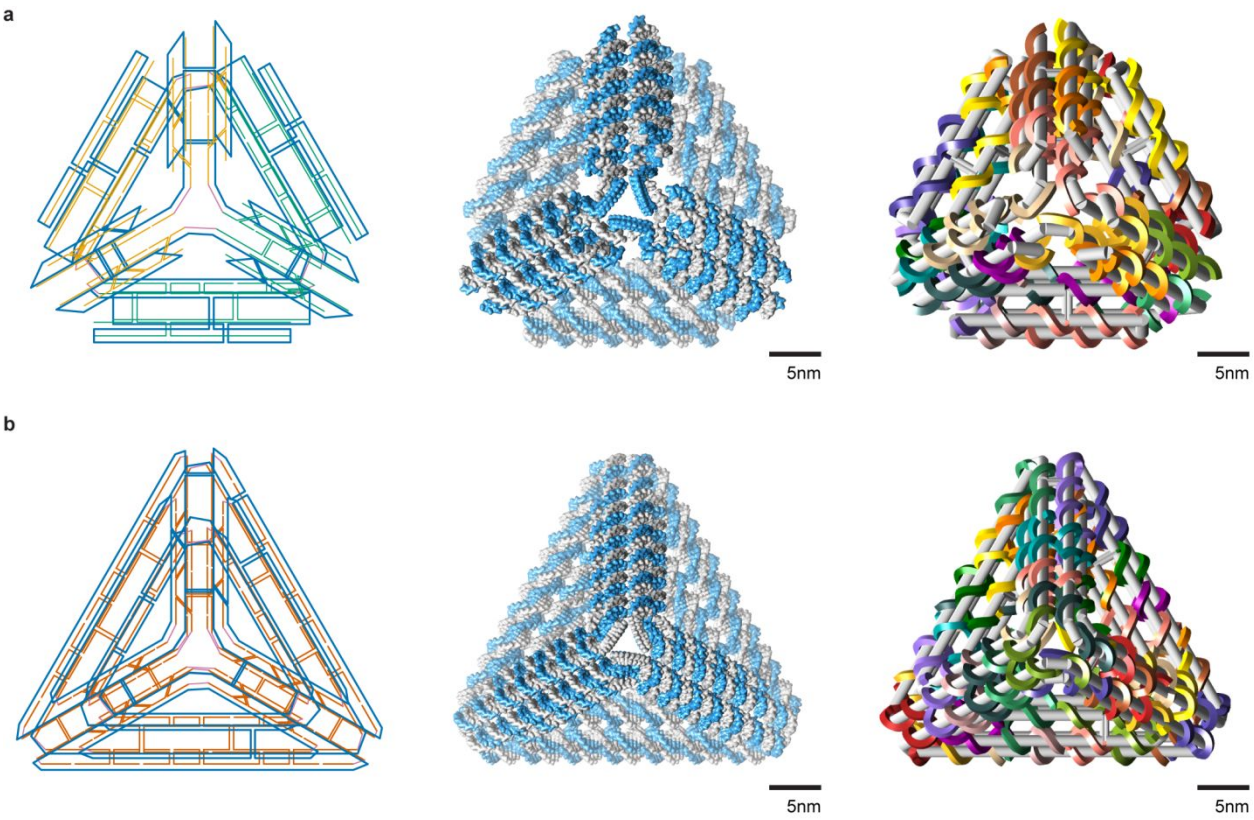

Figure S32. The staple and scaffold routing (left), atomic (middle) and cylindrical (right) model of the tetrahedron of 42-bp edge length. (**a**-**b**) The FV (**a**) and MV (**b**) tetrahedron of 42-bp edge length. In the cylindrical model, the scaffold and staples are represented by gray and multiple colors, respectively; See Table S5 for the required scaffold lengths and Table S6 and Table S7 for design parameters.

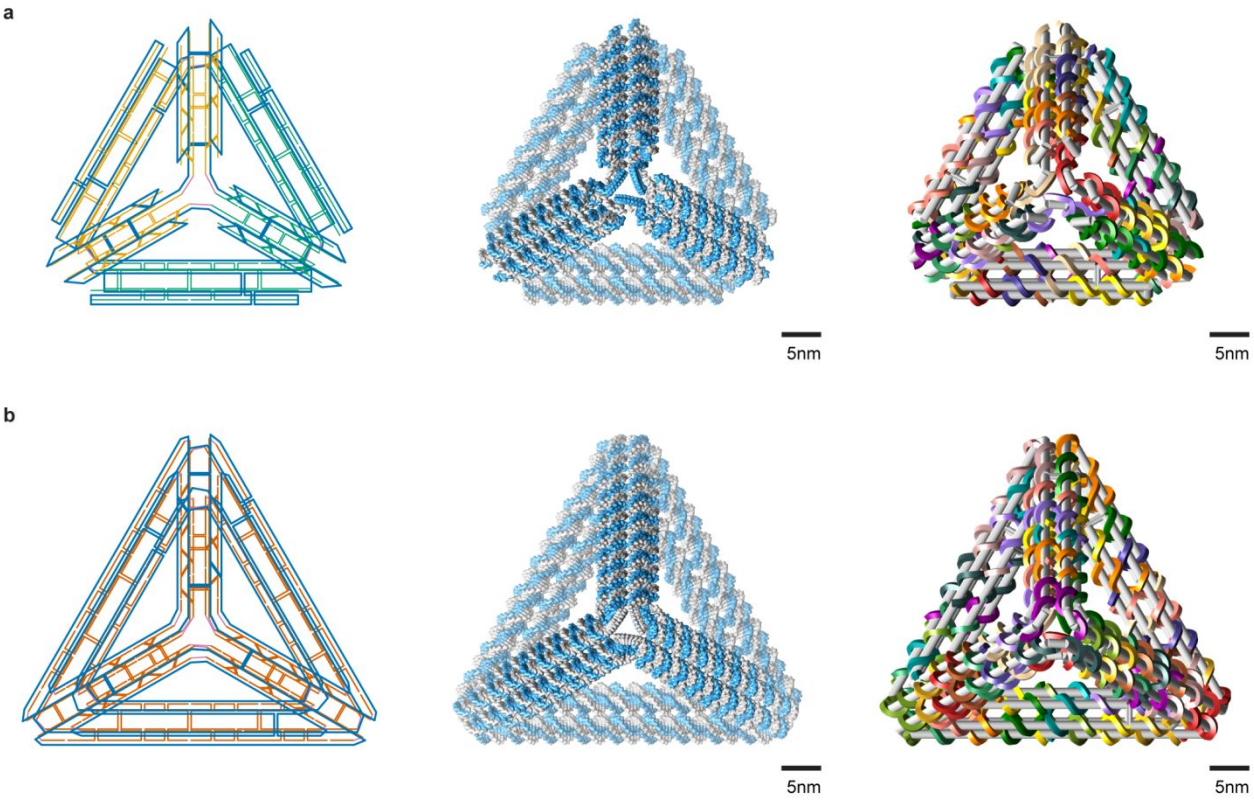

Figure S33. The staple and scaffold routing (left), atomic (middle) and cylindrical (right) model of the tetrahedron of 63-bp edge length . (**a-b**) The FV (**a**) and MV (**b**) tetrahedron of 63-bp edge length. In the cylindrical model, the scaffold and staples are represented by gray and multiple colors, respectively; See Table S5 for the required scaffold lengths and Table S6 and Table S7 for design parameters.

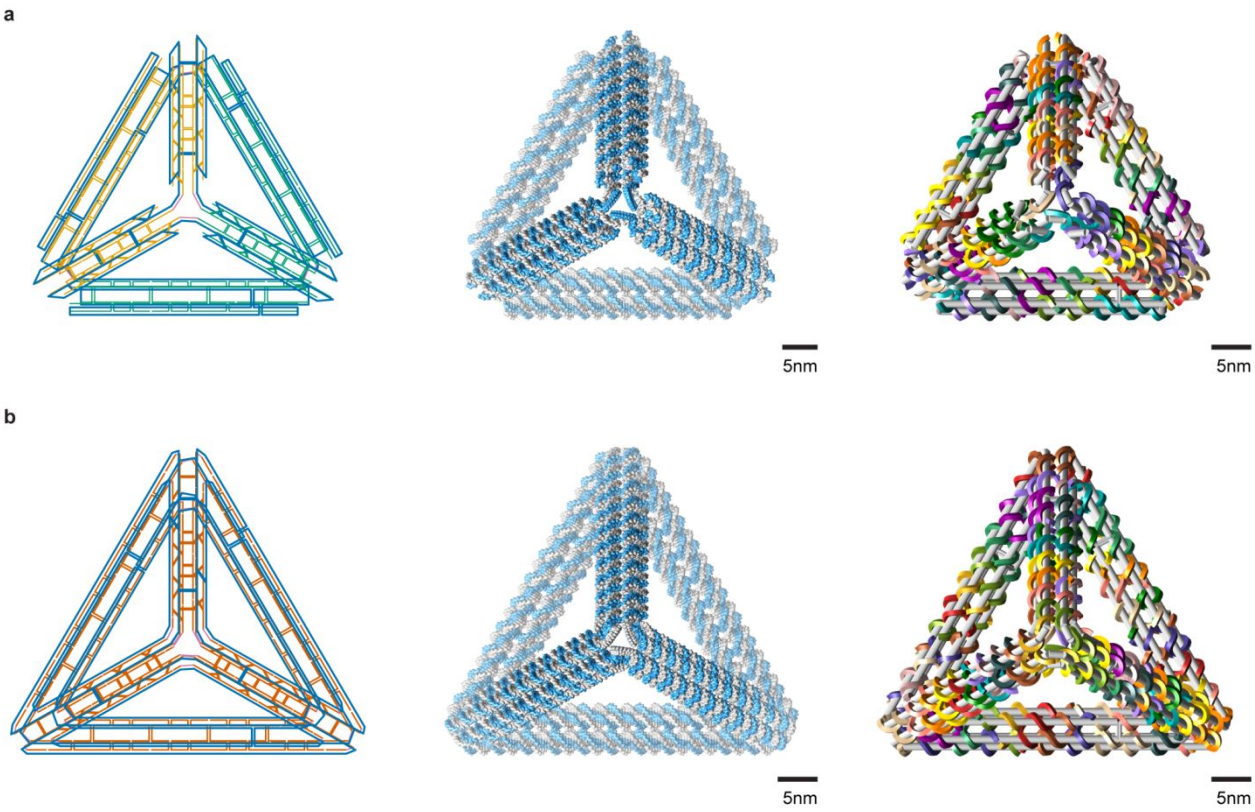

Figure S34. The staple and scaffold routing (left), atomic (middle) and cylindrical (right) model of the tetrahedron of 84-bp edge length. (**a**-**b**) The FV (**a**) and MV (**b**) tetrahedron of 84-bp edge length. In the cylindrical model, the scaffold and staples are represented by gray and multiple colors, respectively; See Table S5 for the required scaffold lengths and Table S6 and Table S7 for design parameters.

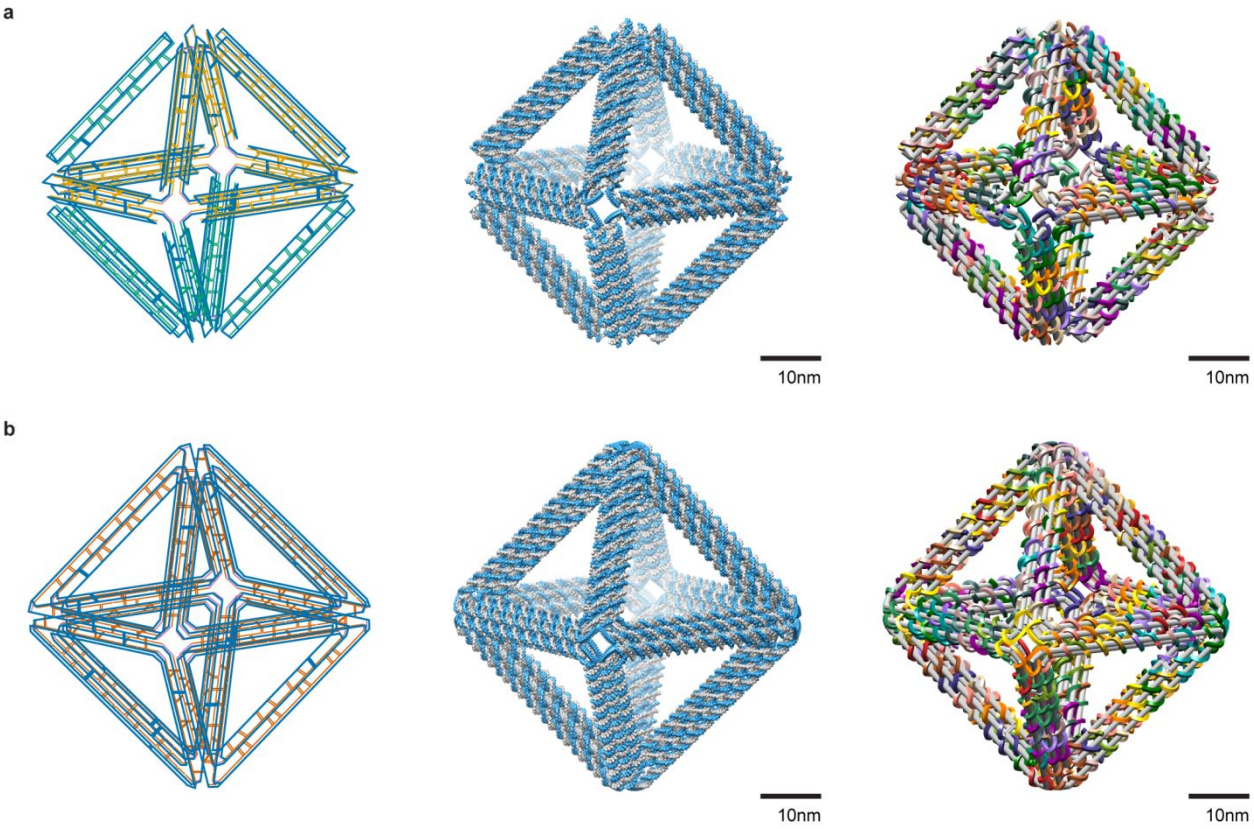

Figure S35. The staple and scaffold routing (left), atomic (middle) and cylindrical (right) model of the octahedron of 84-bp edge length. (**a**-**b**) The FV (**a**) and MV (**b**) tetrahedron of 84-bp edge length. In the cylindrical model, the scaffold and staples are represented by gray and multiple colors, respectively; See Table S5 for the required scaffold lengths and Table S6 and Table S7 for design parameters.

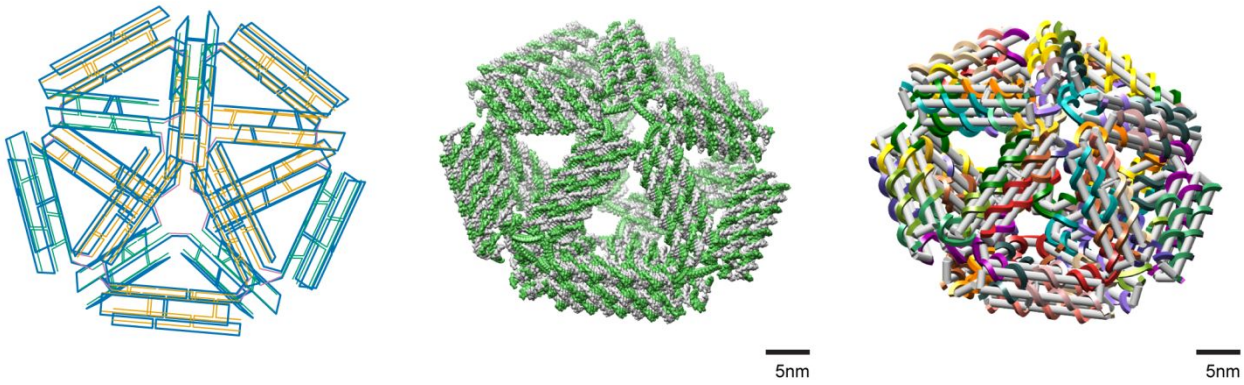

Figure S36. The staple and scaffold routing (left), atomic (middle) and cylindrical (right) model of the pentagonal bipyramid of 42-bp edge length. In the cylindrical model, the scaffold and staples are represented by gray and multiple colors, respectively; See Table S5 for the required scaffold lengths and Table S6 and Table S7 for design parameters.

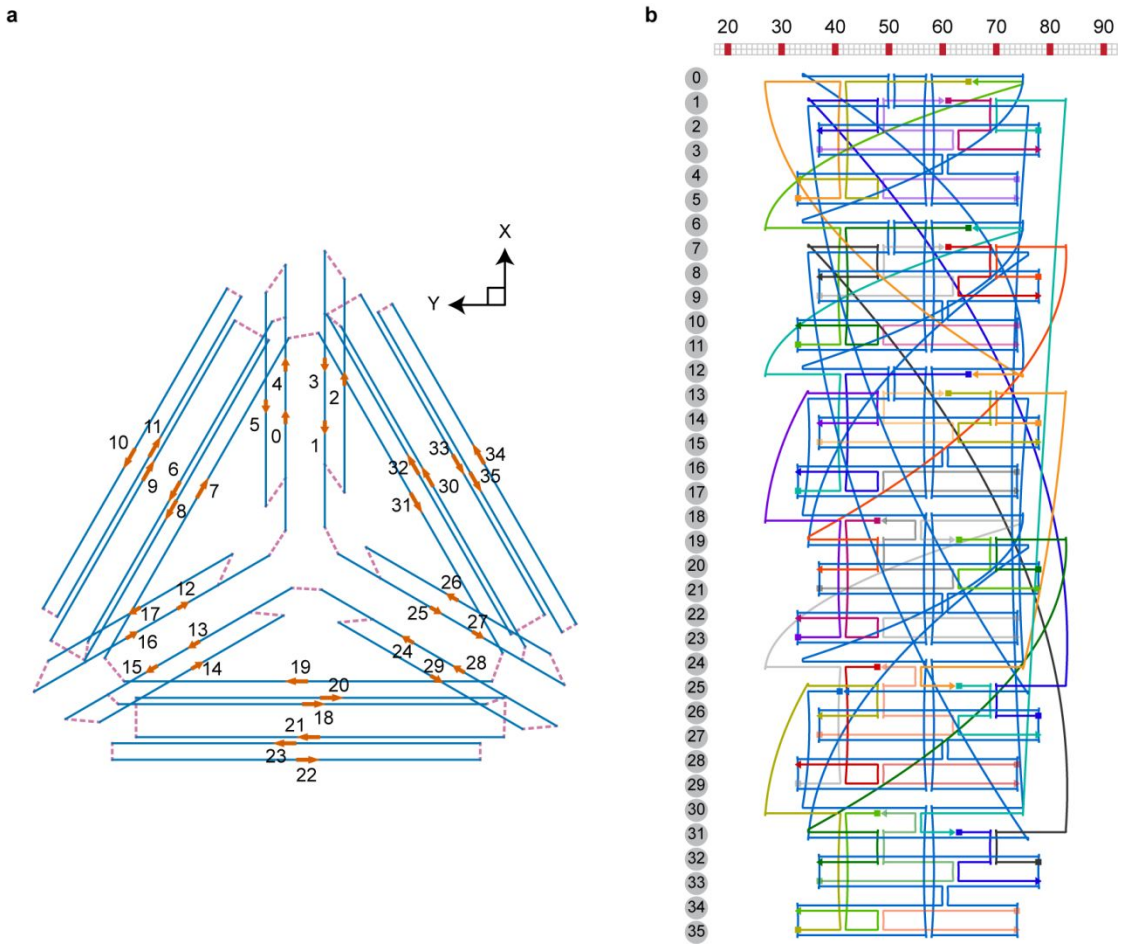

Figure S37. JSON caDNAno for the FV tetrahedron of 42-bp edge length. (**a-b**) Scaffold routing model (**a**) and staple oligonucleotide strand and scaffold organization (**b**) from caDNAno. The numbers in the scaffold routing model are associated with the cross-section number in caDNAno.

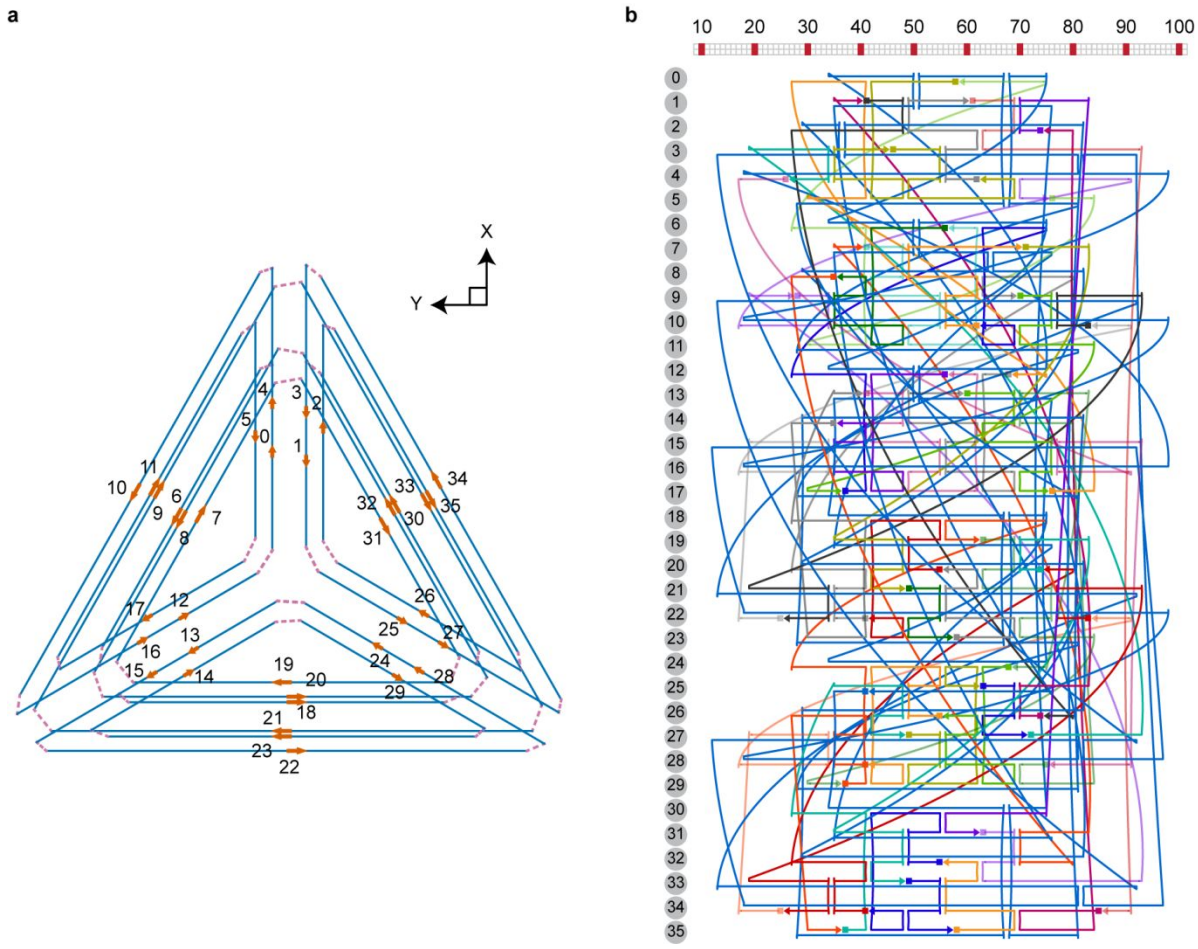

Figure S38. JSON caDNAno for the MV tetrahedron of 42-bp edge length. (**a-b**) Scaffold routing model (**a**) and staple oligonucleotide strand and scaffold organization (**b**) from caDNAno. The numbers in the scaffold routing model are associated with the cross-section number in caDNAno.

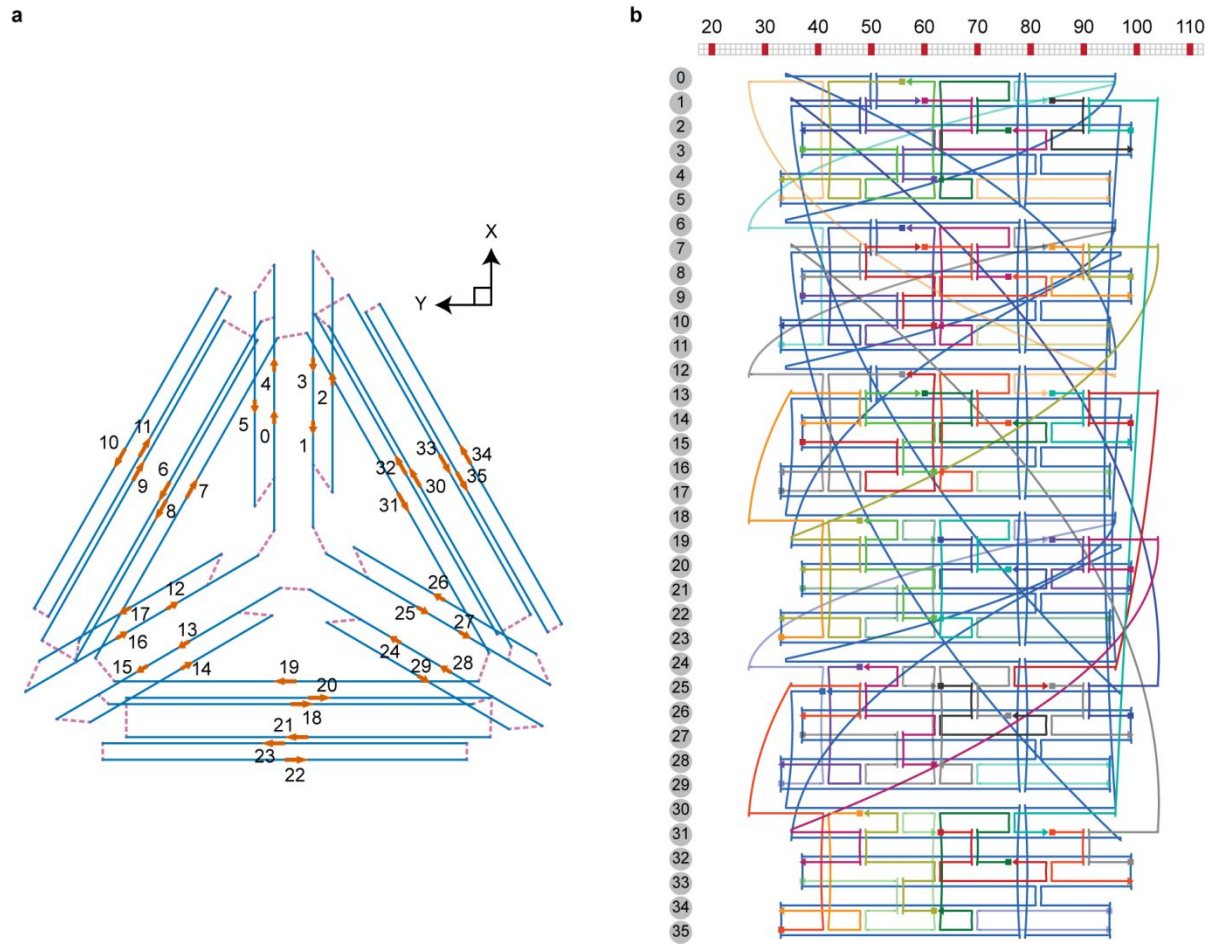

Figure S39. JSON caDNAno for the FV tetrahedron of 63-bp edge length. (**a-b**) Scaffold routing model (**a**) and staple oligonucleotide strand and scaffold organization (**b**) from caDNAno. The numbers in the scaffold routing model are associated with the cross-section number in caDNAno.

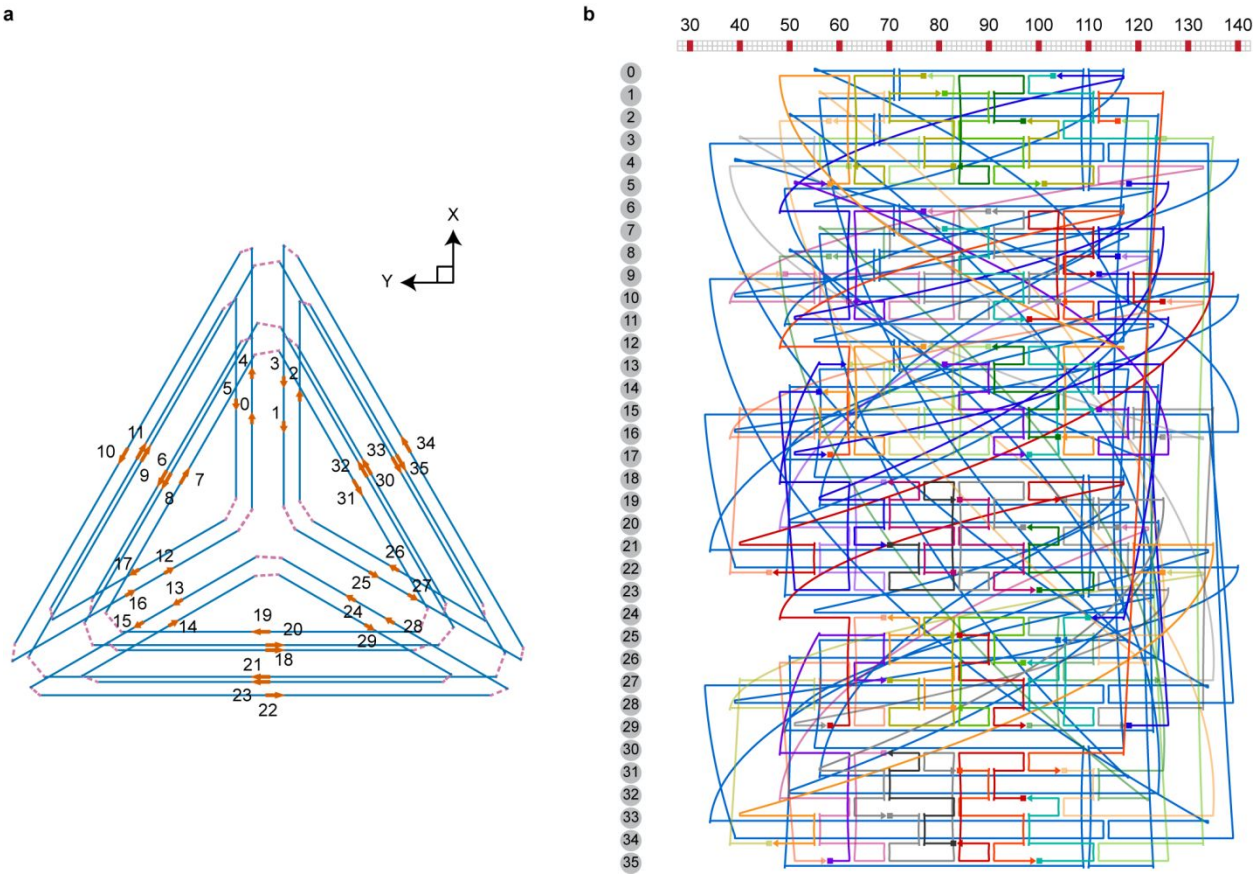

Figure S40. JSON caDNAno for the MV tetrahedron of 63-bp edge length. (**a-b**) Scaffold routing model (**a**) and staple oligonucleotide strand and scaffold organization (**b**) from caDNAno. The numbers in the scaffold routing model are associated with the cross-section number in caDNAno.

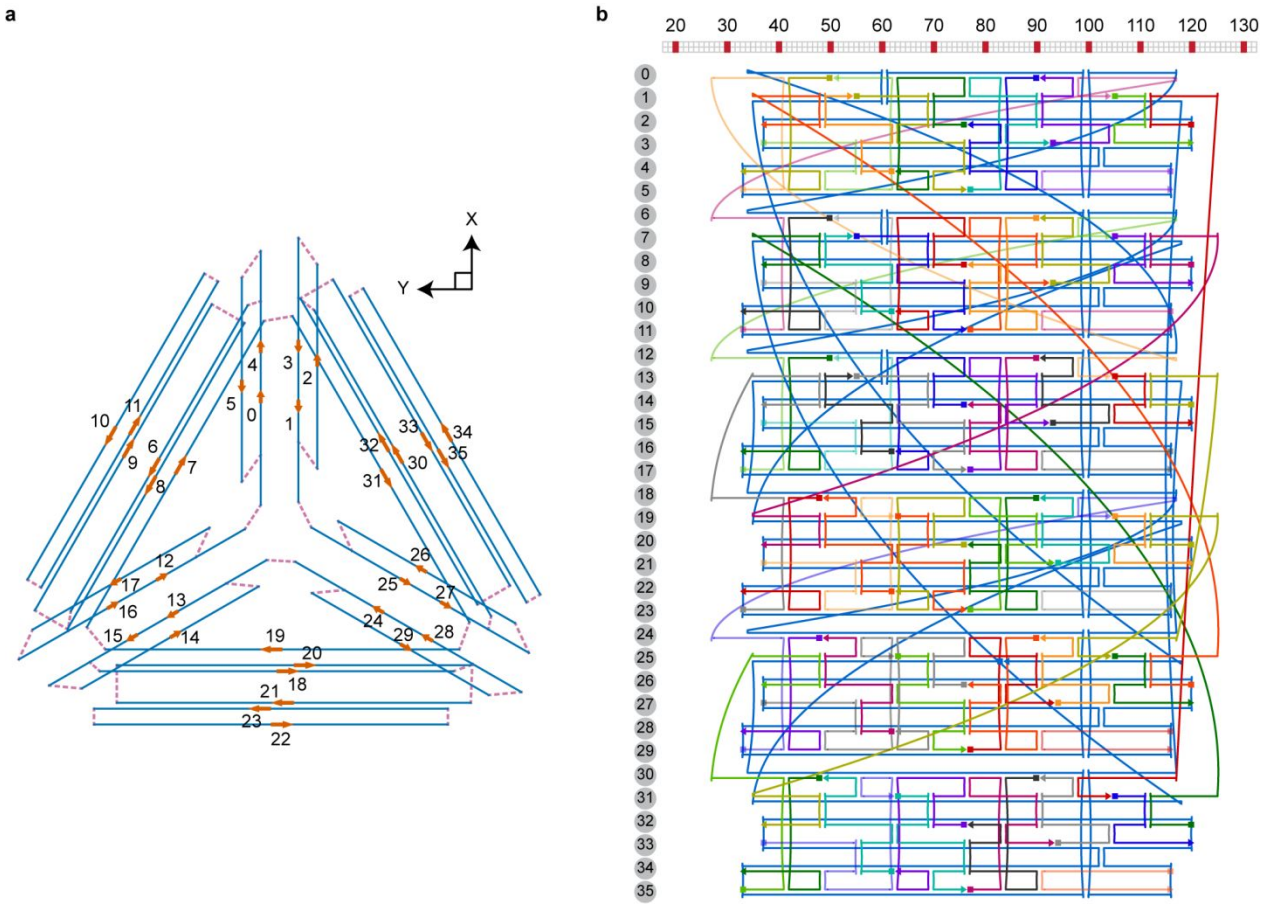

Figure S41. JSON caDNAno for the FV tetrahedron of 84-bp edge length. (**a-b**) Scaffold routing model (**a**) and staple oligonucleotide strand and scaffold organization (**b**) from caDNAno. The numbers in the scaffold routing model are associated with the cross-section number in caDNAno.

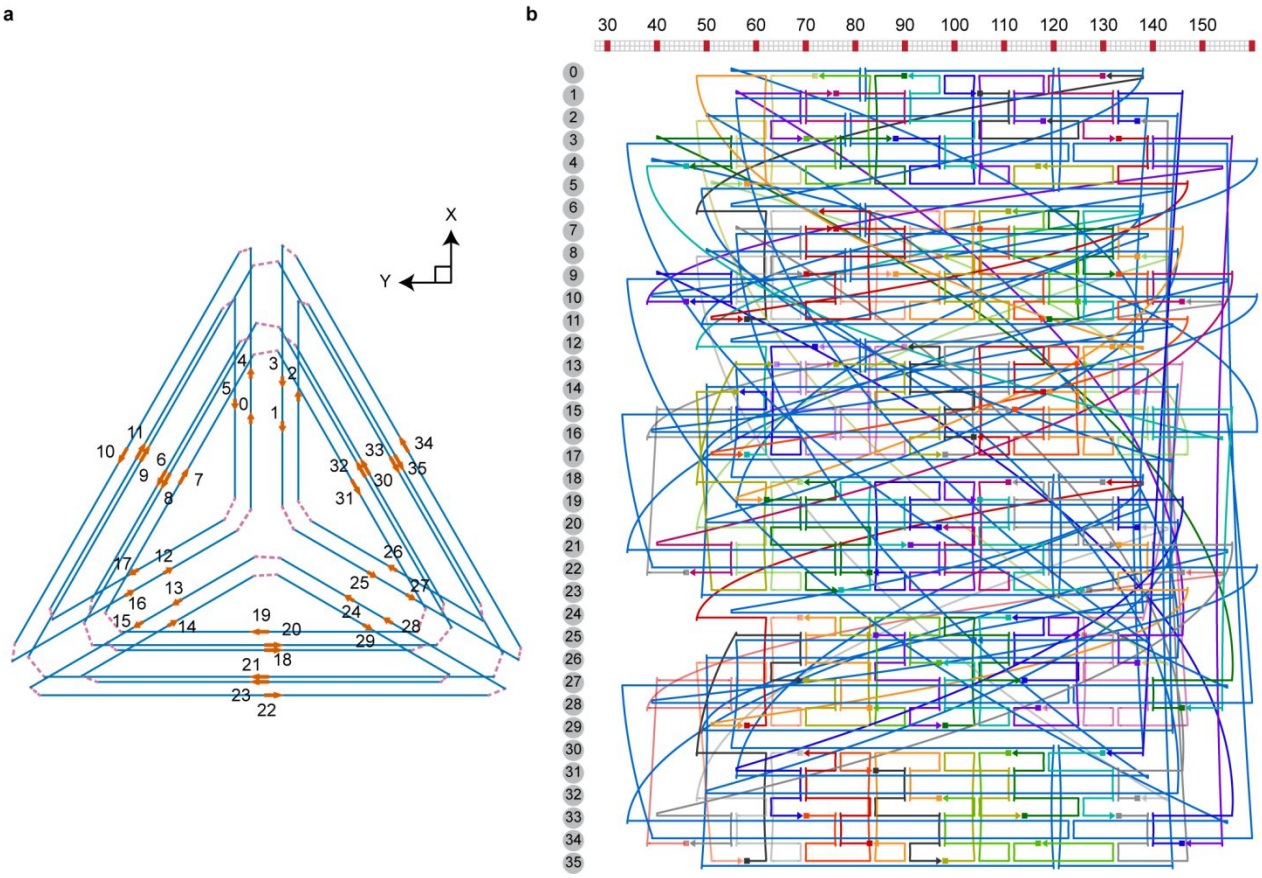

Figure S42. JSON caDNAno for the MV tetrahedron of 84-bp edge length. (**a-b**) Scaffold routing model (**a**) and staple oligonucleotide strand and scaffold organization (**b**) from caDNAno. The numbers in the scaffold routing model are associated with the cross-section number in caDNAno.

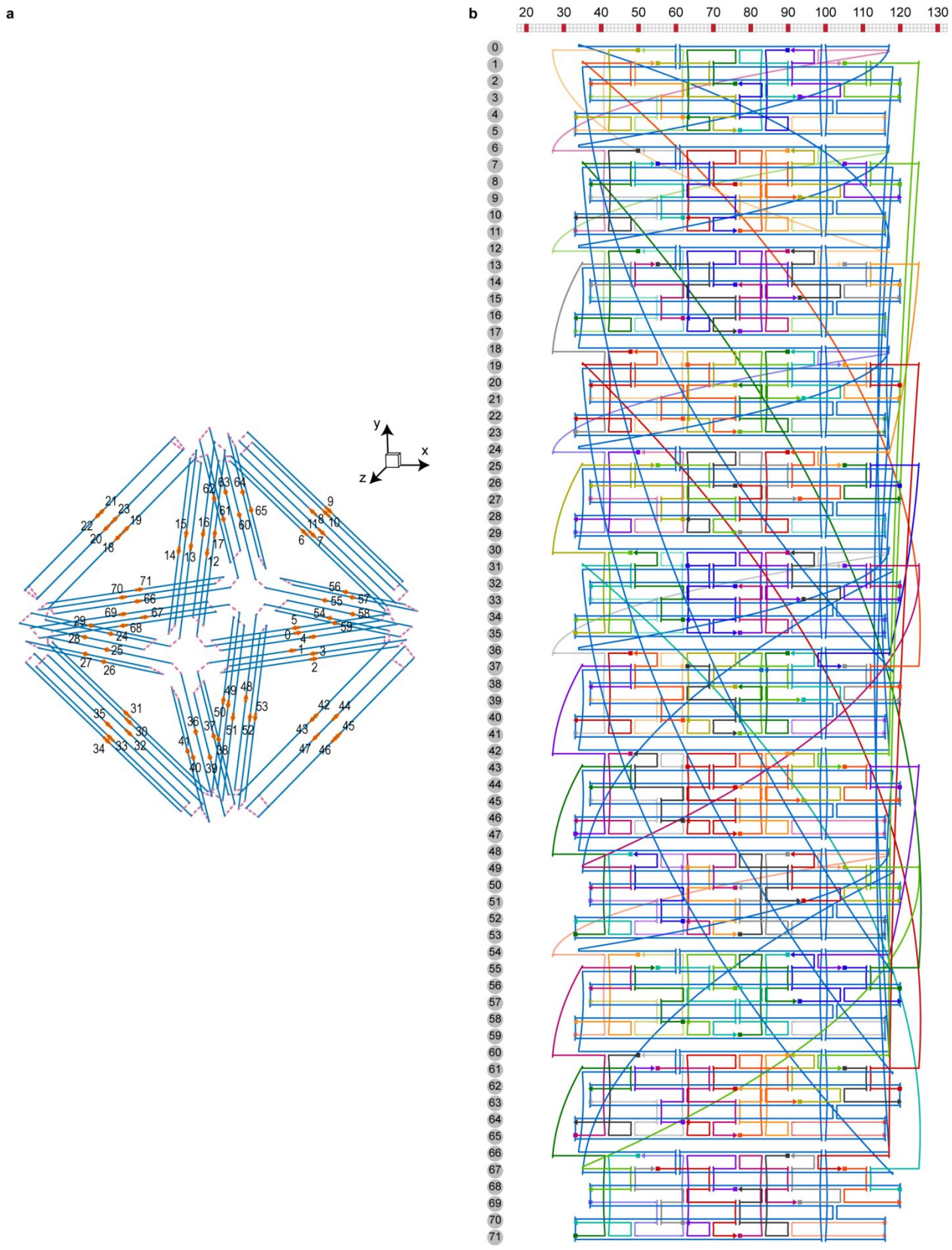
a
b
20 30 40 50 60 70 80 90 100 110 120 130
0 1 2 3 4 5 6 7 8 9 10 11 12 13 14 15 16 17 18 19 20 21 22 23 24 25 26 27 28 29 30 31 32 33 34 35 36 37 38 39 40 41 42 43 44 45 46 47 48 49 50 51 52 53 54 55 56 57 58 59 60 61 62 63 64 65 66 67 68 69 70 71
y
x
z

Figure S43. JSON caDNAno for the FV octahedron of 84-bp edge length. (**a-b**) Scaffold routing model (**a**) and staple oligonucleotide strand and scaffold organization (**b**) from caDNAno. The numbers in the scaffold routing model are associated with the cross-section number in caDNAno.

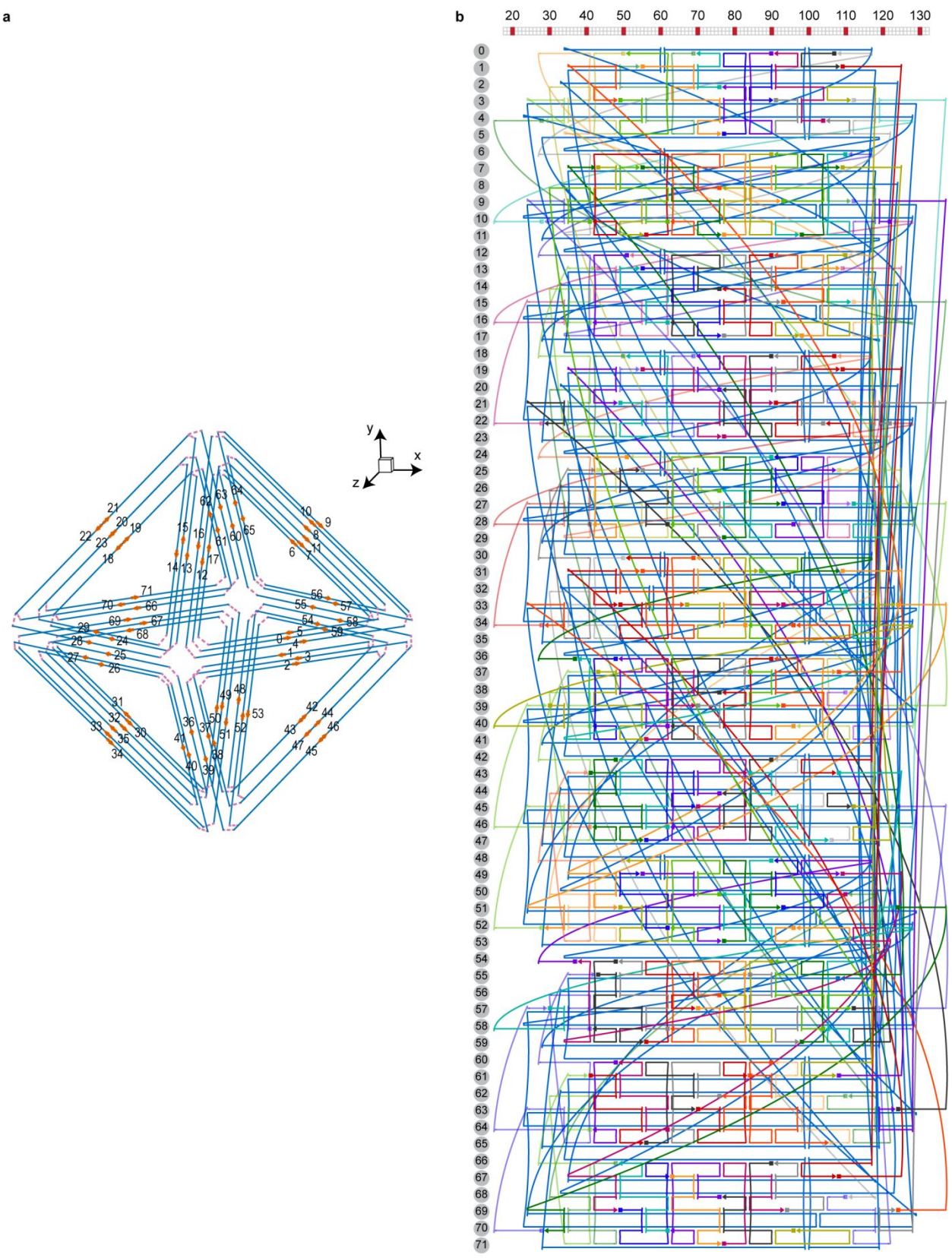
a
b
y
x
z
20 30 40 50 60 70 80 90 100 110 120 130
0 1 2 3 4 5 6 7 8 9 10 11 12 13 14 15 16 17 18 19 20 21 22 23 24 25 26 27 28 29 30 31 32 33 34 35 36 37 38 39 40 41 42 43 44 45 46 47 48 49 50 51 52 53 54 55 56 57 58 59 60 61 62 63 64 65 66 67 68 69 70 71

Figure S44. JSON caDNAno for the MV octahedron of 84-bp edge length. (**a-b**) Scaffold routing model (**a**) and staple oligonucleotide strand and scaffold organization (**b**) from caDNAno. The numbers in the scaffold routing model are associated with the cross-section number in caDNAno.

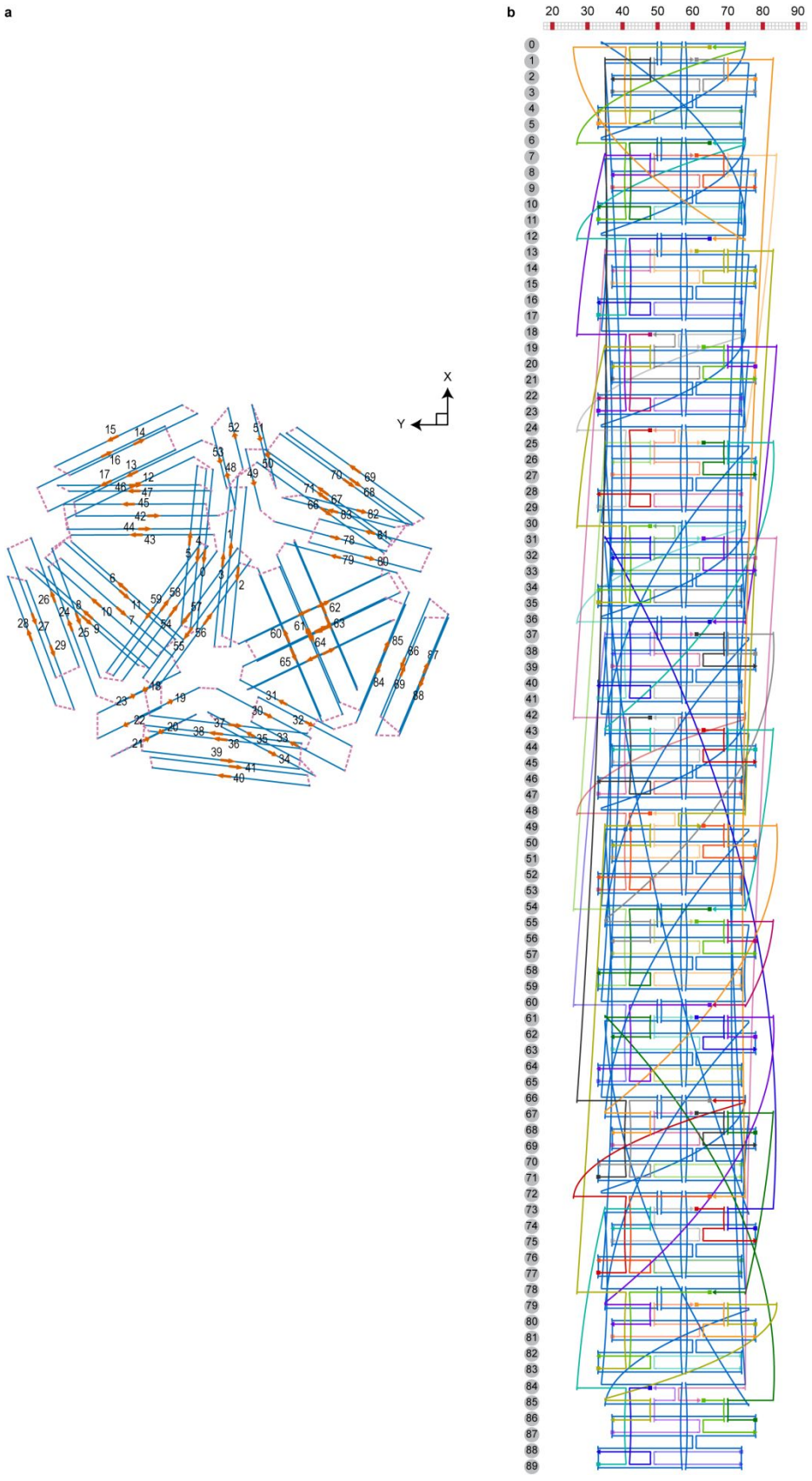
a
b
X
Y
20
30
40
50
60
70
80
90

Figure S45. JSON caDNAno for the FV pentagonal bipyramid of 42-bp edge length. (**a-b**) Scaffold routing model (**a**) and staple oligonucleotide strand and scaffold organization (**b**) from caDNAno. The numbers in the scaffold routing model are associated with the cross-section number in caDNAno.

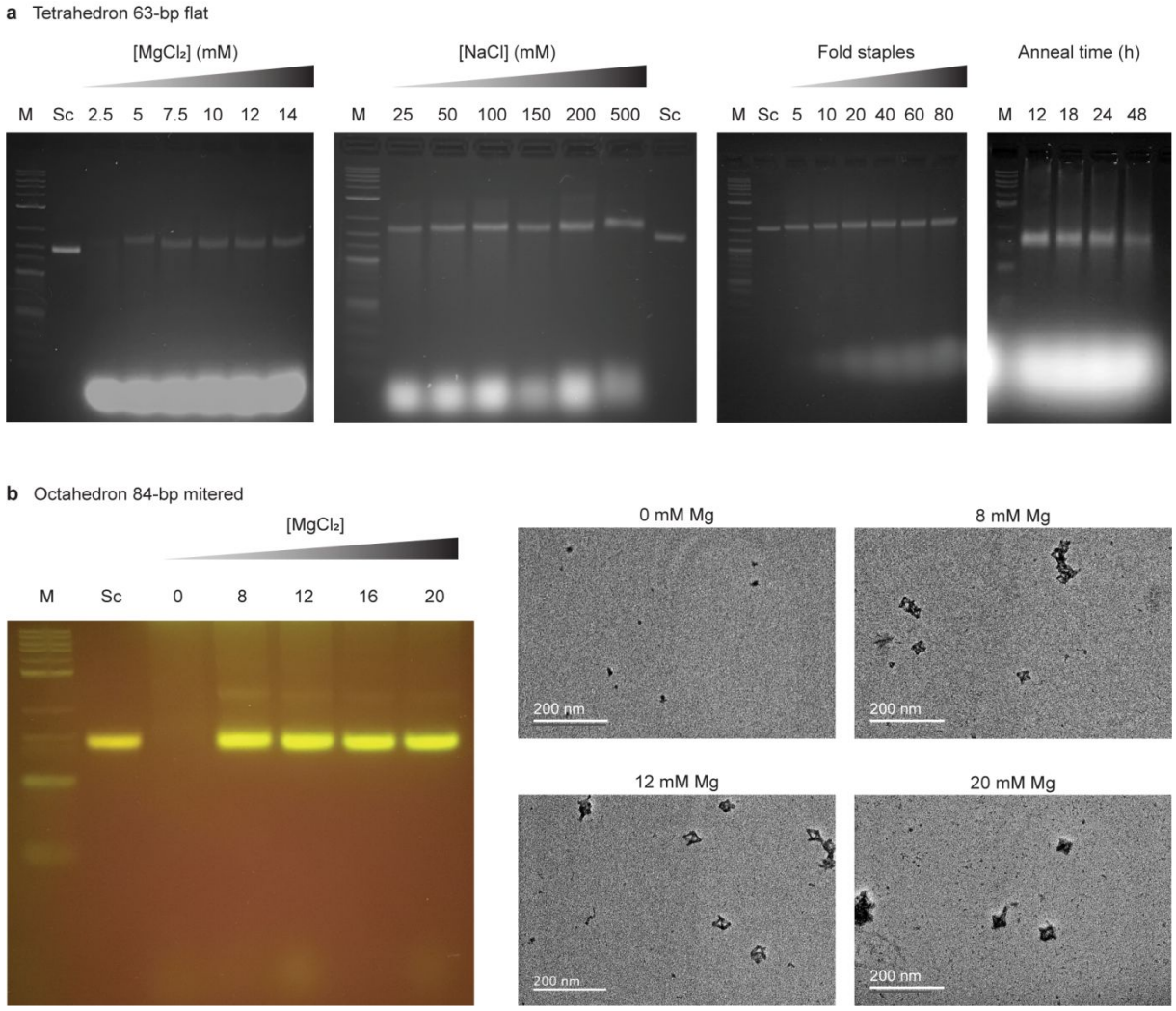

Figure S46. Optimized folding of 6HB DNA-NPs. (**a**) DNA-NP folding were assayed across $MgCl_2$, NaCl, and staple concentrations, and annealing time, prototyped with the FV tetrahedron of 63-bp edge length. (**b**) DNA-NP folding were further assayed by visualizing using electron microscopy, with particles beginning to form in 8 mM $MgCl_2$.

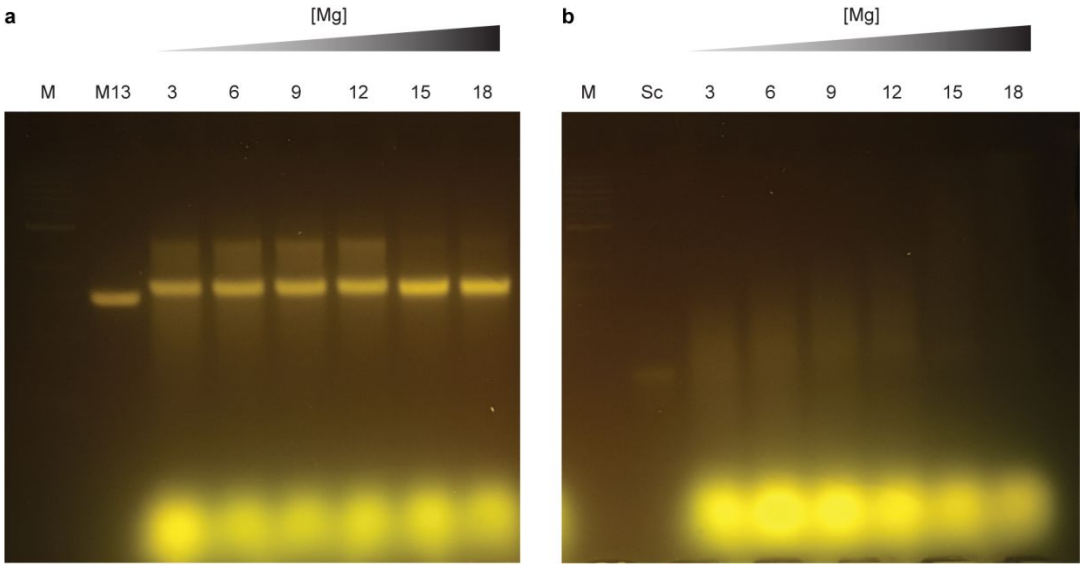

Figure S47. Single strand full-length M13 vs. asymmetric-PCR-produced scaffold. (**a**) Single-stranded M13 genomic DNA used to fold a MV tetrahedron of 42-bp edge length with increasing concentrations of $MgCl_2$ (mM). (**b**) Linear, single-stranded DNA amplified from the same region of the M13 that folds to the tetrahedron. Annealing the object under the same conditions did not result in a well-folded object.

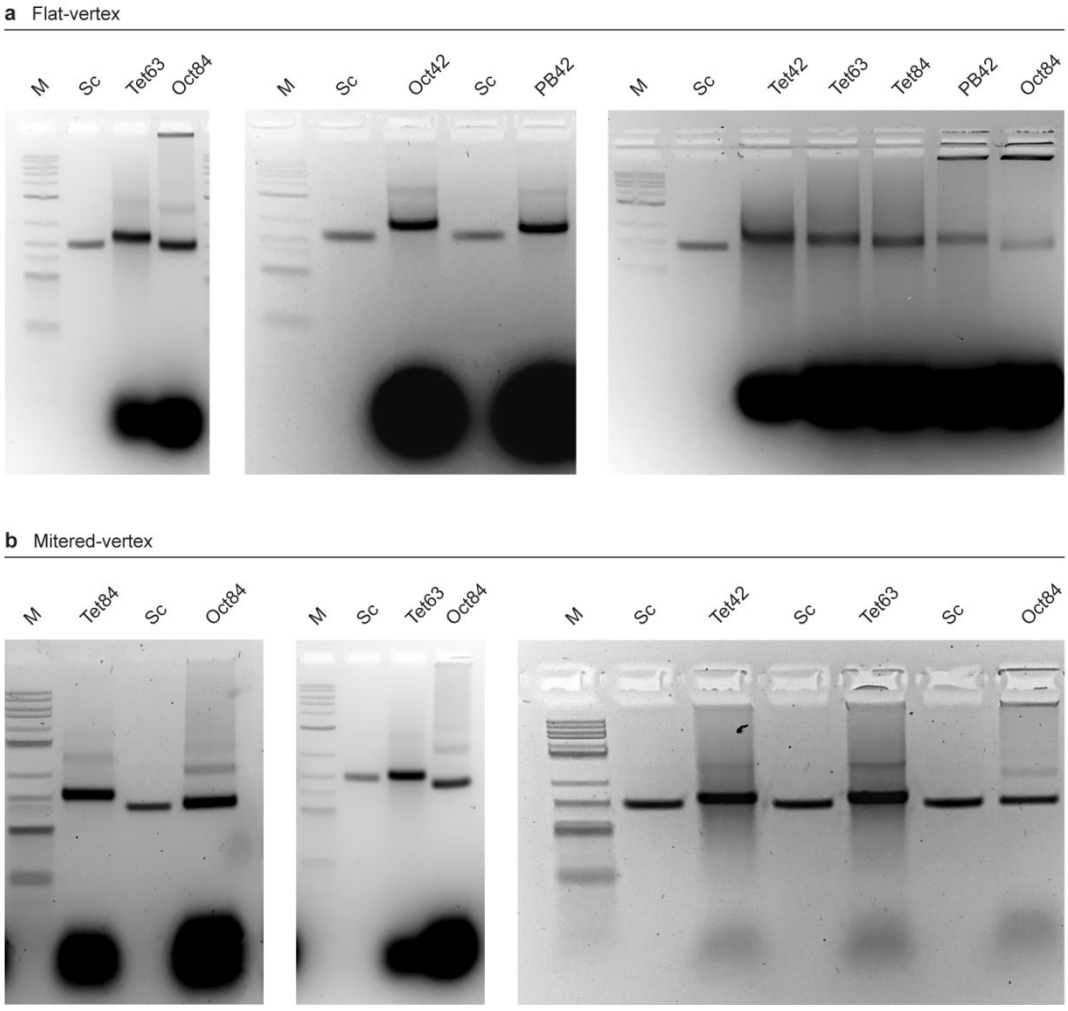

Figure S48. Agarose gels of FV and MV DNA-NPs. (**a**) FV type nanoparticles were folded and ran on a 2% agarose gel in Mg-containing buffer and compared against M13 ssDNA scaffold. (**b**) MV type nanoparticles were folded and ran on a 2% agarose gel in Mg-containing buffer and compared against M13 ssDNA scaffold. M: Marker (2-log ladder, NEB); Sc: genomic M13mp18 ssDNA (NEB); Tet: tetrahedron; Oct: octahedron; PB: pentagonal bipyramid; 42: 42-bp edge length, 63: 63-bp edge length; 84: 84-bp edge length.

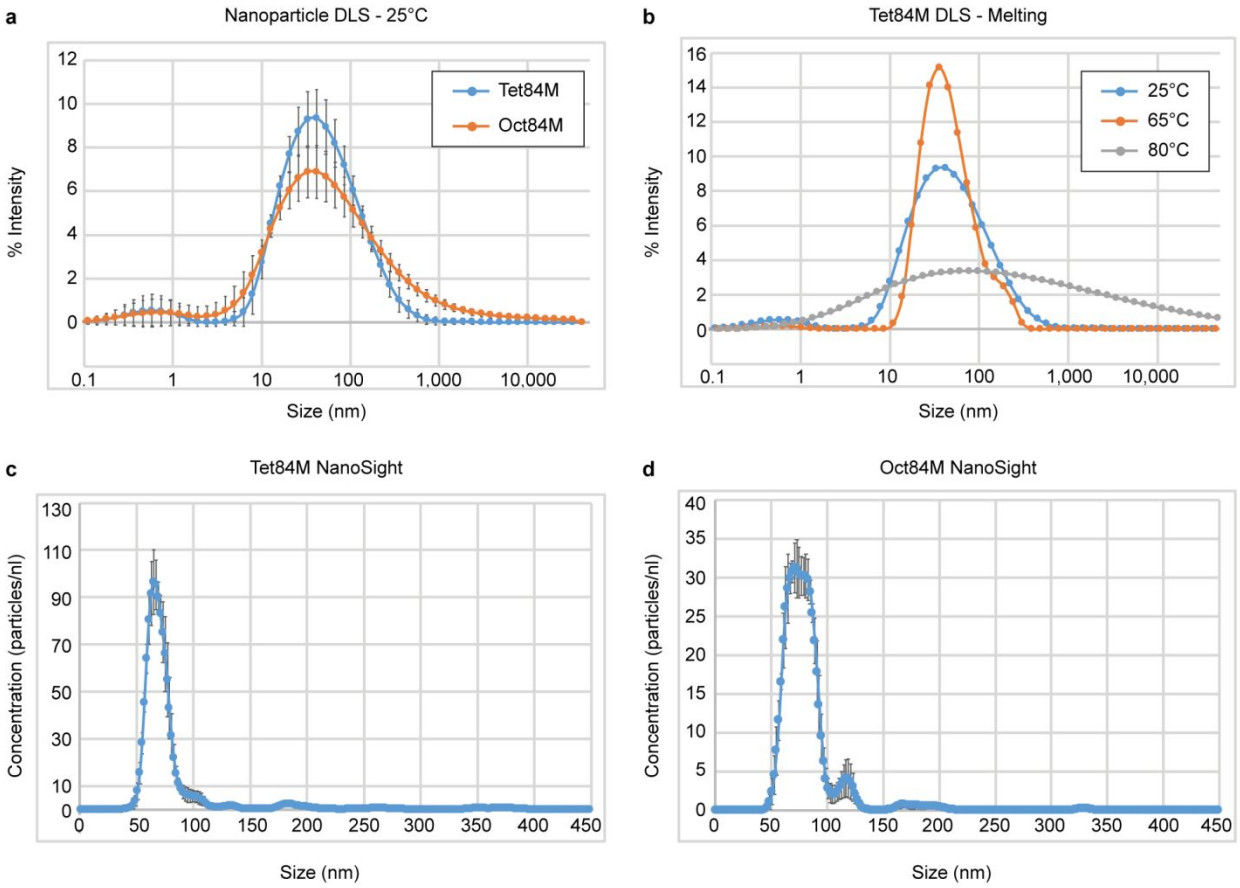

Figure S49. Monodispersed nanoparticles shown by dynamic light scattering. Dynamic light scattering was carried out on an MV octahedron of 84-bp edge length and a MV tetrahedron of 84-bp edge length to check monodispersity. (**a**) Particle size centered around 60 nm. (**b**) Melting of the MV tetrahedron of 84-bp edge length visualized by particle size and monodispersity. Heating the particle to 65°C reduced the particle size spread, while heating above 80°C melted the particle visualized by spreading of the particle size. (**c-d**) Nanoparticle size and uniformity was validated further by particle counting using the NanoSight, for the (**c**) MV tetrahedron 84-bp edge length and the (**d**) MV octahedron of 84-bp edge length. Movies associated with the NanoSight data are shown in Movies S1 and S2.

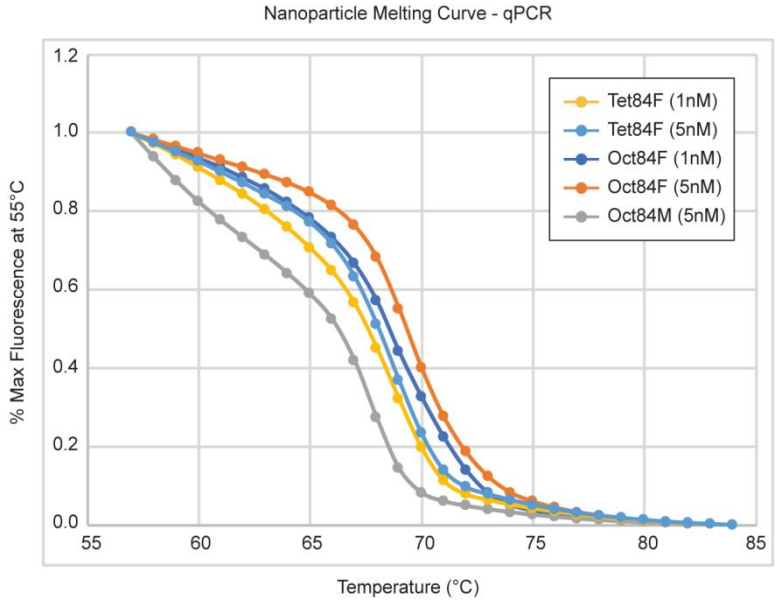

Figure S50. Fluorescent melting curve analysis of 6HB particles. Melting temperature was assayed by following fluorescence from SybrGreen binding to base-paired DNA. Melting temperatures were tested for the FV tetrahedron of 84-bp edge length (Tet84F), FV octahedron of 84-bp edge length (Oct84F), and MV octahedron of 84-bp edge length (Oct84M). Each curve is an average of at least four samples. The inflection point calculated by Newton's method was determined for each.

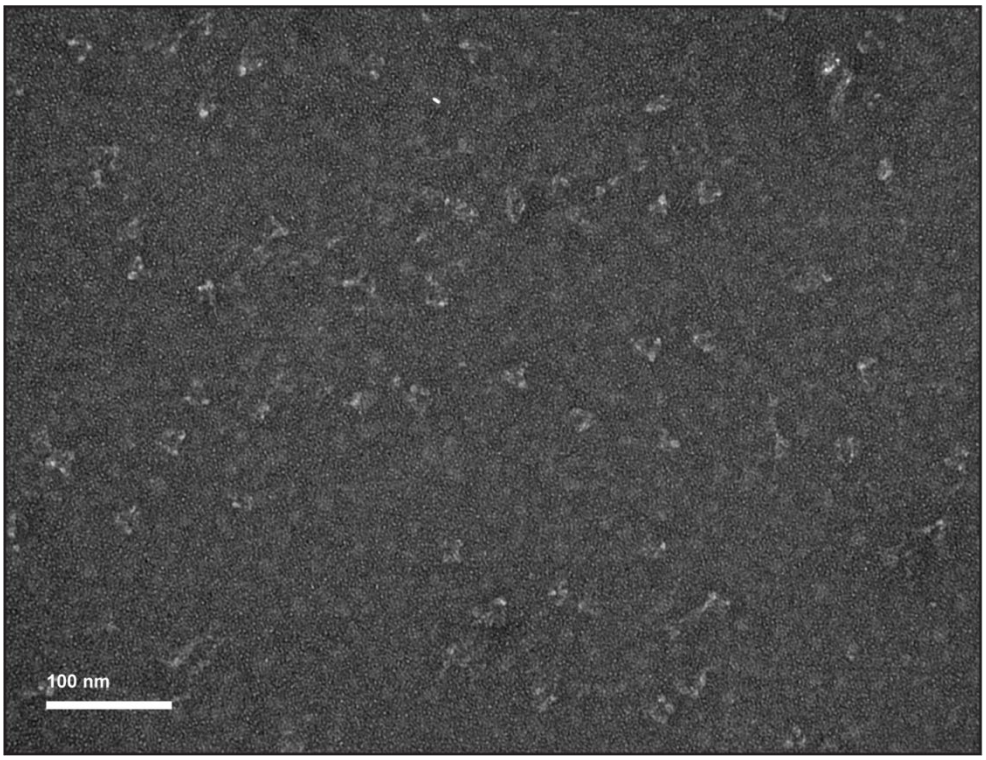

Figure S51. TEM imaging of a FV tetrahedron of 42-bp edge length.

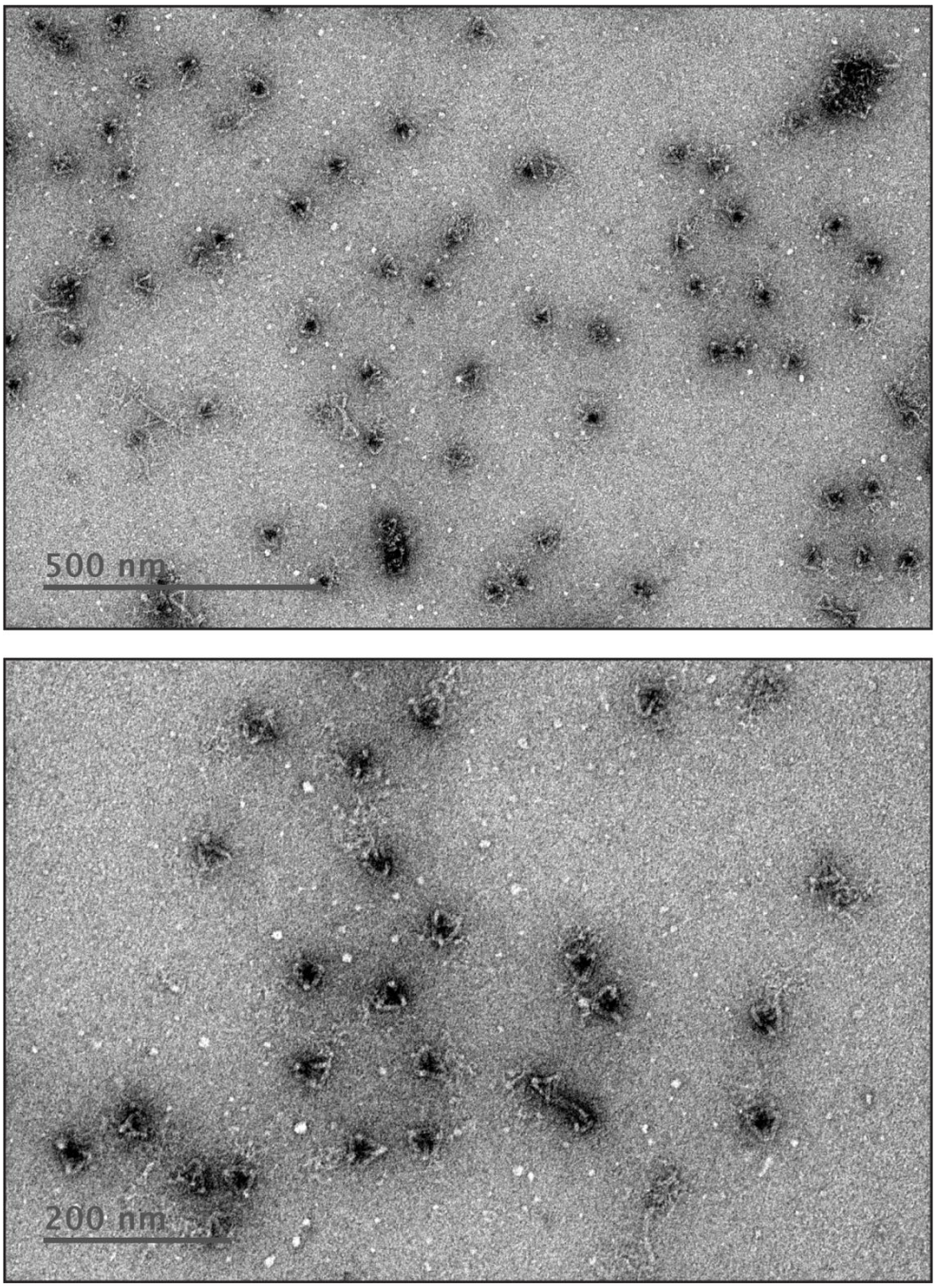

Figure S52. TEM imaging of a FV tetrahedron of 84-bp edge length.

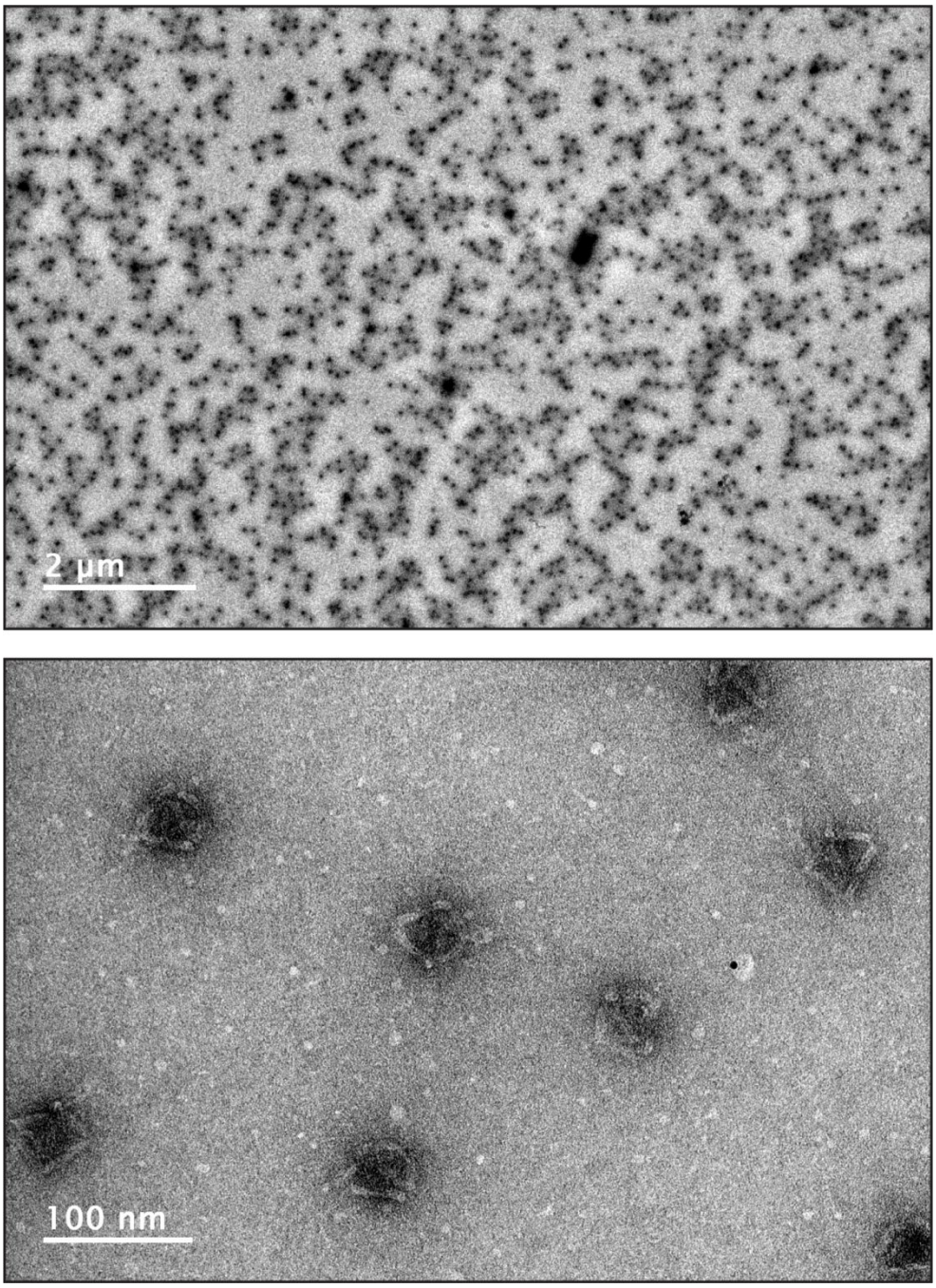

Figure S53. TEM imaging of a FV octahedron of 84-bp edge length.

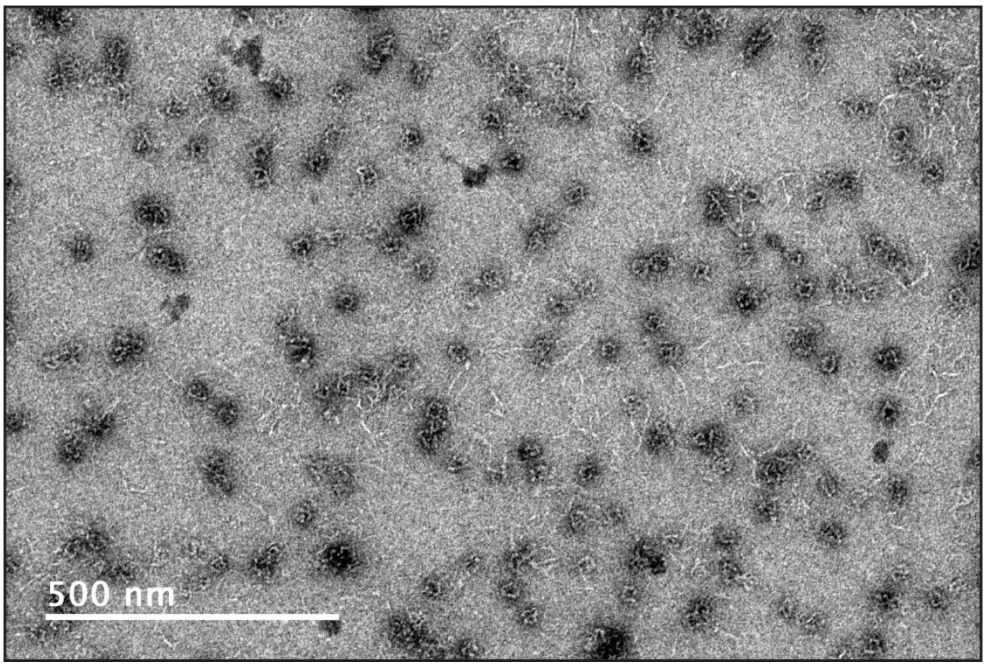

Figure S54. TEM imaging of a FV pentagonal bipyramid of 42-bp edge length.

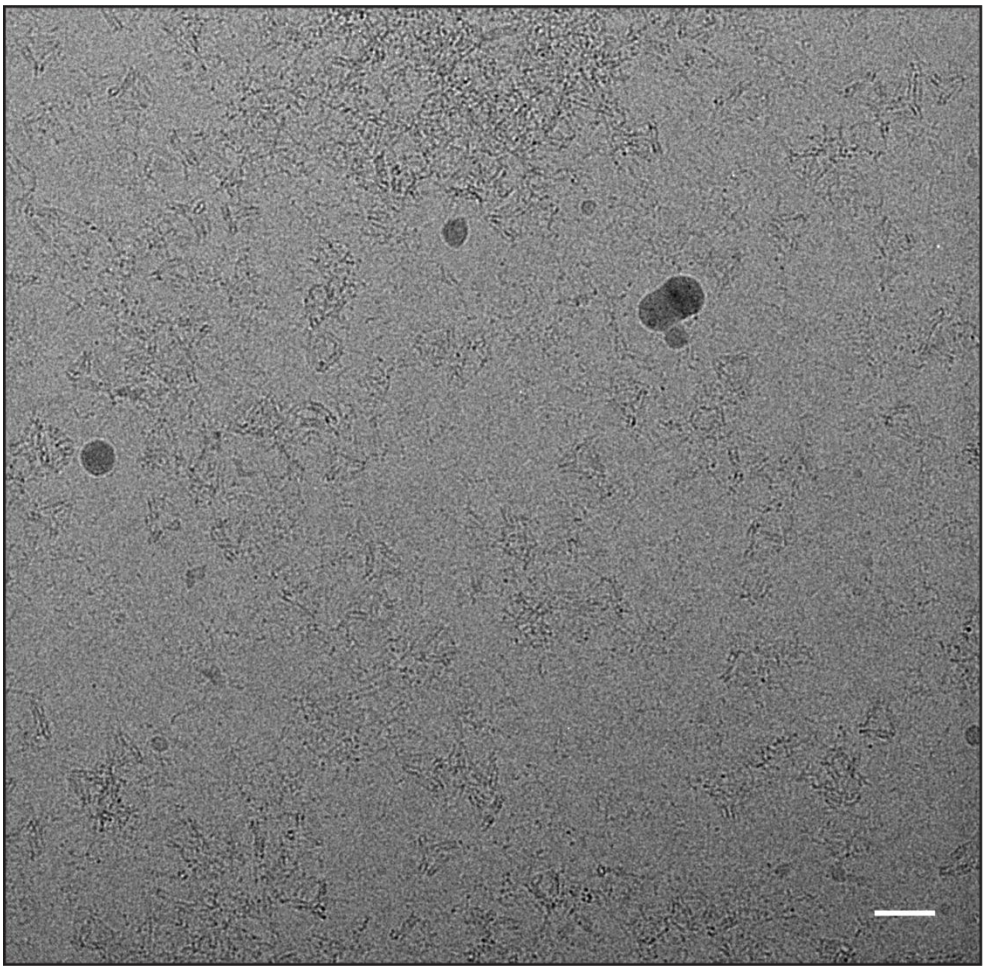

Figure S55. Cryo-EM imaging of a FV tetrahedron of 63-bp edge length. Electron micrograph. Scale bar 50 nm.

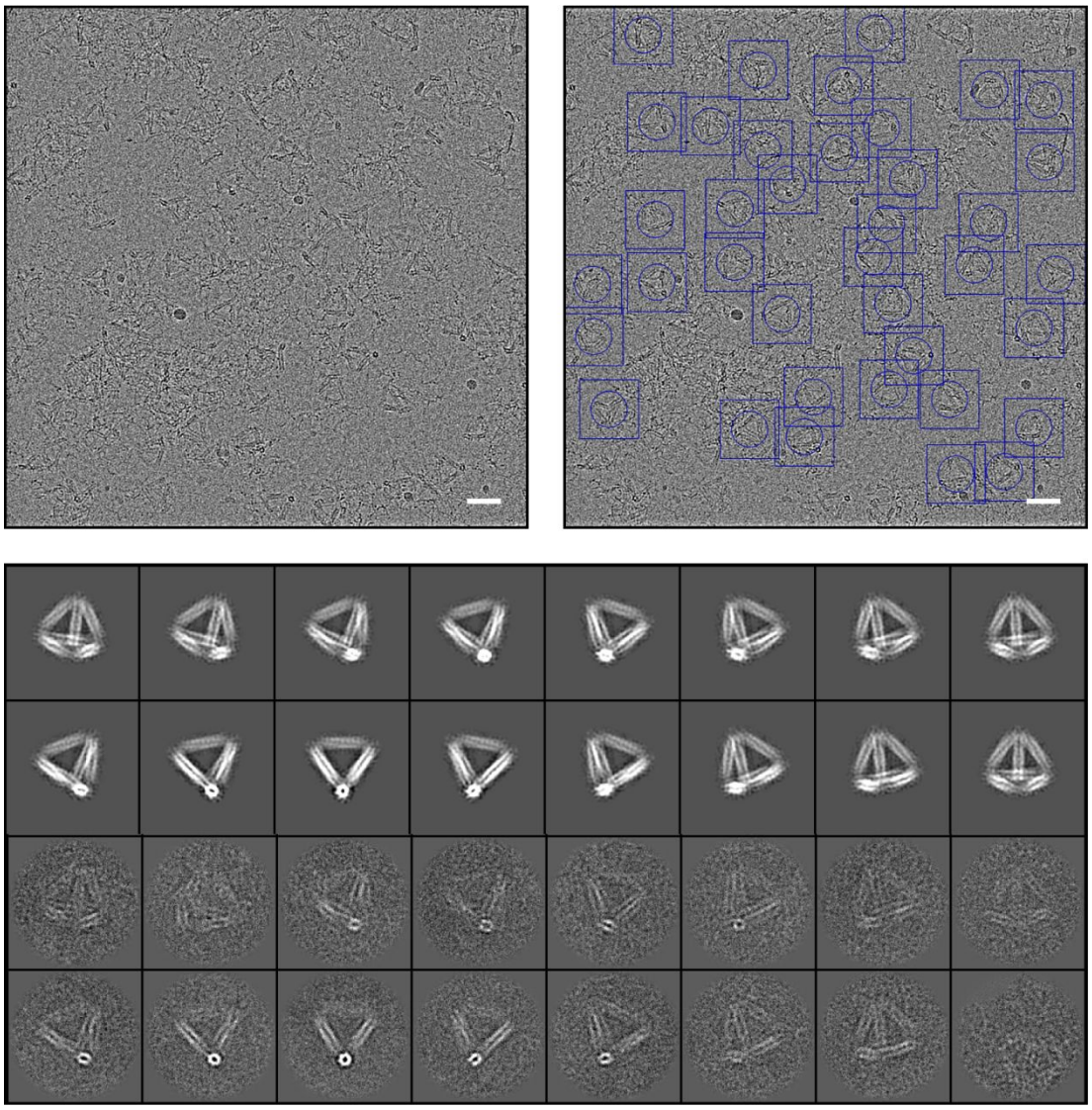

Figure S56. Cryo-EM imaging of a FV tetrahedron of 84-bp edge length. (Top) Example cryo-EM micrograph without and with boxed particles. Scale bar 50 nm. (Bottom) Representative class averages and corresponding projections of 3D reconstruction map.

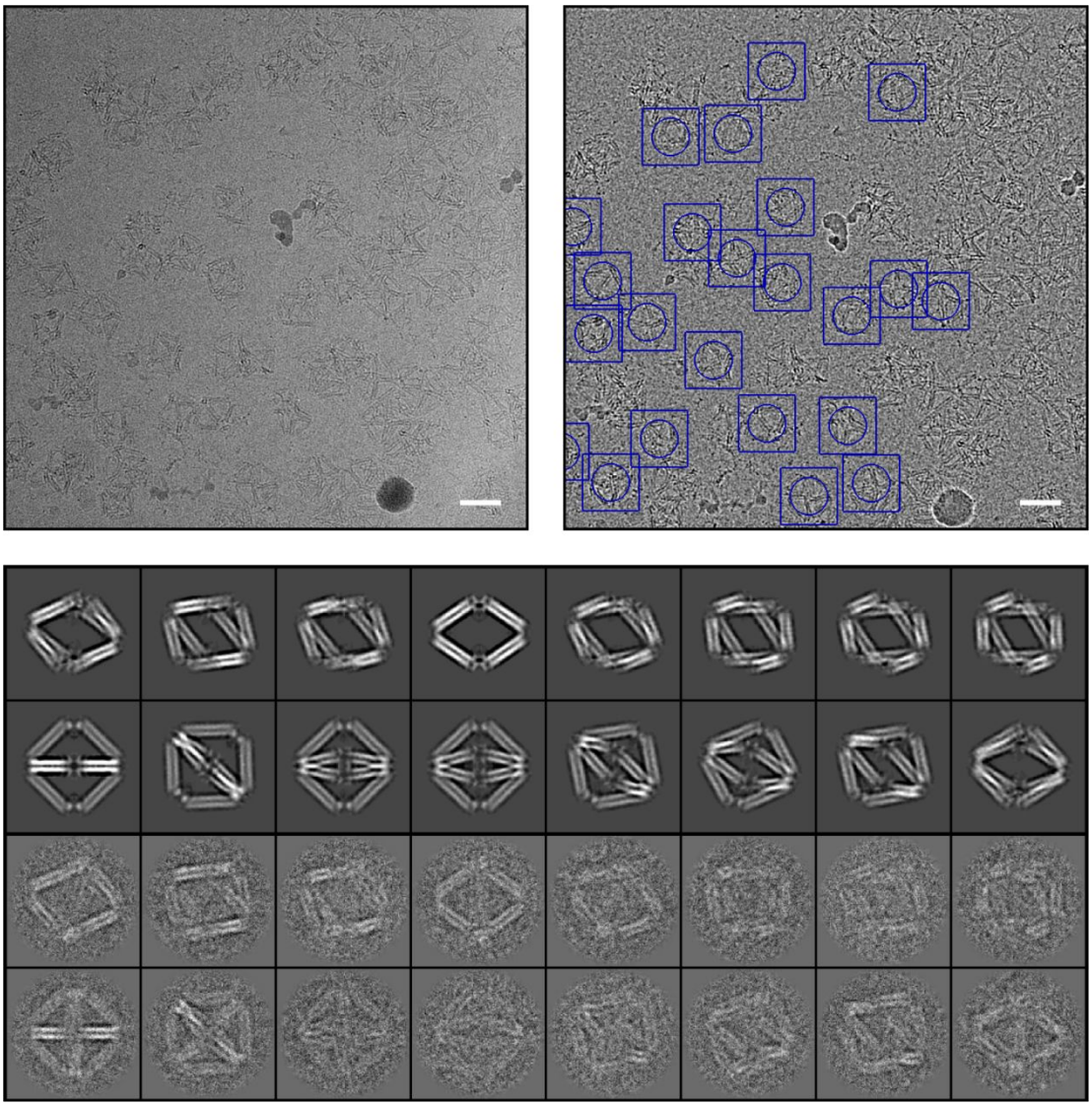

Figure S57. Cryo-EM imaging of a FV octahedron of 84-bp edge length. (Top) Example micrograph images showing unboxed (left) and boxed (right) particles. Scale bar 50 nm. (Bottom) Representative class averages and corresponding projections of 3D reconstruction map.

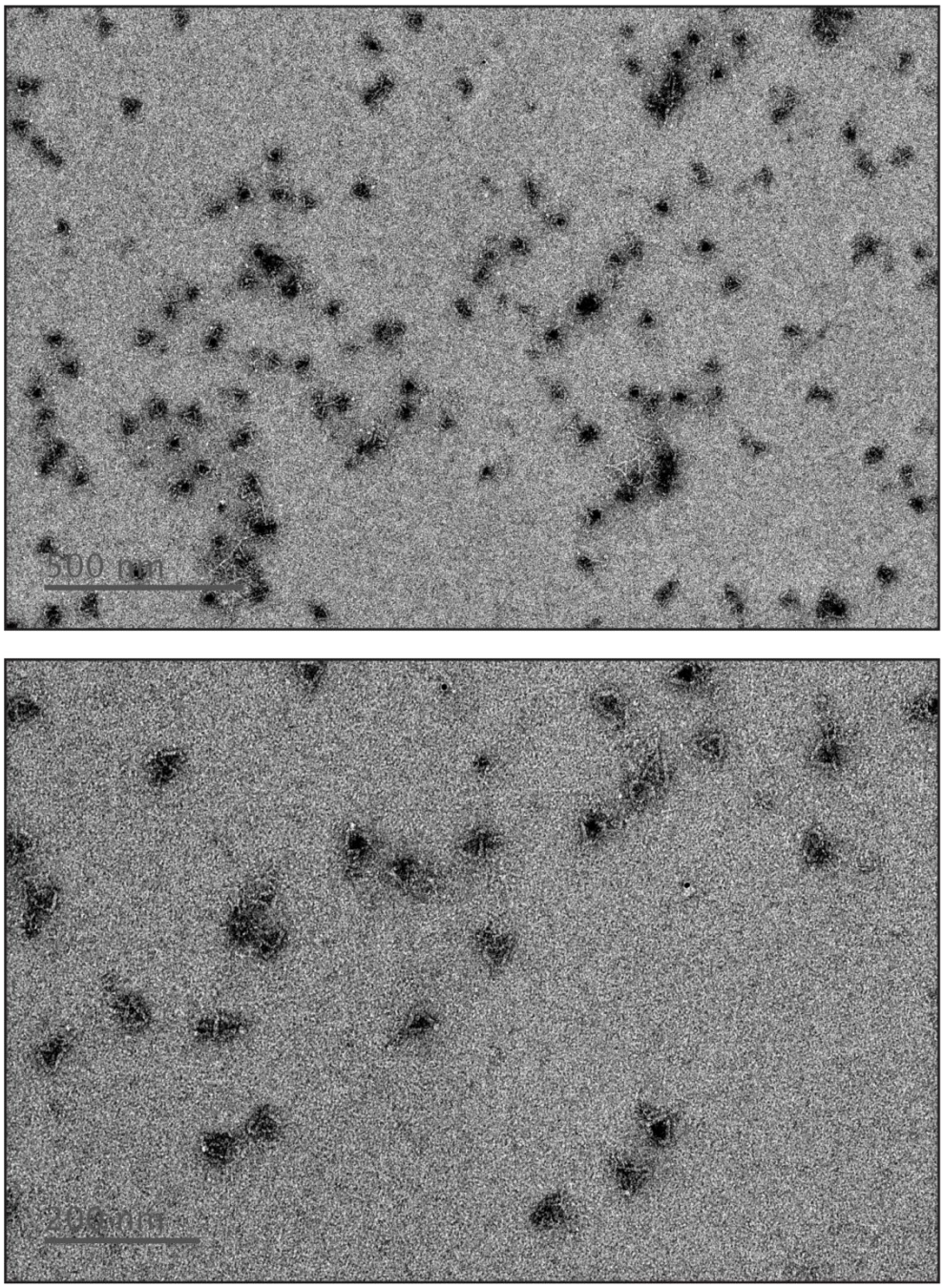

Figure S58. TEM imaging of a MV tetrahedron of 84-bp edge length.

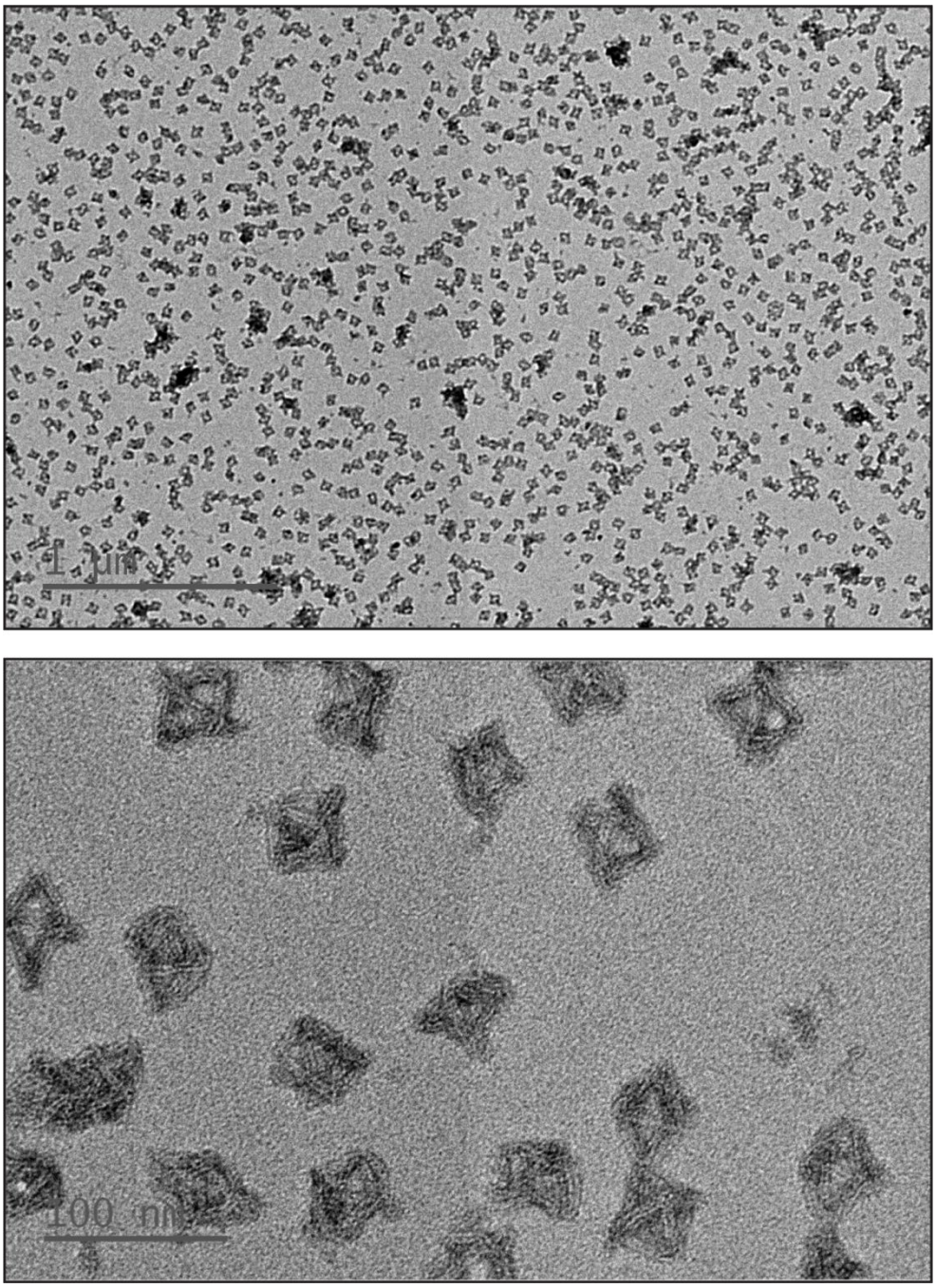

Figure S59. TEM imaging of a MV octahedron of 84-bp edge length.

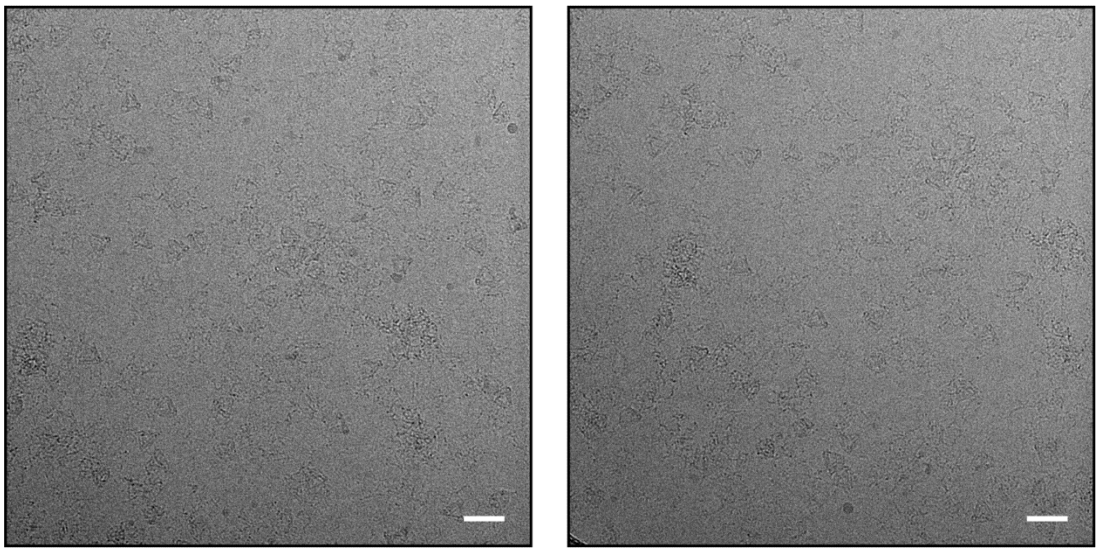

Figure S60. Cryo-EM imaging of a MV tetrahedron of 42-bp edge length. Two micrographs showing folded tetrahedra. Scale bar 50 nm.

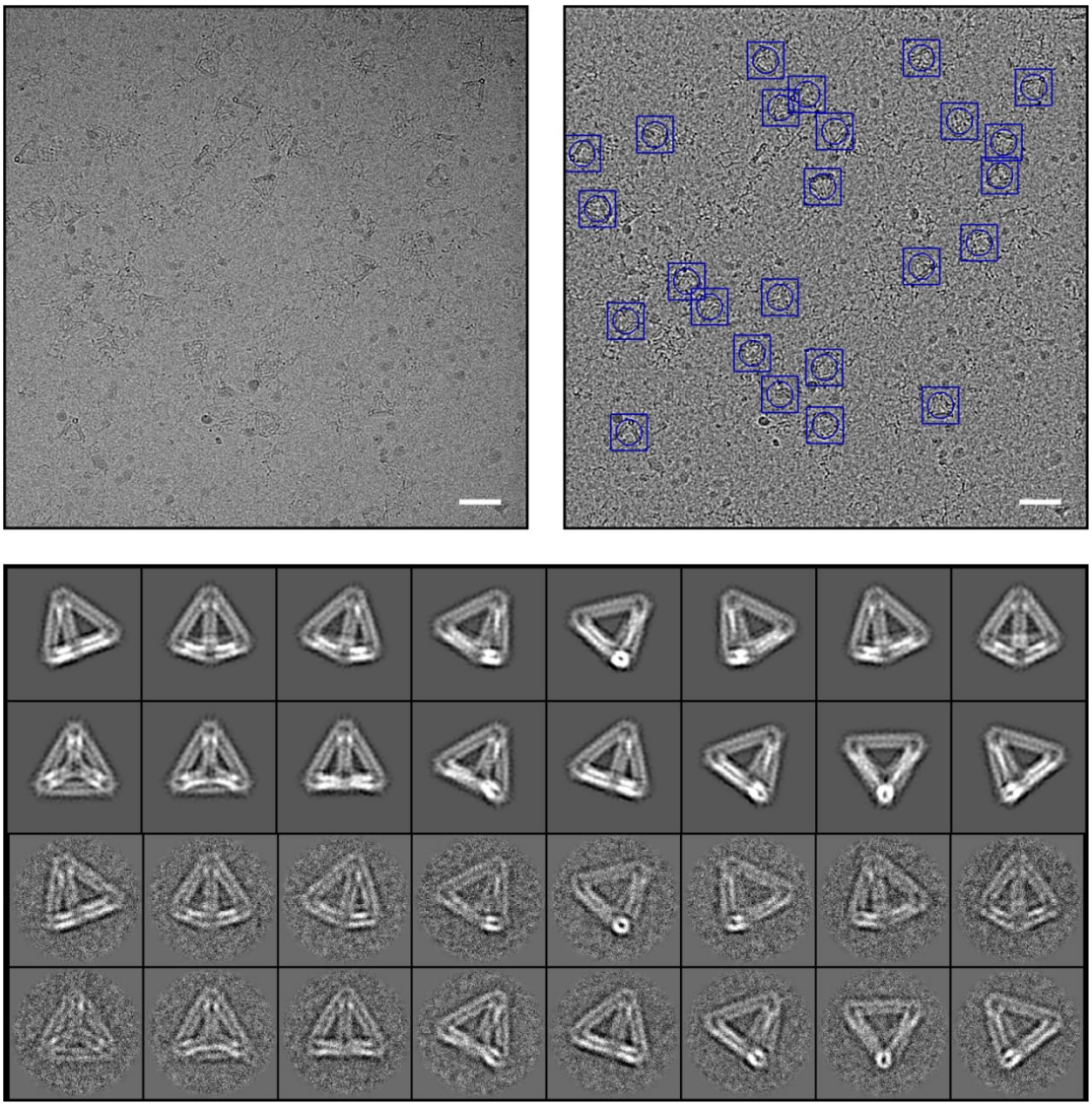

Figure S61. Cryo-EM imaging of a MV tetrahedron of 63-bp edge length. (Top) Example micrograph images showing unboxed (left) and boxed (right) particles. Scale bar 50 nm. (Bottom) Representative class averages and corresponding projections of 3D reconstruction map.

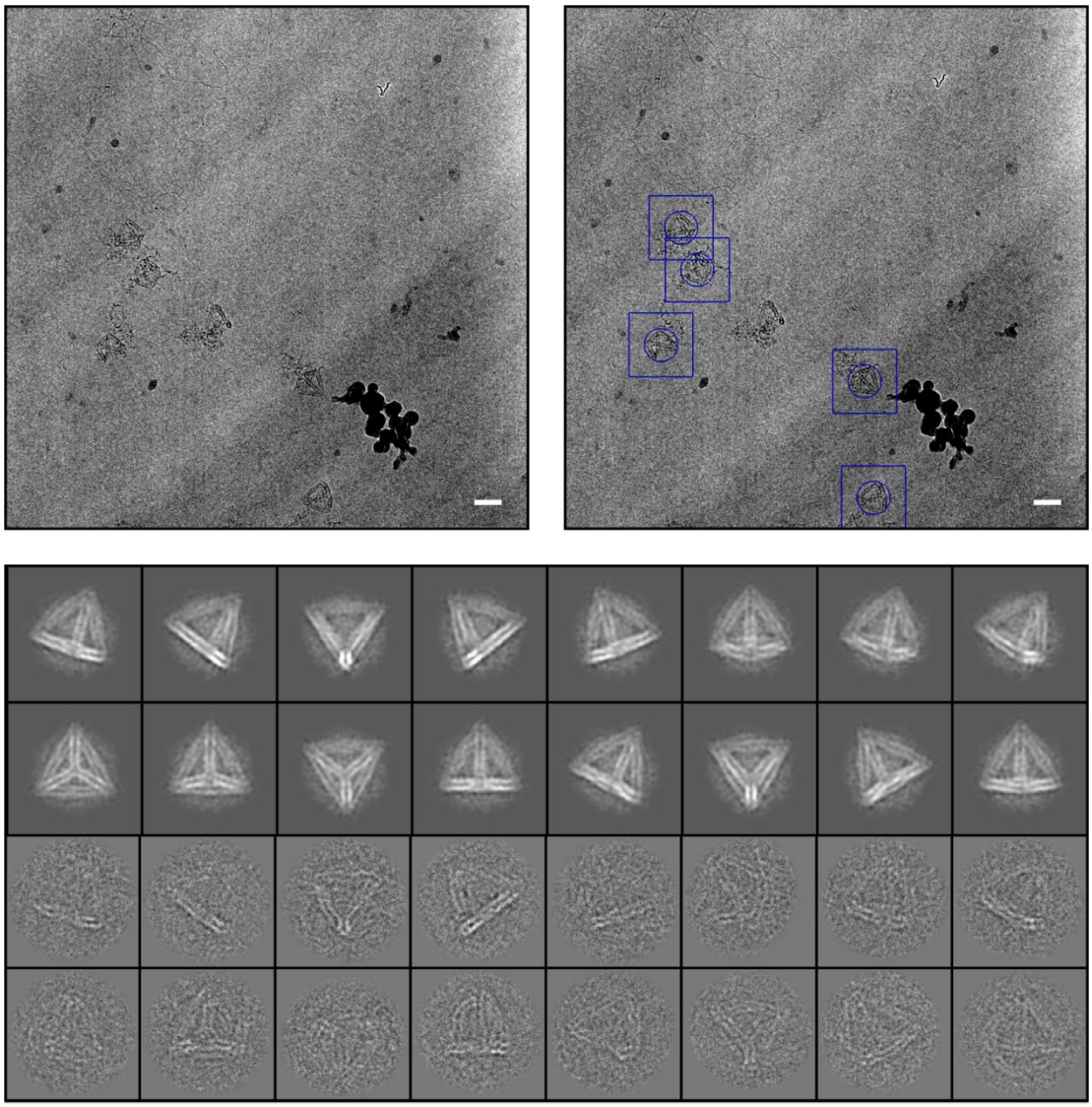

Figure S62. Cryo-EM imaging of a MV tetrahedron of 84-bp edge length. (Top) Example micrograph images showing unboxed (left) and boxed (right) particles. Scale bar 50 nm. (Bottom) Representative class averages and corresponding projections of 3D reconstruction map.

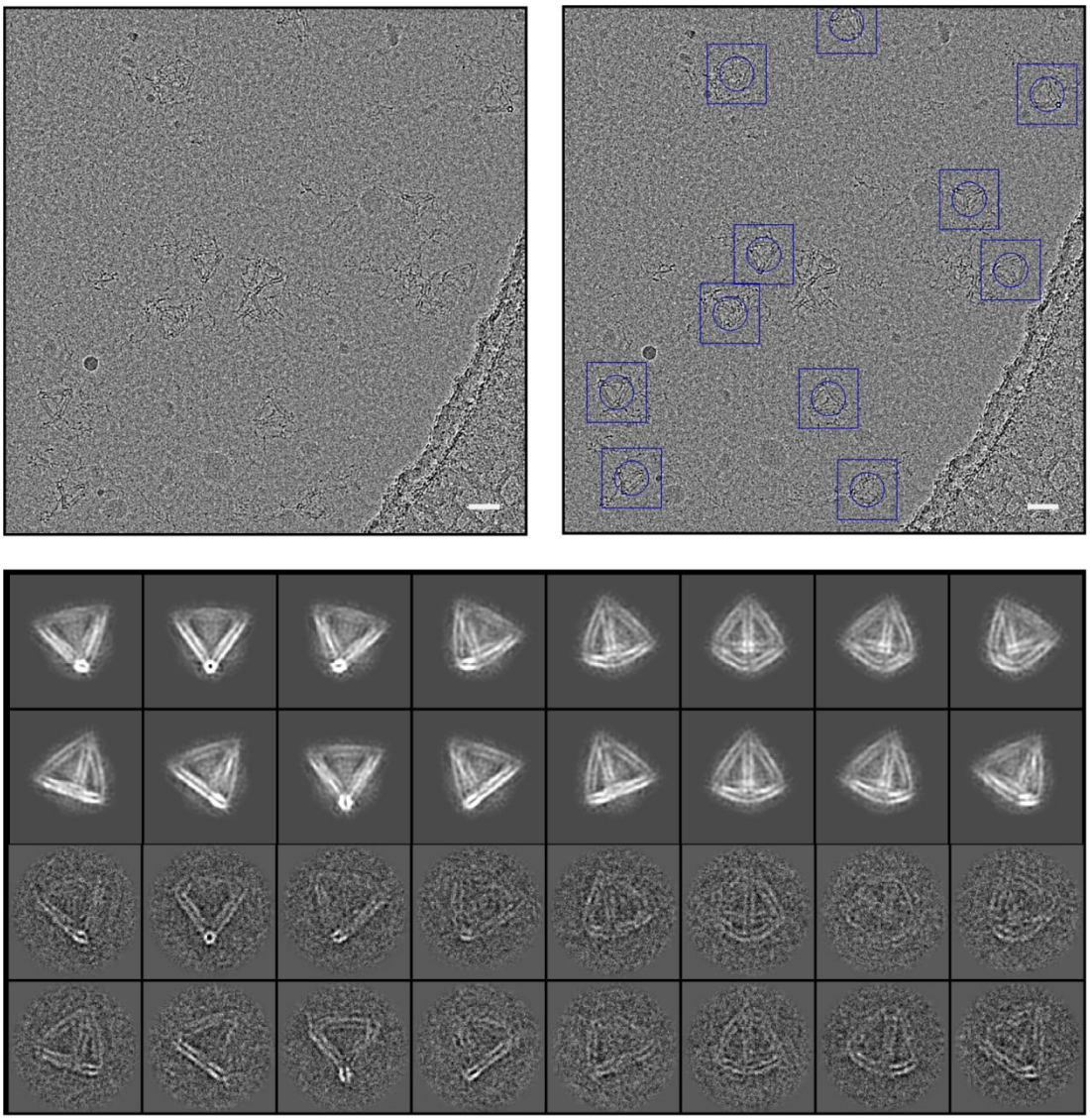

Figure S63. Cryo-EM imaging of a MV tetrahedron of 84-bp edge length using the middle layer for connection scaling. (Top) Example micrograph images showing unboxed (left) and boxed (right) particles. Scale bar 50 nm. (Bottom) Representative class averages and corresponding projections of 3D reconstruction map.

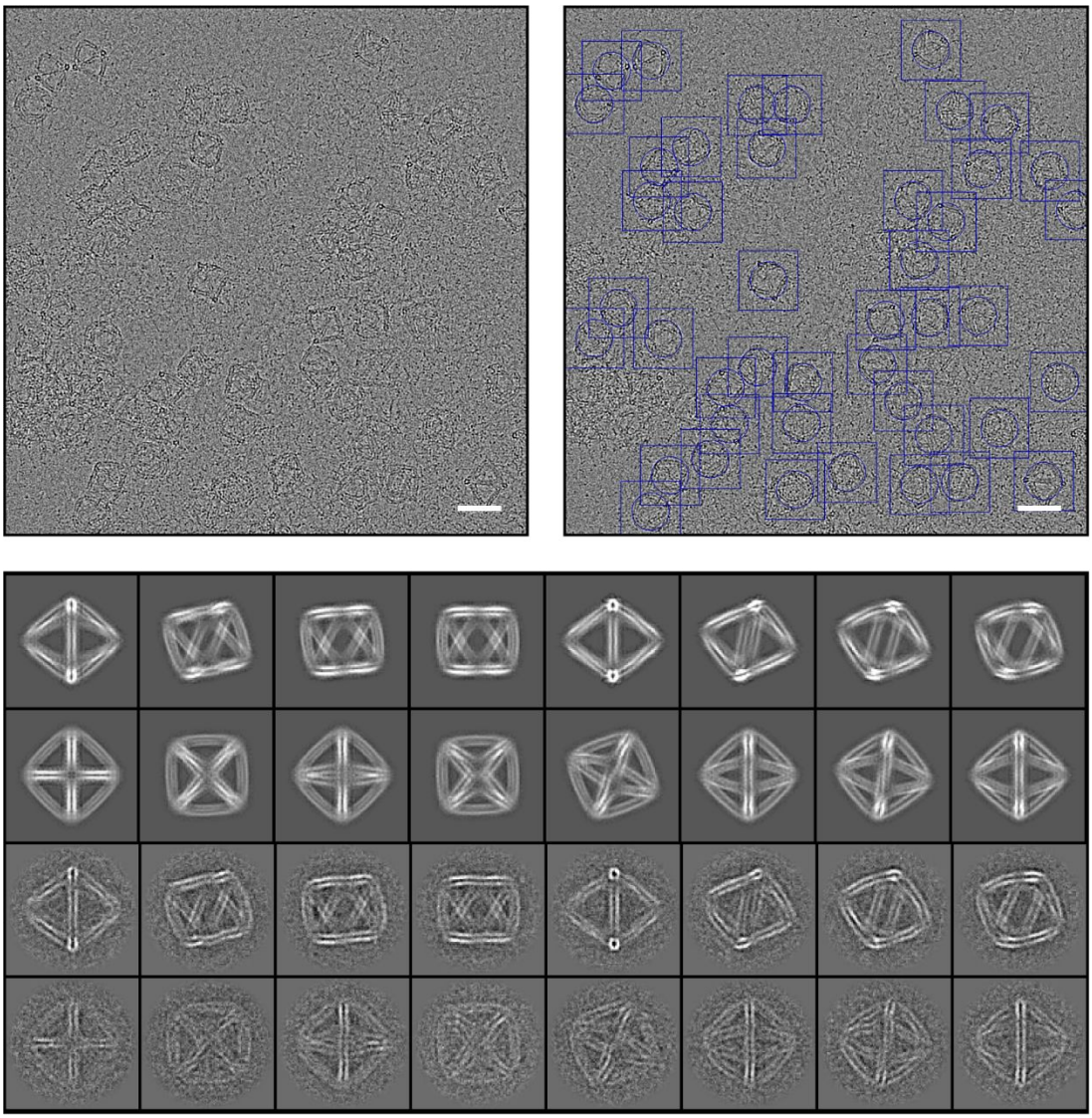

Figure S64. Cryo-EM imaging of the MV octahedron of 84-bp edge length. (Top) Example micrograph images showing unboxed (left) and boxed (right) particles. Scale bar 50 nm. (Bottom) Representative class averages and corresponding projections of 3D reconstruction map.

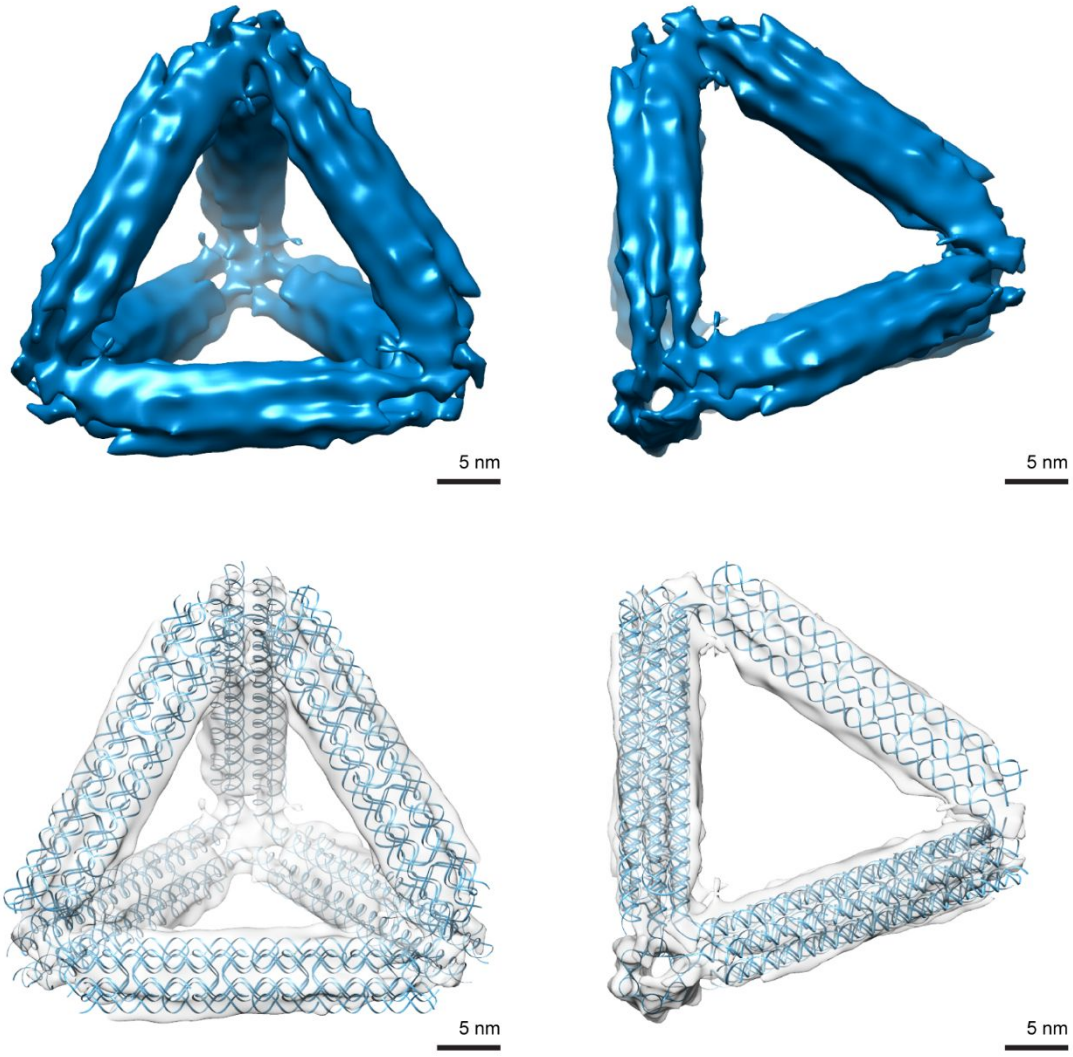

Figure S65. 3D structure characterization of the FV tetrahedron of 84-bp edge length using cryo-EM reconstruction and comparison with model predictions. Movie is shown in Movie S3.

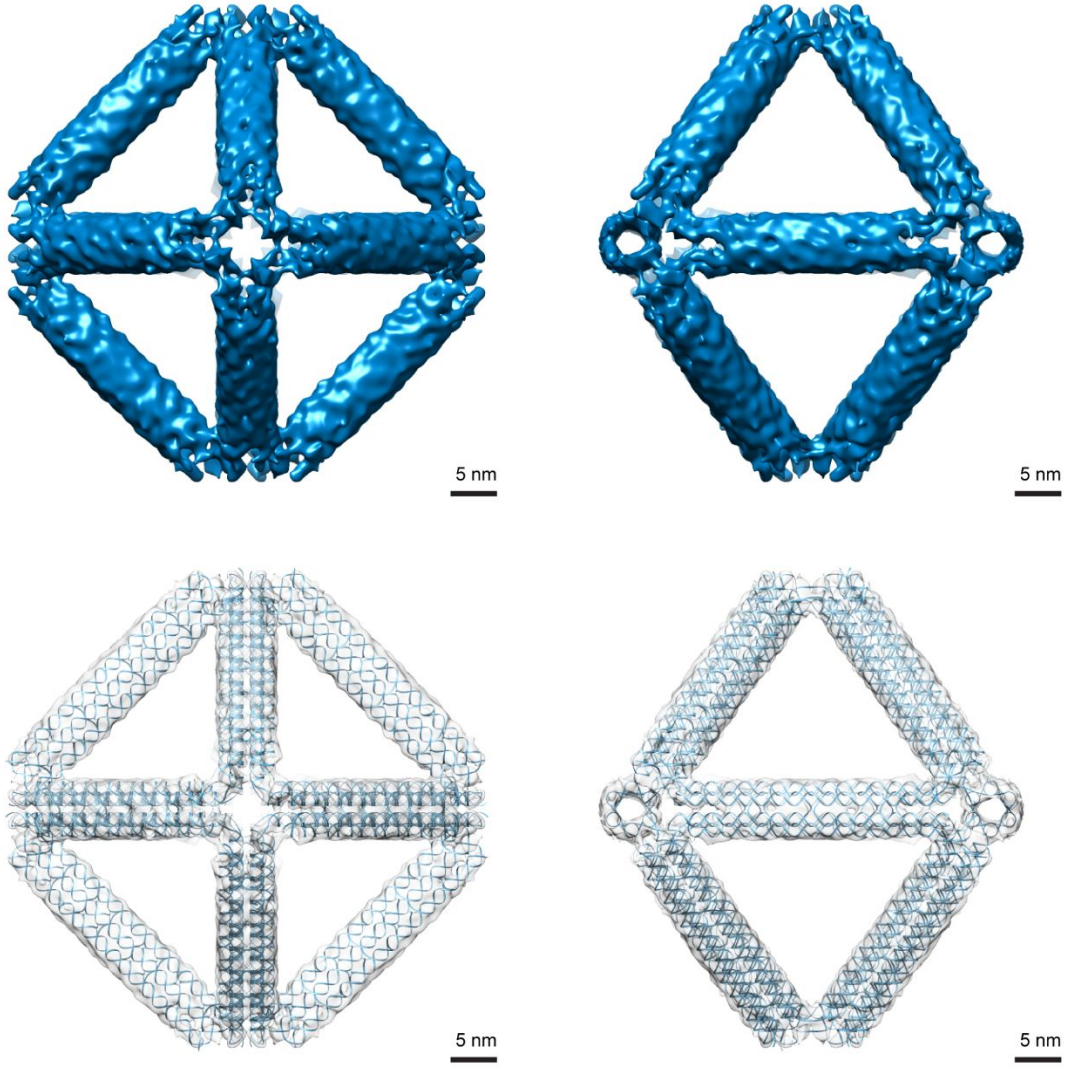

Figure S66. 3D structure characterization of the FV octahedron of 84-bp edge length using cryo-EM reconstruction and comparison with model predictions. Movie is shown in Movie S4.

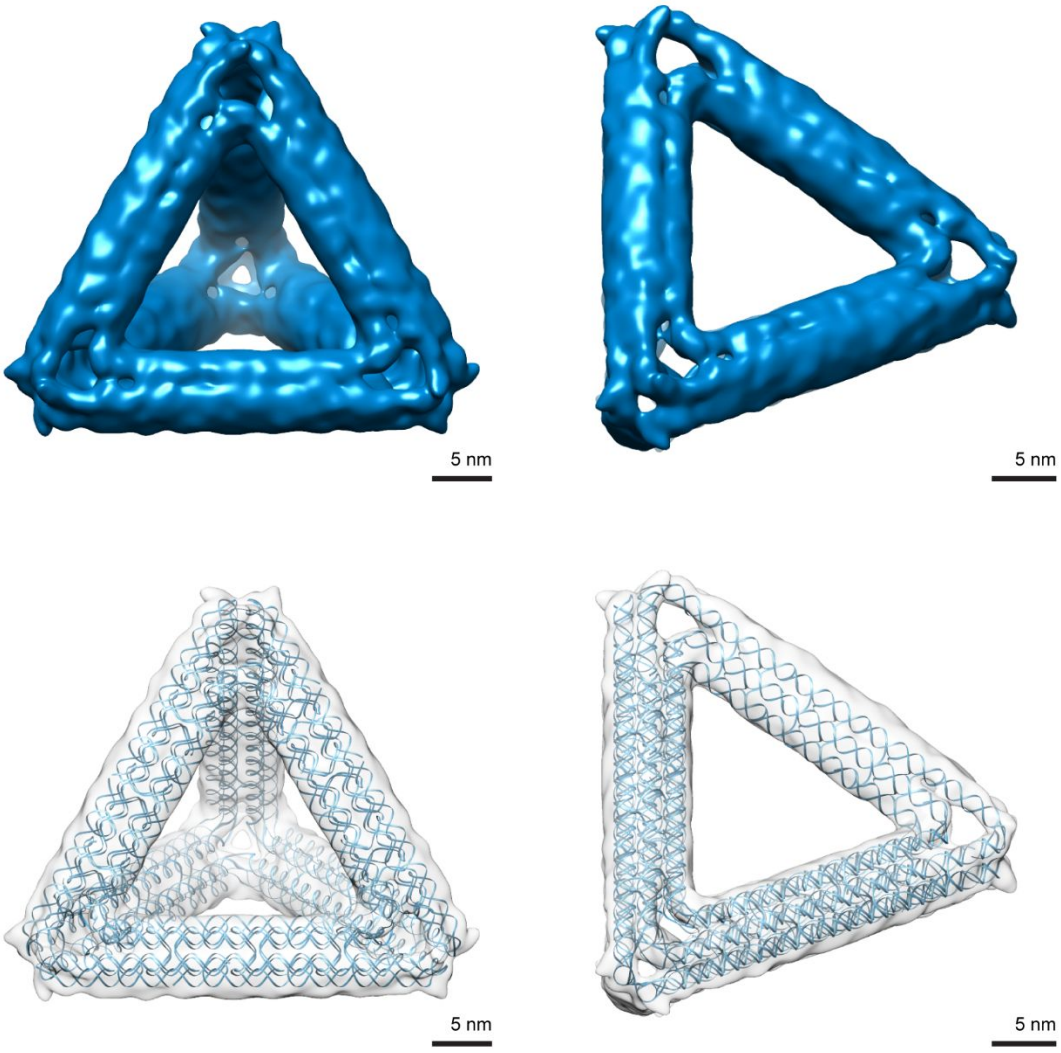

Figure S67. 3D structure characterization of the MV tetrahedron of 63-bp edge length using cryo-EM reconstruction and comparison with model predictions.

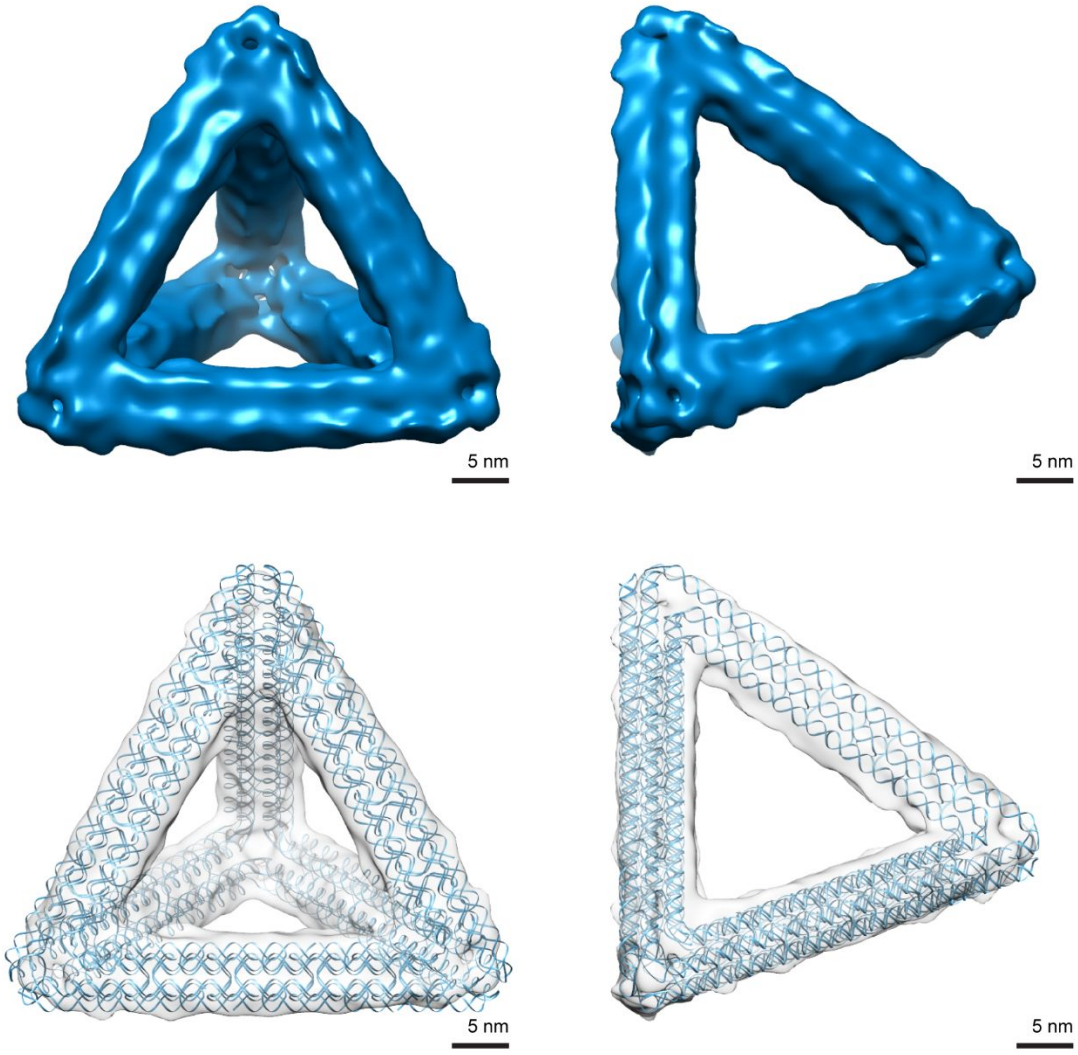

Figure S68. 3D structure characterization of the MV tetrahedron of 84-bp edge length using cryo-EM reconstruction and comparison with model predictions. Movie is shown in Movie S5.

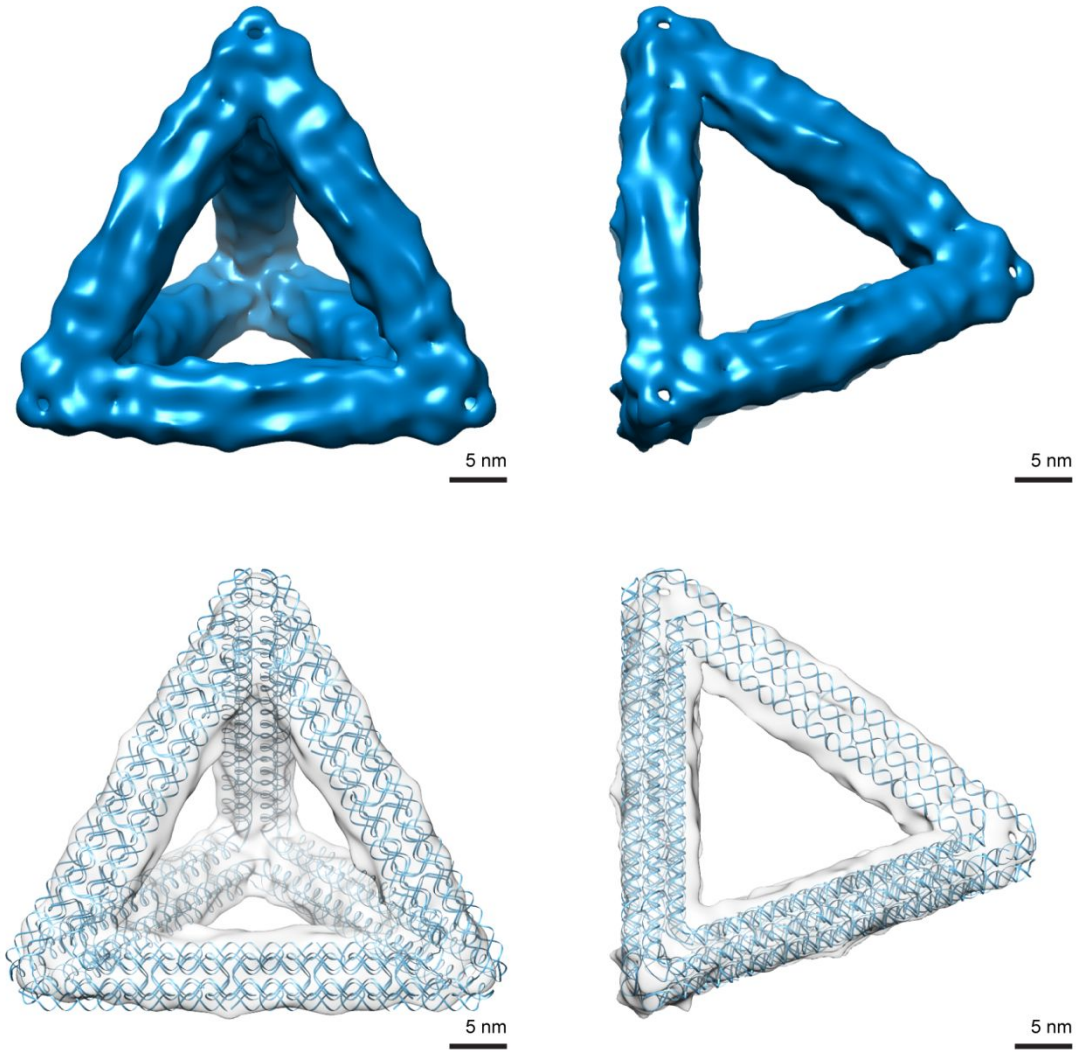

Figure S69. 3D structure characterization of the 84-bp edge length DNA tetrahedron with the MV and middle connection layer using cryo-EM reconstruction and comparison with model predictions.

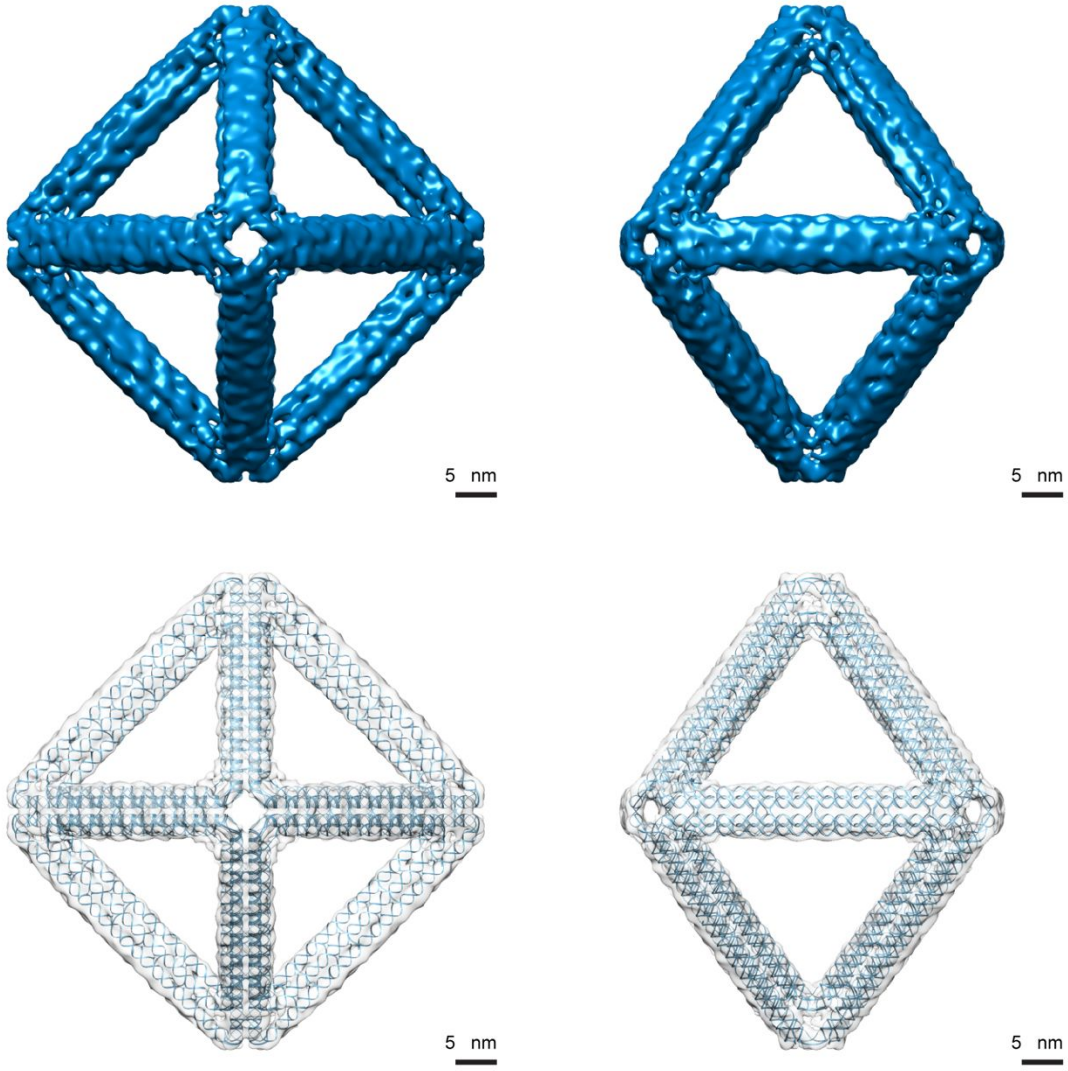

Figure S70. 3D structure characterization of the MV octahedron of 84-bp edge length using cryo-EM reconstruction and comparison with model predictions. Movie is shown in Movie S6.

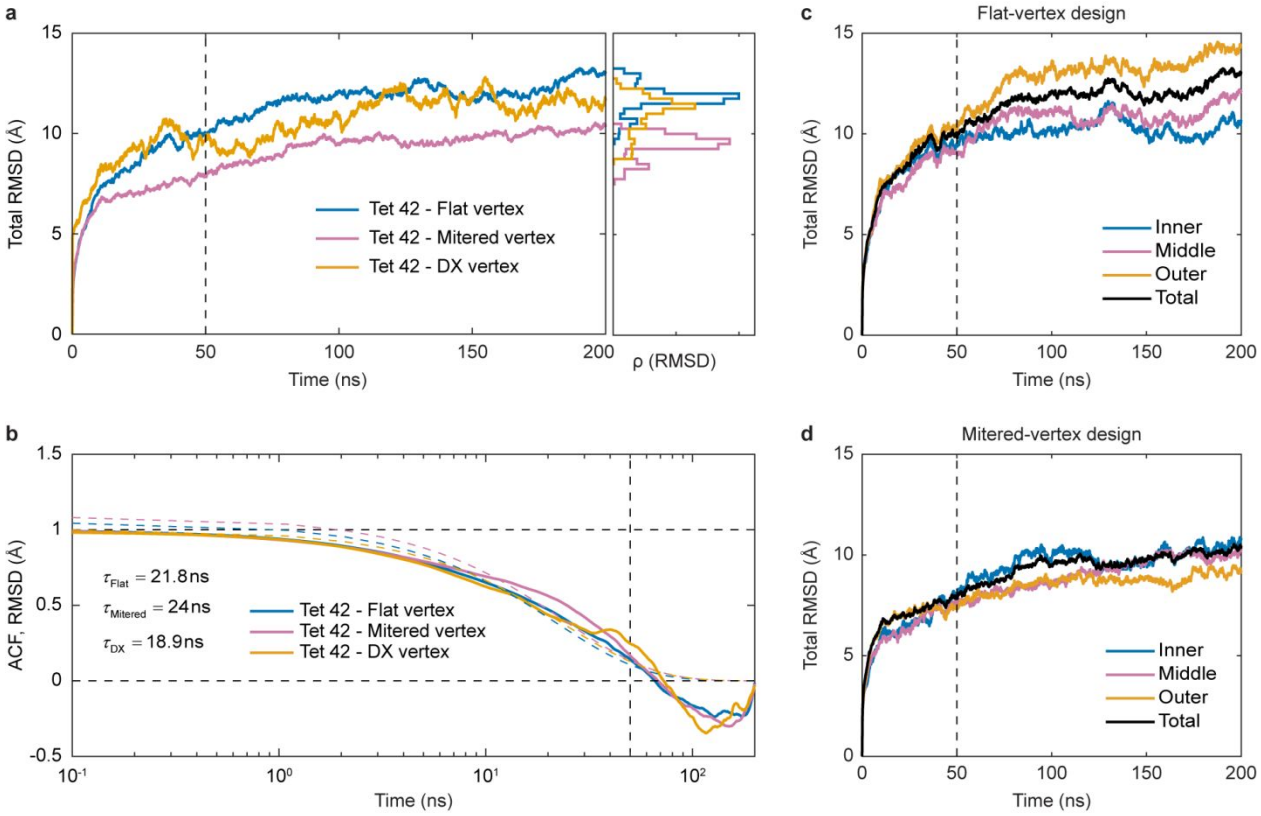

Figure S71. Root-mean-square deviations (RMSD) of tetrahedra of 42-bp edge length from molecular dynamics simulations. (**a**) Total RMSD of all nucleic acid atoms of a FV and MV 6HB tetrahedron compared to a DX tetrahedron compared to their respective atomic coordinates of the initial time point at 0 ns. (**c-d**) Differences in RMSD for the inner, middle, and outer DNA duplexes of the 6HB design for the FV (**c**) and MV (**d**). All molecular dynamics simulations were run for 200 ns.

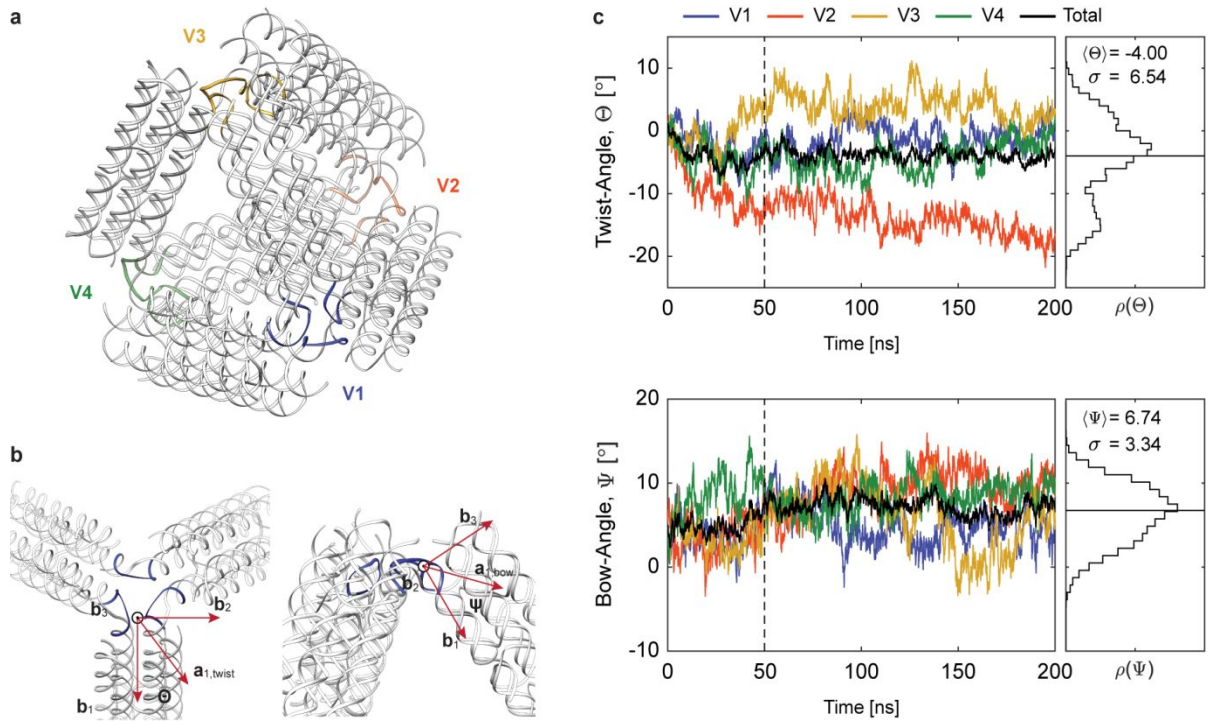

Figure S72. Geometric analysis of a FV 6HB tetrahedron of 42-bp edge length. (**a**) Location of each distinct vertex on the tetrahedron. (**b**) Definition of twist- (Θ) and bow- (Ψ) angles at each vertex with respect to the orthonormal basis ($\mathbf{b_1}$, $\mathbf{b_2}$, $\mathbf{b_3}$). (**c**) Twist-angles in degrees and bow-angles in degrees at each vertex (V1, V2, V3, V4) during a 200 ns MD simulation. The distribution of the twist- and bow-angles are shown separately in the right panel, along with the mean and standard deviation. Mean values are computed using data after the particles have equilibrated, which is distinguished by the vertical dashed line in the trajectory panel.

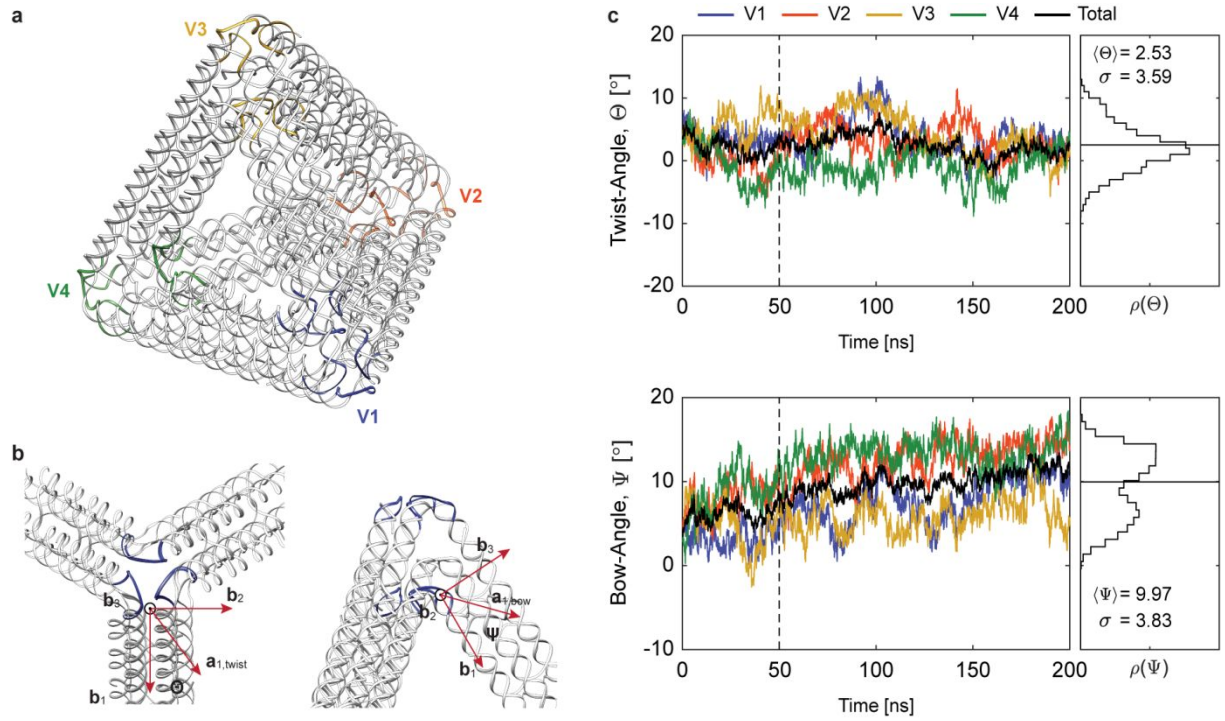

Figure S73. Geometric analysis of the inner vertex of a MV 6HB tetrahedron of 42-bp edge lengths. (**a**) Location of each distinct vertex on the tetrahedron. Both an inner vertex connection, and an outer vertex connection are defined. (**b**) Definition of twist- (Θ) and bow- (Ψ) angles at each inner vertex with respect to the orthonormal basis ($\mathbf{b_1}$, $\mathbf{b_2}$, $\mathbf{b_3}$). (**c**) Twist-angles in degrees and bow-angles in degrees at each inner vertex (V1, V2, V3, V4) during a 200 ns MD simulation. The distribution of the twist- and bow-angles are shown separately in the right panel, along with the mean and standard deviation. Mean values are computed using data after the particles have equilibrated, which is distinguished by the vertical dashed line in the trajectory panel.

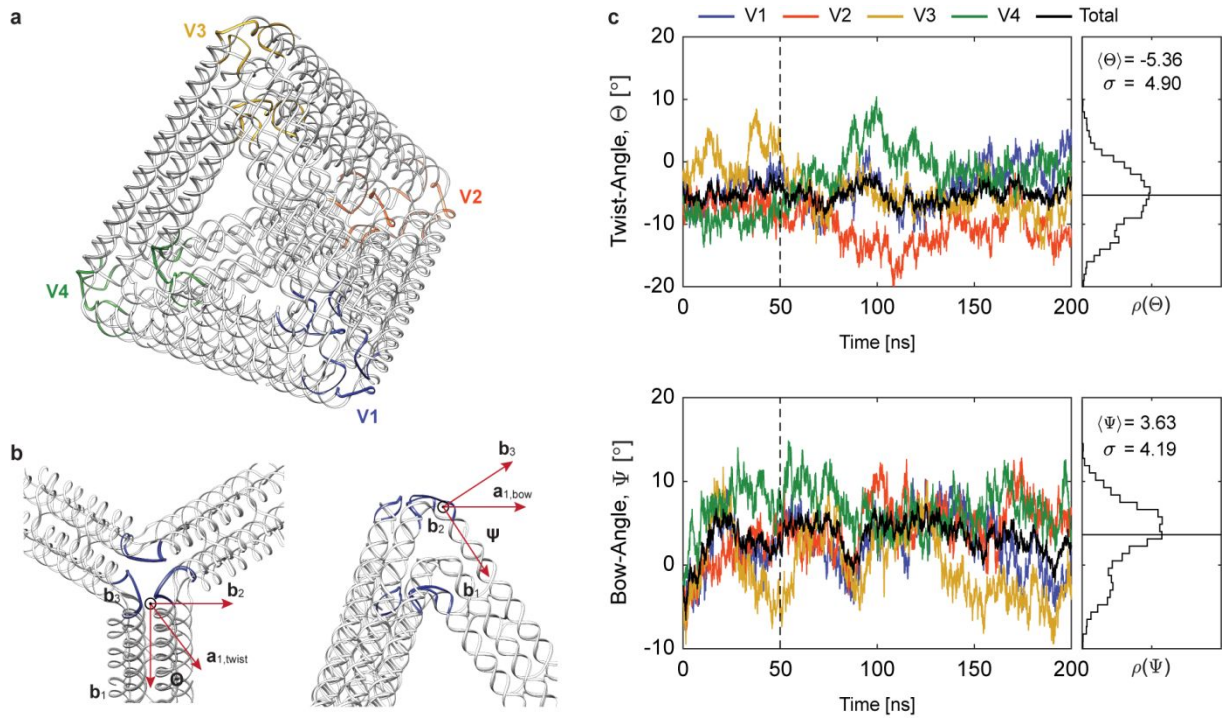

Figure S74. Geometric analysis of the outer vertex of a MV 6HB tetrahedron of 42-bp edge lengths. (**a**) Location of each distinct vertex on the tetrahedron. Both an inner vertex connection, and an outer vertex connection are defined. (**b**) Definition of twist- (Θ) and bow- (Ψ) angles at each outer vertex with respect to the orthonormal basis ($\mathbf{b_1}$, $\mathbf{b_2}$, $\mathbf{b_3}$). (**c**) Twist-angles in degrees and bow-angles in degrees at each outer vertex (V1, V2, V3, V4) during a 200 ns MD simulation. The distribution of the twist- and bow-angles are shown separately in the right panel, along with the mean and standard deviation. Mean values are computed using data after the particles have equilibrated, which is distinguished by the vertical dashed line in the trajectory panel.

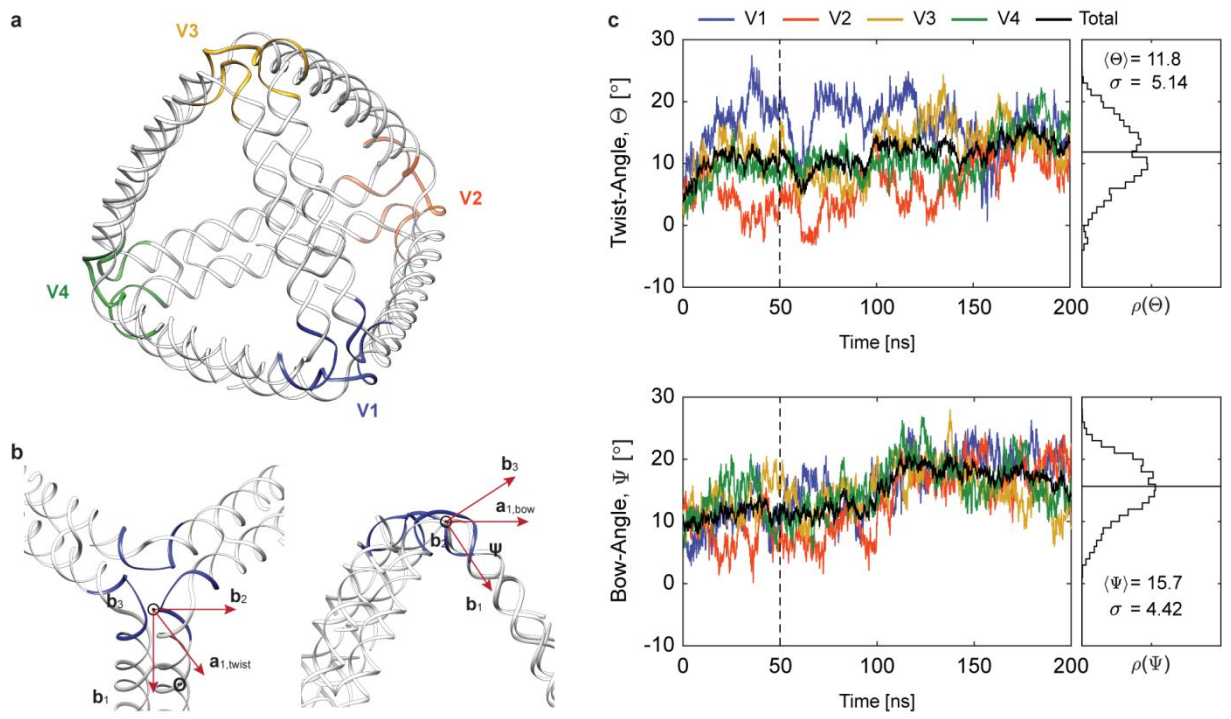

Figure S75. Geometric analysis of a DX tetrahedron of 42-bp edge lengths. (**a**) Location of each distinct vertex on the tetrahedron. (**b**) Definition of twist- (Θ) and bow- (Ψ) angles at each vertex with respect to the orthonormal basis ($\mathbf{b_1}$, $\mathbf{b_2}$, $\mathbf{b_3}$). (**c**) Twist-angles in degrees and bow-angles in degrees at each vertex (V1, V2, V3, V4) during a 200 ns MD simulation. The distribution of the twist- and bow-angles are shown separately in the right panel, along with the mean and standard deviation. Mean values are computed using data after the particles have equilibrated, which is distinguished by the vertical dashed line in the trajectory panel.

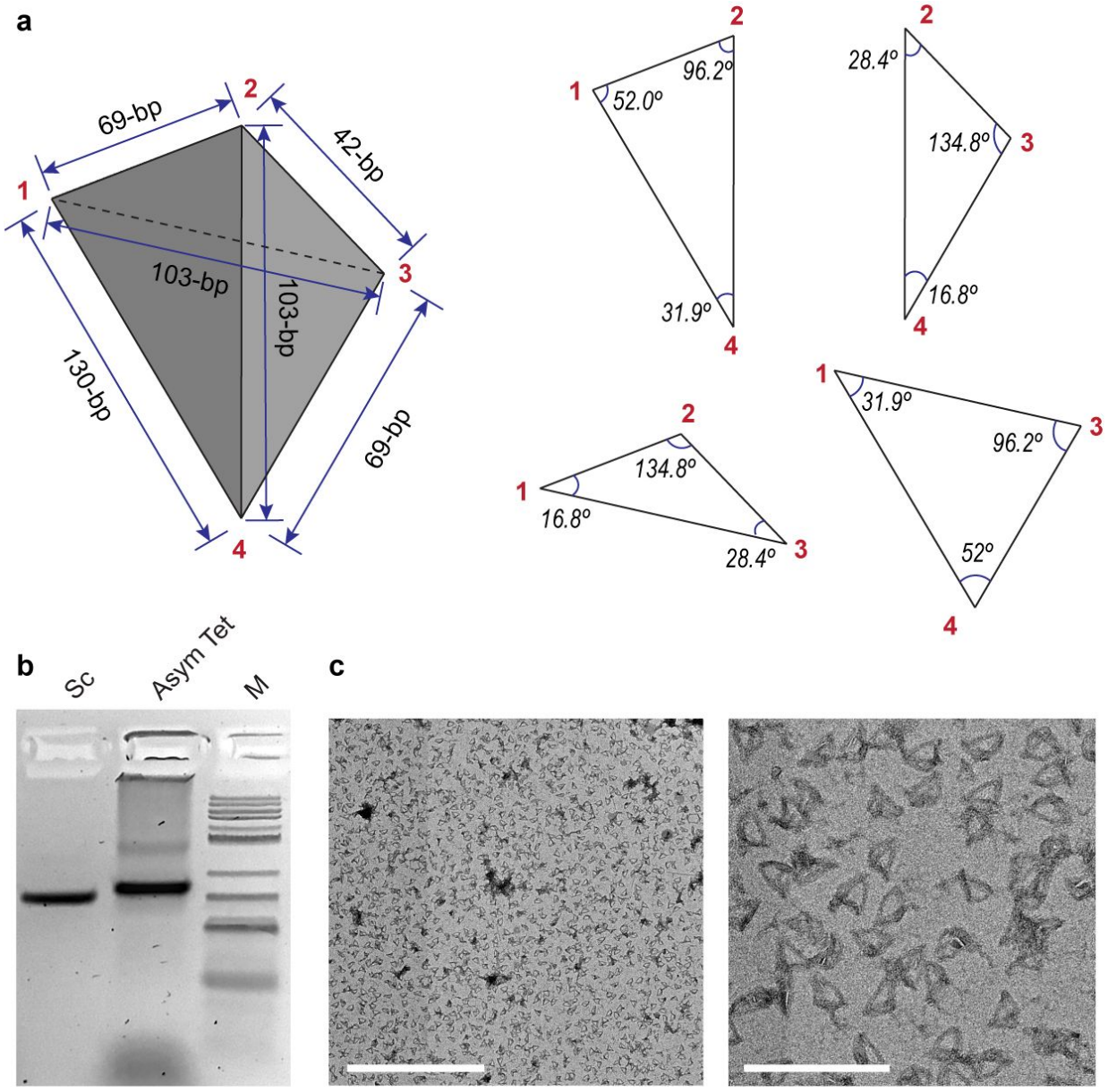

Figure S76. Design and folding characterization of a fully asymmetric wireframe tetrahedron. (a) Design of an asymmetric tetrahedron with incongruent triangular faces shown at right (**b**) Agarose gel electrophoresis shows a subtle shift in the folded band compared to scaffold. (**c**) Wide-field and near-field TEM shows mainly monodispersed and well-folded tetrahedra. Scale bar is 1 um for the wide-field image and 200 nm for the zoomed image.

Table S1. The percentage of the staples with the 14-nt dsDNA seed dsDNA domain in total staples when applying the inner connection layer. The values in parenthesis denote the fraction of basepairs that reside on strands with seeds. The patterns used are shown in Figure S4.

Pattern	Prior block (ID = 3)						Posterior block (ID = 13)					
	Tetrahedron			Octahedron			Tetrahedron			Octahedron		
	42bp	63bp	84bp	42bp	63bp	84bp	42bp	63bp	84bp	42bp	63bp	84bp
Pattern #1	68.2 (39.9)	80.4 (40.9)	81.1 (38.4)	70.6 (39.9)	83.5 (43.0)	83.3 (38.4)	**91.7 (46.6)**	**100 (44.6)**	**100 (40.9)**	**90.3 (46.1)**	**100 (44.6)**	**100 (40.9)**
Pattern #2	54.0 (29.1)	62.9 (31.8)	67.5 (33.4)	59.4 (30.5)	64.8 (33.0)	69.2 (33.4)	81.6 (49.6)	94.4 (48.9)	95.8 (39.7)	78.9 (48.5)	95.4 (49.0)	95.1 (39.6)
Pattern #3	71.1 (50.6)	80.4 (43.2)	73.0 (39.4)	75.3 (53.3)	83.5 (44.5)	75.0 (39.4)	76.9 (44.7)	80.0 (39.3)	79.2 (34.7)	77.9 (45.2)	80.0 (39.3)	78.5 (34.6)
Pattern #4	54.0 (29.1)	62.9 (31.8)	67.5 (33.4)	58.3 (29.9)	65.3 (33.8)	69.2 (33.4)	81.6 (49.6)	94.4 (48.9)	95.8 (39.7)	86.3 (50.2)	95.4 (49.0)	95.1 (39.6)
Pattern #5	71.1 (50.6)	80.4 (43.2)	73.0 (39.4)	75.3 (53.3)	83.5 (44.5)	75.0 (39.4)	76.9 (44.7)	80.0 (39.3)	79.2 (34.7)	77.9 (45.2)	80.0 (39.3)	78.5 (34.6)
Pattern #6	61.4 (38.9)	69.6 (40.7)	77.0 (38.9)	63.1 (38.8)	71.3 (40.6)	78.5 (39.0)	100 (52.6)	100 (46.4)	95.8 (40.1)	100 (53.0)	100 (46.7)	95.1 (39.9)
Pattern #7	71.1 (50.6)	80.4 (43.2)	73.0 (39.4)	75.3 (53.3)	83.5 (44.5)	75.0 (39.4)	76.9 (44.7)	80.0 (39.3)	79.2 (34.7)	77.9 (45.2)	80.0 (39.3)	78.5 (34.6)
Pattern #8	51.1 (32.1)	61.0 (36.1)	70.1 (36.4)	53.9 (33.1)	63.7 (36.8)	72.5 (36.9)	100 (55.3)	94.4 (48.2)	95.8 (39.7)	100 (55.3)	95.4 (48.2)	95.1 (39.6)
Pattern #9	68.2 (39.9)	80.4 (41.0)	81.1 (38.4)	70.6 (39.9)	83.5 (43.0)	83.3 (38.4)	91.7 (46.6)	100 (44.6)	100 (40.9)	90.3 (46.1)	100 (44.6)	100 (40.9)
Pattern #10	58.5 (43.2)	69.6 (41.2)	73.0 (39.4)	60.8 (42.4)	71.3 (41.0)	75.0 (39.3)	84.6 (48.7)	89.5 (43.8)	87.5 (37.2)	85.7 (49.2)	90.3 (44.1)	88.2 (37.5)
Pattern #11	68.2 (39.9)	80.4 (40.9)	81.1 (38.4)	70.6 (39.9)	83.5 (43.0)	83.3 (38.4)	91.7 (46.6)	100 (44.6)	100 (40.9)	90.3 (46.1)	100 (44.6)	100 (40.9)
Pattern #12	54.0 (29.1)	62.9 (31.8)	67.5 (33.4)	58.3 (29.9)	65.3 (33.8)	69.2 (33.4)	81.6 (49.6)	94.4 (48.9)	95.8 (39.7)	82.7 (49.6)	95.4 (49.0)	95.1 (39.6)
Average	71.0 (38.9)						90.2 (43.9)					

Table S2. The percentage of the staples with the 14-nt dsDNA seed dsDNA domain in total staples when applying the middle connection layer. The values in parenthesis denote the fraction of basepairs that reside on strands with seeds. The patterns used are shown in Figure S4.

Pattern	Prior block (ID = 1)						Posterior block (ID = 11)					
	Icosahedron			Cuboctahedron			Icosahedron			Cuboctahedron		
	42bp	63bp	84bp	42bp	63bp	84bp	42bp	63bp	84bp	42bp	63bp	84bp
Pattern #13	78.5 (43.3)	70.0 (36.6)	79.2 (35.4)	77.4 (43.7)	70.0 (36.8)	79.7 (35.9)	**94.2 (48.1)**	**85.4 (41.0)**	**79.2 (37.4)**	**92.9 (46.9)**	**84.6 (40.3)**	**78.5 (36.8)**
Pattern #14	73.2 (42.2)	72.9 (40.4)	69.2 (33.8)	76.4 (44.5)	77.8 (43.4)	69.2 (34.1)	66.7 (39.4)	83.7 (37.5)	86.8 (43.8)	66.7 (39.3)	82.8 (36.7)	86.1 (43.2)
Pattern #15	67.9 (36.3)	80.5 (38.1)	76.1 (31.5)	67.8 (35.7)	84.8 (40.0)	77.1 (31.7)	72.8 (39.9)	87.1 (44.4)	85.2 (41.4)	74.1 (41.1)	85.8 (44.3)	86.0 (41.5)
Pattern #16	72.1 (39.2)	75.0 (39.8)	70.7 (32.8)	74.1 (41.3)	79.6 (42.9)	70.4 (33.3)	68.1 (38.3)	86.4 (40.1)	89.4 (44.5)	67.8 (38.5)	84.8 (38.7)	88.0 (43.8)
Pattern #17	66.7 (35.6)	79.8 (37.3)	78.1 (31.7)	66.7 (35.0)	82.8 (38.6)	78.8 (31.9)	75.4 (43.3)	84.8 (44.9)	85.2 (41.4)	76.4 (44.2)	83.8 (44.8)	86.0 (41.5)
Pattern #18	75.0 (48.5)	72.4 (40.0)	74.1 (36.0)	77.4 (49.8)	74.0 (40.9)	75.4 (36.4)	84.3 (44.7)	80.0 (35.7)	69.7 (32.3)	84.5 (44.1)	80.0 (35.7)	70.5 (32.5)
Pattern #19	68.6 (36.7)	81.4 (38.8)	75.0 (31.3)	69.0 (36.4)	87.5 (41.7)	75.0 (31.5)	71.4 (37.9)	88.4 (44.1)	85.2 (41.4)	71.4 (37.4)	88.3 (43.8)	86.0 (41.5)
Pattern #20	75.8 (48.1)	72.9 (41.1)	69.2 (35.0)	83.3 (51.8)	77.8 (44.0)	69.2 (35.2)	77.2 (44.2)	79.2 (34.4)	71.9 (34.6)	75.7 (43.4)	79.0 (34.1)	73.3 (35.4)
Pattern #21	77.8 (40.6)	71.4 (36.1)	79.2 (34.3)	76.5 (40.2)	71.8 (36.2)	79.7 (34.5)	94.1 (49.9)	85.1 (42.7)	82.4 (39.2)	92.6 (49.2)	84.2 (42.4)	82.5 (39.1)
Pattern #22	75.0 (47.9)	72.4 (40.6)	70.5 (33.4)	80.0 (50.7)	75.7 (42.3)	72.5 (35.8)	79.2 (44.3)	79.5 (34.8)	71.3 (34.0)	80.7 (43.8)	79.6 (35.0)	71.7 (33.8)
Pattern #23	77.2 (38.2)	72.7 (35.7)	79.2 (33.4)	75.7 (37.3)	73.4 (35.7)	79.7 (33.4)	93.9 (51.4)	84.8 (43.3)	85.2 (40.8)	92.4 (51.1)	83.8 (44.1)	86.0 (41.0)
Pattern #24	71.4 (37.9)	75.8 (39.6)	71.2 (32.4)	71.4 (37.4)	82.0 (42.3)	71.8 (32.4)	68.6 (37.9)	87.5 (41.0)	90.4 (44.8)	69.0 (37.4)	87.5 (41.1)	90.4 (44.5)
Average	75.0 (38.3)						81.6 (41.0)					

Table S3. Fraction of staples with 14-nt seed domains and basepairs that reside on strands with 14-nt seed domains when using the FV design. Ratio, A (%) = (# of staples with one or more 14-nt seed domains / total # of staples) and Ratio, B (%) = (# of nucleotides in 14-nt seed domains / total # of staple nucleotides)

Target structures	Edge length	Staple-break	# of staples with 14-nt seed domains	# of staples with 4-nt dsDNA domains	Ratio A	# of nucleotides in 14-nt seed domains	# of nucleotides in 4-nt dsDNA domains	Ratio B
Tetra-hedron	42	*Max. length*	33	0	91.7	744	0	46.6
		Max. seeds	36	6	100	813	21	50.9
	63	*Max. length*	54	0	100	1050	0	44.6
		Max. seeds	66	36	100	1218	168	51.8
	84	*Max. length*	72	0	100	1272	0	40.9
		Max. seeds	102	75	100	1707	420	54.9
Octa-hedron	84	*Max. length*	144	0	100	2544	0	40.9
		Max. seeds	202	147	100	3381	812	54.4
Pentagonal bipyramid	42	*Max. length*	81	0	90.0	1833	0	45.8
		Max. seeds	90	18	100	2040	63	51.0

Table S4. Fraction of staples with 14-nt seed domains and basepairs that reside on strands with 14-nt seed domains when using the MV design. Ratio, A (%) = (# of staples with one or more 14-nt seed domains / total # of staples) and Ratio, B (%) = (# of nucleotides in 14-nt seed domains / total # of staple nucleotides)

Target structures	Minimum edge length	Staple-break	# of staples with 14-nt seed domains	# of staples with 4-nt dsDNA domains	Ratio A	# of nucleotides in 14-nt seed domains	# of nucleotides in 4-nt dsDNA domains	Ratio B
Tetra-hedron	42	*Max. length*	31	1	64.5	603	4	28.2
		Max. seeds	45	36	77.6	693	158	32.4
	63	*Max. length*	51	0	82.3	907	0	31.3
		Max. seeds	76	73	82.6	1174	378	40.5
	84	*Max. length*	67	0	80.7	1143	0	31.3
		Max. seeds	104	101	85.2	1577	581	43.2
Octa-hedron	84	*Max. length*	111	6	68.5	1712	24	24.3
		Max. seeds	189	182	82.5	2829	1036	40.1

Table S5. Required scaffold lengths for 40 rendered 6HB DNA-NPs of 42-bp edge length. The values in parenthesis denote required scaffold lengths for the MV DNA-NPs. 28 (FV) and 32 (MV) of the 40 structures, indicated with (*), require a scaffold length longer than the 7,249-nt M13mp18. These each used a random sequence of the appropriate length to demonstrate the theoretical scaffold and staple routing.

Category	Required scaffold length (nt)				
Platonic	Tetrahedron **1,512 (2,218)**	Cube **3,024 (3,704)**	Octahedron **3,024 (3,738)**	Dodecahedron **7,560* (8,590*)**	Icosahedron **7,560* (9,708*)**
Archi-medean	Cuboctahedron **6,048 (8,736*)**	Icosidodecahedron **15,120* (22,140*)**	Rhombi-cuboctahedron **12,096* (18,282*)**	Snub cube **15,120* (20,340*)**	Truncated cube **9,072* (14,700*)**
	Truncated Cuboctahedron **18,144* (23,760*)**	Truncated dodecahedron **22,680* (36,900*)**	Truncated icosahedron **22,680*(27,000*)**	Truncated octahedron **9,072* (11,676*)**	Truncated Tetrahedron **4,536 (6,732)**
Johnson	Gyroelongated pentagonal pyramid **6,680* (8,334*)**	Triangular pyramid **2,292 (3,075)**	Pentagonal bipyramid **3,780 (4,794)**	Gyroelongated square bipyramid **6,096 (7,897*)**	Square gyrobicupola **8,192* (11,992*)**
	Pentagonal orthocupola-rotunda **12,830* (18,710*)**	Pentagonal orthobirotunda **15,120* (22,100*)**	Elongated pentagonal gyrobicupola **15,300* (22,935*)**	Elongated pentagonal gyrobirotunda **20,340* (30,110*)**	Gyroelongated square bicupola **14,720* (19,658*)**
Catalan	Rhombic dodecahedron **6,048 (7,232)**	Rhombic triacontahedron **15,120* (18,240*)**	Deltoidal icositetrahedron **13,824* (16,018*)**	Pentagonal icositetrahedron **16,992* (19,724*)**	Triakis octahedron **11,088* (14,227*)**
	Disdyakis dodecahedron **23,040* (29,086*)**	Triakis Icosahedron **28,260* (36,215*)**	Pentakis dodecahedron **22,980* (29,988*)**	Tetrakis hexahedron **9,912* (12,664*)**	Triakis tetrahedron **5,364 (7,063)**
Miscel-laneous	Twisted Triangular prism **3,024 (4,359)**	Heptagonal bipyramid **10,668* (12,786*)**	Enneagonal Trapezohedron **40,716* (43,897*)**	Small stellated dodecahedron **34,560* (46,302*)**	Rhombic hexe-contahedron **30,720* (42,270*)**
*** indicates designs that require scaffold length greater than the 7,249-nt M13mp18**					

Table S6. Design parameters of the automatic sequence design for the FV DNA-NPs.

	Tetrahedron			Octahedron	Pentagonal bipyramid
	42bp	63bp	84bp	84bp	42bp
Geometry					
# of faces, N_f	4	4	4	8	10
# of vertices	4	4	4	6	7
# of edges, N_e	6	6	6	12	15
# of arms at the junction	3	3	3	4	4,5
Maximum edge length (bp)	42	63	84	84	42
Minimum edge length (bp)	42	63	84	84	42
The minimum spanning tree of the dual graph of the loop-crossover structure					
# of nodes, $N_f + 2N_e$	16	16	16	32	40
# of edges, $4N_e$	24	24	24	48	60
# of members of the spanning tree	15	15	15	31	39
Scaffold					
# of unpaired nucleotides, N_{un}	0	0	0	0	0
Required length (bp) $= 6 \times \left[\sum_{i=1}^{N_e} i \text{ th edge length(bp)}\right] + N_{un}$	1,512	2,268	3,024	6,048	3,780
# of double crossovers	15	15	15	31	39
Staples					
# of staples	36	54	72	144	90
# of nucleotides in staples	1,596	2,352	3,108	6,216	4,000
Minimum length (bp)	30	30	30	30	30
Maximum length (bp)	54	54	54	54	54
Average staple length (bp)	44.33	43.56	43.17	43.17	44.44
# of double crossovers	33	69	105	209	81
# of unpaired nucleotides	84	84	84	168	220

Table S7. Design parameters of the automatic sequence design for the MV DNA-NPs.

	Tetrahedron			Octahedron
	42bp	63bp	84bp	84bp
Geometry				
# of faces, N_f	4	4	4	8
# of vertices, N_v	4	4	4	6
# of edges, N_e	6	6	6	12
# of arms at the junction	3	3	3	4
Maximum edge length (bp)	42	63	84	84
Minimum edge length (bp)	74	95	116	106
The minimum spanning tree of the dual graph of the loop-crossover structure				
# of nodes, $4N_f$	12	12	12	24
# of edges, $4N_e$- N_f	20	20	20	40
# of members of the spanning tree	11	11	11	23
Scaffold				
# of unpaired nucleotides	102	102	102	138
Required length (bp)	2,118	2,874	3,630	6,762
# of double crossovers	11	11	11	23
Staples				
# of staples	48	62	83	162
# of nucleotides in staples	2,142	2,898	3,654	7,056
Minimum length (bp)	23	29	25	21
Maximum length (bp)	59	61	60	60
Average staple length (bp)	44.63	46.74	44.02	43.56
# of double crossovers	61	97	133	253
# of unpaired nucleotides	126	126	126	432

Table S8. Staple sequences for the FV tetrahedron of 42-bp edge length. The sequence is represented by colors; unpaired nucleotides with blue, and crossovers with orange, the 14-nt seed dsDNA domain with green, and the 4-nt dsDNA domain with red.

Staple ID	Length (bp)	Staple sequences
1	54	AACAAAATTAATTACATTTAACAAAGGAAGATGATGAAACACGTTATTGAATAA
2	54	AGAACTCAAACTATCGGCCTTGCTCAGTAATAACATCACTGCCCCCGGAAATAC
3	54	AAGAATACGTGGCACAGACAATATACATAGAACCCTTCTGTTTACAATTAAAAA
4	52	ACAAAATCGCGCAGTTTCATTTGAATATATATGTGGCTTTGAATACCAAGTT
5	52	GTCTGTCCATCACGGGTAATATCCAGAAACGCTCAGGCCACCGAGTAAAAGA
6	52	TCACCAGTCACACGTTTTGAATGGCTAAACATCGCTATTTACATTGGCAGAT
7	52	TAGCGGTCACGCTGTTCCTCGTTAGAAAGGGATTTTAGGGCGCTGGCAAGTG
8	52	CCAGCAGCAAATGAGAATTGAGGAAGCTAATAGATCAGTGCCACGCTGAGAG
9	52	GATGATGGCAATTCAACAGAAATAAAATGAATATACATATTCCTGATTATCA
10	52	CATATCAAAATTATTTGCACGTAAATTGAATAATGGAAGGCGAGTACCTTTT
11	52	AGTTGGCAAATCAACAGTTGAAAGAAATCAAACCCTCAATGGGTCAATAGAT
12	52	TTTGACGAGCACGTATAACGTGCTCGCGCTACAGGGCGCGACGAACGGTACG
13	51	GCCATTGCATTGACGCTTTTTTTCAATCGTCTGAAATGGATCAACAATTC
14	50	AACAGTACATCTGTAAATTTTTTTTCGTCGCAAAGGGATGCCTGAGTAGA
15	50	GCCGCGCTTTGAGAAGTTTTTTTTGTTTTTATAATCAGTGATGATTTAGA
16	50	GTTTGGATTGAAACAATTTTTTTTAACGGATTCGCCTGATTAGTAATTTT
17	50	CGAACTGATCGAACCACTTTTTTTCAGCAGAAGATAAATACTATGGTTGC
18	49	ATTCTGGCCCGTATTATTTTTTTAATCCTTTGCCCGAAAACATCAAGAA
19	49	TTGCTGAACGAGGATTTTTTTTTAGAAGTATTAGACACCTGAAAGCGT
20	49	AATTACCTGTGAGTAATTTTTTTCATTATCATTTTGCCAATATCTGGTC
21	49	AATACTTCTGGGGAAATTTTTTTGCCGGCGAACGTGGGTTAGAACCTAC
22	47	GCGGGCGCTAGACAGAGAGGTGAGCCGATTAATCAGAGCGGGAGCTA
23	47	GCCTGCAATAGAGCCAACAAAGAACTAACAAGTTATCTAAAATATCT
24	47	ATTATCATCAGTAACAGAAAGGAAACGTCAGGAAATTGCGTAGATTT
25	34	AACAGGAGGGCGGTCAGTTTTTTTATTAACACC
26	34	TCAGGTTTAGGGAAGAATTTTTTTAGCGAAAGGA
27	34	TTAGGAGCAACCACCAGTTTTTTTAAGGAGCGGA
28	32	CCAGAATCCAATGCGCCGTAACCACCACACCC
29	32	AATACATTTCTCAAATAATCTAAAGCATCACC
30	32	ACATCGGGAATACTTCCAATATAATCCTGATT
31	30	AAAAGTTAGCAAAAGCGAATTATTCATTTC
32	30	GCTTGACTTGATTAAATTAACCGTTGTAGC
33	30	GACAACTAACAGAGCAGTAATAAAAGGGAC
34	30	CCTTGCTTAAATCATACCTTTTTTAATGGA
35	30	CTACATTACAGGAAAACAATATTACCGCCA
36	30	TACCGAAAGCCCTAATTAGTCTTTAATGCG

Table S9. Staple sequences for the FV tetrahedron of 63-bp edge length. The sequence is represented by colors; unpaired nucleotides with blue, and crossovers with orange, the 14-nt seed dsDNA domain with green, and the 4-nt dsDNA domain with red.

Staple ID	Length (bp)	Staple sequences
1	54	ATCGGAACGAGGGTAGCAAAACGGGCCTAAAACGAAAGAACCCCCACGTTAAT
2	54	TTCATTCCATATAACAGTTGCAAATGGGGCGCGAGCTGAAATTAACATAGGAAT
3	54	CTGTATGGGATTTTGCTAAATTGCGAAAAAAGGCTCCAAAGCTTTCGTCCTCAT
4	52	GTCATTTTTGCGGATTTAGTTTGACCCATCAATTCGCTCCTTTTGATAAGAG
5	52	AACTACAACGCCTGGAGAATAGAAAGTTTAATTGTGTTTCGTCACCAGTACA
6	52	TCGCCCACGCATAAGACTTTTTCATGGAATACACTGACAATGACAACAACCA
7	52	GTCAGTGCCTTGAGTACCAGGCGGATCCACCCTCATAATAAGTTTTAACGGG
8	52	CTTAGCCGGAACGAATTCATTACCCATGGGCTTGACGACCTGCTCCATGTTA
9	52	AAATAGCGAGAGGCCGAGAATGACCAGAAGCCCGAGACGACGATAAAAACCA
10	51	AATAGGTGTCGCCTGATTTTTTTTAAATTGTGTCGAAATCCGGACTGGCTC
11	51	CTTGCCCTGAACACTATTTTTTTTCATAACCCTCGTTTACCAAACAAACTC
12	51	GTTGAAAATAACAGCTTTTTTTTGATACCGATAGTTGCGCCAAGAACAAC
13	51	TCAGAAGCACTTTTGATTTTTTTTGATACAGGAGTGTACTGGGAATAGCAA
14	50	ACTACGAAGCGCGAAACTTTTTTTTAAAGTACAACGGAGTATTAAGAGGCT
15	50	GCTATATTTCAGGCAAGTTTTTTTGCAAAGACACAAACTAAATGAATTTT
16	50	CAGTTAATGAGGAACCTTTTTTTTCATGTACCGTAACACTGAATAAAGCGC
17	50	GCCAGAGGGTCAGGATTTTTTTTTAGAGAGTACCTTTAATTTAATGCAGA
18	49	GAGGCTTGCCAGGTAGTTTTTTTAAAGATTCATCAGTGTGTCTGGAAGT
19	49	CCTCATAGTGAATTTATTTTTTTCCGTTCCAGTAAGCGGAATCGTCATA
20	49	TAAGGGAACCAGTCAGTTTTTTTGACGTTGGGAAGAAGCGAAAGACAGC
21	49	CTGAATATACGCCAAATTTTTTTTAGGAATTACGAGGCGACCAGGCGCAT
22	46	GAGACTCCTCAAGAGAAGGGGGTTGATACTCAGGAGGTTTAACCGC
23	46	AATATTCATTGAATCCCCCGGTCTTTTTGCATCAAAAAGACGTTTT
24	46	AGGCTGGCTGACCTTCATCAGCTGCTACACCAGAACGAGTCTTTAA
25	45	CACCCTCATTTATTATTTTAGCGGGGTTTTGCTCAGTACCTATTT
26	45	TTATGCGATTAGGACAGATCTTGACAAGAACCGGATGGACCAACT
27	45	GCGAACCAGACTGGATACTTTAAACAGTTCAGAAAATTGTAAAAT
28	42	ACCACATTAAATATAATTCTGCGAACGAGTAGATGAGCTCAA
29	42	TTGAAAGTTAAGAATGGTTTAATTTCAAAGTAAATAATCAAC
30	42	TAAAGCCTGTCGTCTCAACAGTTTCAGCGGAGTTAACGATCT
31	42	AAAACGAGCGGGATAGAGGCTTTGAGGACTAAACCTAAAGGC
32	42	CGGAACCTTCAGGGACCGCCACCCTCAGAGTACCGAAGTGCC
33	42	TTCCATTCGGCTACCGTCACCCTCAGCAAAATCTAGCGATTA
34	42	GTTTAGACCGGAAGGACTTCAAATATCGTTAAGAGTAAATCA
35	42	CATGTTTTCAACTACTAATAGTAGTAGCAAGGTGGATTAGAT
36	42	ACATTTCGATTCCCGCAACTAAAGTACGTGAGATTTCCAATA
37	42	AAAGTTTAGAATGGCGGTTTATCAGCTTAGGAGCCGAACAAC
38	42	TAAAGGAACAACTTTTTCCAGACGTTAGAAATAAAAGGTGAA
39	42	CGCTTTTACTAACGAACACTCATCTTTGGGCAAAAAGGAAGT
40	39	GTCGAGAATTAGGACTGAAACATGAAAGATCAGAGCCAC
41	39	GTAACAAAAGAGTAATGAACGGTGTACAATTGAATTACC
42	39	AAAATCATCAAATGGCGTCCAATACTGCGTAGCTTCAAA
43	38	TCATTGAGTAAGAGCACGAGAACATTCAGTGAATAAGG

44	38	AATTCGCATACATGGAAGCGGAACCCTGACTATTATAG
45	38	CACCCTTTGTATCATATCACCGTATAAGTATAGCCCGG
46	30	TACATAAATGCTGTGCTTAGAGCTTAATTG
47	30	AGTCTCTTAGCGTAGCATTCCACAGACAGC
48	30	ATTATTAAGGGAGTGATATATTCGGTCGCT
49	30	GCCCAATCCCCCTGACAGTGCCCGTATAAA
50	30	ATTATACCGAACTGCGCAGACGGTCAATCA
51	30	CAACAGGGGTAATATTGCAAAAGAAGTTTT
52	30	AATCATATCATTTGGTCAATAACCTGTTTA
53	30	TTTCTTACTCCAAAATAATAATTTTTTCAC
54	30	TACCAAGGCACCAATAAAATACGTAATGCC

Table S10. Staple sequences for the FV tetrahedron of 84-bp edge length. The sequence is represented by colors; unpaired nucleotides with blue, and crossovers with orange, the 14-nt seed dsDNA domain with green, and the 4-nt dsDNA domain with red.

Staple ID	Length (bp)	Staple sequences
1	54	GAGTACCTTTAATTGCTCCGGTGTCTAATTCTGCGAACGAGCGAGCTGGCTGAC
2	54	CACCACCAGAGCCGCCGCCCTGAATTGATGATACAGGAGTTATTTCGCCAATAA
3	54	CCTCAGAACCGCCACCCTCCAAACTATAGTTAGCGTAACGCAGTTTCCGCAGAC
4	52	AAGCGGATTGCATCAATATAATGCTGTTCGCAAATTATTATAGTCAGAAGCA
5	52	CTTTTCATAATCAACACAAACAAATAGTGCCTTGATTATTAGCGTTTGCCAT
6	52	ATTAGGATTAGCGGGCCCAATAGGAATTAGTAAATGACTCCTCAAGAGAAGG
7	52	AAAAGAACTGGCATACCGATTGAGGGAAGGCCGGAATAATAACGGAATACCC
8	52	TATCAGCTTGCTTTAGCAACGGCTACAACACTCATCTTTAATTGTATCGGTT
9	52	CTTTAATCATTGTGAAAAGGAATTACTTAGACTGGAGATGGTTTAATTTCAA
10	52	ATTTTGTCACAATCAATAGAGGTGAAATTAGAGCCAGCAATCTTTTTTCACG
11	52	AGGTAGAAAGATTCATCAGTTTACCATTTGCAAAAGAAGTTTGCAGATAGCC
12	52	GGAGTTAAAGGCCGCTTTTAGTTTCCAAGGCACCAACCTAGTCTTGCCCTGA
13	51	AAAATAGCGTACCAGAATTTTTTTTGGAAACCGAGGAAACGCAAATGTAGCG
14	51	ACGTAATGCCCAGAACGTTTTTTTTAGTAGTAAATTGGGCTTGATAGAATGA
15	51	GTCATACATGAAACATGTTTTTTTTAAAGTATTAAGAGGCTGAGAAAAGAGG
16	51	CTTGAGCCATCCAAAAATTTTTTTTAAAGGCTCCAAAAGGAGCCTCGAAATC
17	50	ATAACAGTTAATTCTACTTTTTTTTAATAGTAGTAGCACGCCACCAGAAC
18	50	CGCAGTATGATCGGCATTTTTTTTTTTTCGGTCATAGCCCCCGTTGAAATA
19	50	CCACAGACAAGAAAGGATTTTTTTTACAACTAAAGGAATCGGAATAAGTTT
20	50	TAATAAAGTAGCGACAAAAGAAATATGGTTTACCAGTTGACGGAGTAGCA
21	50	ATAAGGACAACGGAGATAACCGCGTCACCCTCAGCACTAAAGAAGAGGCA
22	50	TAAGAACTGTCAAAAATTTTTTTTCAGGTCTTTACCCTGACGGTCATTAC
23	50	AAGTAAGAATCCCCCTAATAAATTAGGAATACCACAGCAACACGAGGGGG
24	49	GCGGATAAGAACGGTGTTTTTTTTACAGACCAGGCGCGTCAGGATTAGA
25	49	CAGCTTGATTGCTCCATTTTTTTTGTTACTTAGCCGGTAGTACCGCCAC
26	49	CCCGAAAGAAACGTAATTTTTTTCAAAGCTGCTCATTTGAGGCTTGCAG
27	49	CACCACCGGCTATCTTTTTTTTTACCGAAGCCCTTTTCAACATTATTAC
28	45	TTTTAACAAACAGTGCAAAGAAGAGCAACACCCTCGACGATTGGC
29	45	CGTCTTTATTTTGCGAACCGAACTGACCAAGTATATCATTTTCAG
30	45	ACCATTAAGCTATAATCTTGACAAGAACTCGAGCTGCTTAGAGCT
31	44	AAAGAATTTATACCTCATCGCCTGATAAGACAACAACAGCATCG
32	44	CCATTACCCATCGAAGTTTGCCTTTAGCTACATAAGACAAAAGG
33	44	TAATAGTCGGAATCCTTTAAACAGTTCAGTTGGGAAATGCAGAT
34	42	CTTCATCACCGGAAAAGAGGTCATTTTTTTAAATATAGTTTG
35	42	ATCATACCAGAGCCACAGGAGGTTGAGGCCAGAATTAATAAG
36	42	GGTCAATTATCACCCACCCTCAGAGCCCACTGAGGTTTTGT
37	42	AATACTGAAAATGTGAGGCATAGTAAGATTCAACTAGAAAAA
38	42	AATGAAACATTAGCAGGGAAGGTAAATACGCCAAAAGGTGGC
39	42	TCTACGTTCAAATGGTCATAAATATTCATTTGCCATATCATA
40	42	CCAGCGAACACTAAAGAGGCTTTGAGGAGCGAAAGACCATCG
41	42	AACATATAGAATCATAGCAGCACCGTAAAATCACCAATTAT
42	42	CCTGTTTGATACATTAGCTCAACATGTTGCGGATGTCAAAGC
43	42	GAACCAGAAGAGTATTTTCATTTGGGGCGTAGATTTGCAACT
44	42	AAAGTACTTTGATGCAAACTCCAACAGATAGGCTGAAAAGG
45	42	CCCGTATGGGGTCAAATCCTCATTAAAGCAGGTCAAGAACCG

46	42	CCACCCTAGGCAAGTAATGCCCCCTGCCGTACTGGGAAAGC
47	42	GCAGTCTAGCATTGACCACCCTCAGAGCTTAACATGAACCTA
48	42	CCCACGCATTTGTAAAGCGCGAAACAAAAAACGAACTTTTTC
49	42	GTATGGGCCAGACGCCCATGTACCGTAAACCACCCGCCCGGA
50	42	ATAGGTGCATAAGGTAAACAACTTTCAAATCTAAATTCGTC
51	42	ACCAGTAAGAACCGGTACTCAGGAGGTTAACGAGGAGCGGAG
52	40	ACATAACGCCAAATACCAGTCAGGACGAAAACGAGCGTCC
53	40	GAACGAGGGTCGGTTGCGCCGACAATATTGTGTTTGACCC
54	40	GCGACATTCAGAACGTAGAAAATACAGTCAGACCGTCACC
55	39	TAATTGCTGAATATCGCGTTTTAATCGGATATTCAATAA
56	39	CTTGATATTAATCCCTCAGAGCCGCGAAACAAACAGTG
57	39	GGATAGCAAGGGAGAGGGTTGATATAACTTTGATTTTCT
58	34	TCATTAAAAAATTCACGCAAAGACACCATGCGAA
59	34	ATGAGGAGCGGGATATATATTCGGTCGCCAGTGA
60	34	ACCCTCGTTGAGATACGAACTAACGGAATAAGAA
61	32	CGAGAAACACACTACGATTAAACGGGTAAAAT
62	32	GAACAAAGTAGAGGCTGACGACGATAAAAACC
63	32	TTGAAAATCTTTGGGATTATCACCGTCACCGA
64	30	CCAAATCCTTCAAAAAAGATTAAGAGGAAG
65	30	GCAATAGAACCGCCTCACCGGAACCAGAGC
66	30	ACAGATGTGCCGTCTTTTGCTCAGTACCAG
67	30	CGTTTTCTTAGCAATTAAGACTCCTTATTA
68	30	CGCGACCACCGATAAGGTGAATTTCTTAAA
69	30	CCATAAAGCTCATTTTACCTTATGCGATTT
70	30	TGGCATCGATTCCCGGAAGTTTCATTCCAT
71	30	TTATTCTGGCTTTTTACCGTTCCAGTAAGC
72	30	TGAGAATGCCCTCACAACGCCTGTAGCATT

Table S11. Staple sequences for the FV octahedron of 84-bp edge length. The sequence is represented by colors; unpaired nucleotides with blue, and crossovers with orange, the 14-nt seed dsDNA domain with green, and the 4-nt dsDNA domain with red.

Staple ID	Length (bp)	Staple sequences
1	54	GAGTACCTTTAATTGCTCCGGTGTCTAATTCTGCGAACGAGCGAGCTCCATCGC
2	54	ATGCAAATCCAATCGCAAGTAAGGCGCTAGAAAAAGCCTGCGCCATATAGAAAA
3	54	GCAGCAAATGAAAAATCTATAAAATAGCCGTCAATAGATATTATTAACCAATAA
4	54	CACAGACAGCCCTCATAGTGGAGTGATAATAATTTTTTCAGAATTTCAACGGGG
5	54	TTTGCACGTAAAACAGAAATTGCTTTATTATTCATTTCAAATTACCTGAAAGCG
6	52	GGTGAATTATCACCGGCATTTTCGGTCACCACCCTGGAAATTATTCATTAAA
7	52	AAGAAACGATTTTTAGAGCAAGAAACAACTGGCATTTTATCCCAATCCAAAT
8	52	ATCGGAACGAGGGTAACAAAGTACAAGAAAGAGGACAGCAGCGAAAGACAGC
9	52	AACCGCCACCCTCAGAATTTTCTGTAAAAAGGAGCAGAACCGCCACCCTCAG
10	52	AAGCGGATTGCATCAATATAATGCTGTTCGCAAATTATTATAGTCAGAAGCA
11	52	CTGATAGCCCTAAATGGTCAGTTGGCCTTTACAAAAGTCTTTAATGCGCGAA
12	52	CGGAATTATCATCAGTAACAGTACCTAAACATCAAGAAACCACCAGAAGGAG
13	52	GAATCAGAGCGGGAAGAAGAACTCAACATTGGCAGACGTGCTTTCCTCGTTA
14	52	GCTTAGATTAAGACTCTTCTGACCTATTACCAGTATTGAAAACATAGCGATA
15	52	GCGAAAATCCTGTTATCACCCAAATCCGAAAGGAGCTGGTTTGCCCCAGCAG
16	52	CAACATGTTCAGCTCCGTTTTTATTTAAGCCTTAACAGACGACGACAATAAA
17	52	CTTTAATCATTGTGAAAAGGAATTACTTAGACTGGAGATGGTTTAATTTCAA
18	52	GAACGTGGACTCCAACGTCATCGGAAGGGGAAAGCCGGCGGCAATAAGAGAA
19	52	AGGTAGAAAGATTCATCAGTTTACCATTTGCAAAAGAAGTTTCCCTTCACCG
20	52	TGTCTTTCCTTATCATTCCCAAATCAGCGAGGCGTTTTAGTTCTTGCCCTGA
21	52	AGCACCGTAATCAGTAGCGAATCAAACTCCCTCAGAGCCGAGTATTAAGAGG
22	52	TCAGAGGGTAATTGAGCGCTTTAAGAAAGGAAACCGAGGATATCAGTACCAG
23	52	TCCATCACGCAAATTAACCTACCGCCTACCTACATTTTGACTTGCTTCTGTA
24	52	ACGAAAGAGGCAAAAGAATAAATCCGGCGCAGACGGTCAATGAATAGGTGTA
25	51	AAAACGCTCTATTAATTTTTTTTAATTTTCCCTTAGAATCCTAGACATTC
26	51	CGATTTAGACCGACAAATTTTTTTAGGTAAAGTAATTCTGTCATGAGCCTA
27	51	AAAATAGCGGAGAGAGTTTTTTTTTGCAGCAAGCGGTCCACGCGACAGGGC
28	51	CAACTAATAGTAACATTTTTTTTTATCATTTTGCGGAACAAAGACATGGCT
29	51	ACTTAGCCGTCAGGAGGTTTTTTTTTTAGTACCGCCACCCTCCTTAATGCC
30	51	CCGGTATTCCCAGAACGTTTTTTTAGTAGTAAATTGGGCTTGATAGAATGA
31	50	TGAAAGCATTGACAGGCCGGAACAAGTTTGCCTTTATAGCGTTCAGAACC
32	50	ACCGGAATCCATGTAATTTTTTTTTTAGGCAGAGGCATTCCACTATTAAA
33	50	CGGCAAAATATGGTTGTTTTTTTCTTTGACGAGCACGTATAATAAGAATA
34	50	TTTTGCGAAAATACAGACGGGAAGAGAGATAACCCAAGCTATCTAATAAC
35	50	GCCCGGACCTTCATCTACGTAAAACACTCATCTTTGATCGCCTGGAACCG
36	50	CCACCACCGCTCAAGAGTTTTTTTAAGGATTAGGATTACCCTGAACAAAG
37	50	TGAATTTATTGAGGGATTTTTTTGGGAAGGTAAATATTGACCATTGATAT
38	50	TTATCAACAAGTTACATTTTTTTAAATAAACAGCCATATTAGAACGCAAA
39	50	CTAAAGGAAACCGATAGTTTTTTTTTGCGCCGACAATGGTCAGGATTAGA
40	50	ATAACAGTTAATTCTACTTTTTTTTAATAGTAGTAGCACGCTGAGAGCCA
41	50	CCCGAAAGAGCCGCTTTTTTTTTTGCGGGATCGTCACCCTCATCATTAC
42	50	TAAGAACTGTCAAAAATTTTTTTTCAGGTCTTTACCCTGACGGGCAGGGA
43	50	TAACCTGGCCAACAGATAATCACAATACTTCTTTGATGGTAATTCGTCTG
44	50	TAAAGGGATCAGACAATTTTTTTTATTTTTGAATGGCTATTCACCAGGGT
45	50	AATCGCGCAAGTACATATTTTTTTAATCAATATATGTGTAAAAGAGTCTG

46	50	GCCAGTGCGTAACCATGTTCCAGAAAAACCGTCTATCGAGGTGCGAGAAA
47	50	ATAAGGATCCTGAATTTACGAGGGTATTAAACCAAGATTACCGCCCGACT
48	50	CGAACAAAGTGCCGTCGTTTTTTTAGAGGGTTGATATACACCAACCTAAA
49	50	TGATTGGAATCCCCCTAATAAATTAGGAATACCACAGCAACACGAGGGGG
50	49	TCAGGGATATATTTCGTTTTTTTGAACCTATTATTCTACCATCGATAGC
51	49	GATGGCAATATACAGGTTTTTTTAGTGTACTGGTAATCCTGTAGCATTC
52	49	TTGGGAATTCAAATAATTTTTTTTATCCTCATTAAAGCATATCAAAATTA
53	49	AAAATAGCACGGAATATTTTTTTAGTTTATTTTGTCAATGTAAATGCTG
54	49	TTTGAGGACAACGTAATTTTTTTCAAAGCTGCTCATTTCAATAATCGGC
55	49	CCGAACGAACTTTTCATTTTTTTCCAGTGAGACGGGCCAACATTATTAC
56	45	TTAGAAGATTAAATGCAAAGATTGCGTAGAGGTGACAAACCCTCA
57	45	GAAGATGACATTTAACCGTTCCAGTAAGTTTGGATAACGTCAGAT
58	45	ACCATTAAGCTATATATATTCGGTCGCTTCGAGCTGCTTAGAGCT
59	45	AAAAAAATTATCAGAACAGTGCCCGTATGTACCGTTTTCCAGACG
60	45	CGTTATACAGTAGGCAGCGCCAAAGACACTACCTTTATATTTTAG
61	44	AACTGACAGACCAGATCTTGACAAGAACGTTTCCAGCGATTATA
62	44	TGCGGGAATTTTGCACGCTAACGAGCGTAAAATAACTCATCGAG
63	44	TAATAGTCGGAATCCTTTAAACAGTTCAGTTGGGAAATGCAGAT
64	44	GCCACCCACCACCAAGGCAGGTCAGACGAGCACCAACTGTAGCG
65	44	AAATGGAACCAGTAACCCTTCTGACCTGAGAATCCTAACATCAC
66	44	GGAAGGGGGCAAGTCGCCGCGCTTAATGGCCCGAGATGGCCCAC
67	44	GGAATACTACGCAGAGGTGGCAACATATTAAAAACTGAGTTAAG
68	42	TGAGTGTCCACACCGTAGCGGTCACGCTAACGTGGCCGTAAA
69	42	TGATAAAACAAAGAGGTTATATAACTATCAATCAATTAACA
70	42	CTGAATATGAATTTACAATTTCATTTGATTACCTGACGGATT
71	42	TCAGTGCTCACCAGACGATCTAAAGTTTACAACTTAATCTCC
72	42	AGTTGCTGGTTTTGTCATCGTAGGAATCTACCGCATATCCCA
73	42	CCACGCAACCGGAAAAGAGGTCATTTTTTTAAATATAGTTTG
74	42	ATCATACACACCGCACCTTGCTGAACCTAAGGAATTGAGGAT
75	42	TCCTAATCTTACCAACCCAGCTACAATTCGAACCTCGCCCAA
76	42	CAGTCTCATGGAAGATTGCGTAGATTTTAACAATAAGCAAAA
77	42	CGCTCAACAAATTCAATTTAATGGTTTGTTTCAAATTTAACC
78	42	TTCATATTAGGTTGACGCGAGAAAACTTAAATACCTCATATG
79	42	TCCGGCTGGTTTACGCTTAATTGAGAATTTTAGTAGACCGTG
80	42	AATACTGAAAATGTGAGGCATAGTAAGATTCAACTAGAAAAA
81	42	CGCCTGATAAAGAAGGTTAGAACCTACCCAGAATGTTTTAA
82	42	CACCAGATCAGAGCCATAGCCCCCTTATGCGTCAGTTACCAT
83	42	TAGCAAGGAGGTTGCCAGAGCCGCCGCCCCACCCTTGCCATC
84	42	TCCTTATCCAAAAGAATGAAATAGCAATCAAGAATAGGGAAG
85	42	CGCATTATACATAATATGTTAGCAAACGAACGCAATTACCGA
86	42	GGTGTACCAACTTTCGGAGATTTGTATCACCCCCATTAAACG
87	42	GGTAAAAAAGAGTAGCGCATAGGCTGGCTCATAAGGATAAAT
88	42	GGGCGCTAAGAAAGAAGTTTTTTGGGGTCAGGGCGATAGGGT
89	42	TCACACGTTATTTAACTATCGGCCTTGCTTAGTAATGAGAAG
90	42	TATCGGTAGGCTCCTGGGATTTTGCTAATGTCGTCAACACTG
91	42	AGTTTCGCTTGAGTCTTGCTTTCGAGGTCGTTGAATCAACAG
92	42	TTTCAGCTAGCGTATACAAACTACAACGAAGTTTTTTAAACA
93	42	CCTGTTTGATACATTAGCTCAACATGTTGCGGATGTCAAAGC
94	42	GAACCAGTAACCGATTTTCATTTGGGGCGTAGATTTGCAACT
95	42	AAAGTACTTTGATGCAAACTCCAACAGACAACAAGAAAAGG
96	42	TCTACGTTCAAATGGTCATAAATATTCATTGCCATATCATA
97	42	TGTTTTTAGATAGAATAAAAGGGACATTCGCTCAAATCCAGA
98	42	AACTCGTTATTAGAAAATCAACAGTTGACAAATATGGCGGTC
99	42	AGTATTAAGGCAAGCCTTTGCCCGAACGATACATTTGAGGAA

100	42	GGTTATCAAGCATCCTGCAACAGTGCCATTAACATTTTTAAA
101	42	ATTAATTATGAAACTTTACATCGGGAGACAGGTTTTATACTT
102	40	TTGCCTGAGTGCAGGAACGGTACGCCAAAGCGTTCACCAG
103	40	AACAAGCAAGAAAGTCCTGAACAAGACTTTCCACAAGATT
104	40	ACATAACGCCAAATACCAGTCAGGACGAAAACGAGCGTCC
105	40	CGTTTTCATCGTGCAAAATCACCAGTATTGGCCGAGCCGC
106	40	CCCAATAATATGCAGAGAGAATAACAAAAAGAATTAAGAC
107	40	TACGTGAACCTGAAATCAAAAGAATACGCCGCTGGCGCTA
108	40	CCAAGCGCGAAGTTTTTCATGAGGAACGGATATGATGAAC
109	39	TTAATTTCAGCATAGGTCTGAGAGAAAAGGGCAAGCCAA
110	39	TTAGTAAATGACAATAGGAACCCATAAACAGTTTAATTG
111	39	TAATTGCTGAATATCGCGTTTTAATGAGGCTTTCAATAA
112	39	ATCAATATCACCAGAAGATAAAACATTGGGCGATTCGAC
113	39	GAATATACATATATAATCCTGATTGCGTCATAAAACAAA
114	34	TTTTCATACAGAATACGTCACCAATGAAGAAACA
115	34	AGCCCTTTAATATCGAATTAACTGAACAGCGGGG
116	34	TGTGTCGACACTAATGCCACTACGAAGGAGTATA
117	34	ACAATATGTTGTAGGTGAGGCCACCGAGAGTGAA
118	34	GCACTAAAAAGGGCGTTTGGAACAAGAGTTTCGA
119	34	TAGCAAGAAGAACGCATGTAGAAACCAACAGTGA
120	34	ACCCTCGTTGAGATACGAACTAACGGAAAACAGC
121	32	TATAAAGTAGCTTGACCCCTAAAGGGAGCCCC
122	32	CGAGAAACATAAGAACGATATAGAAGGCTTAT
123	32	CTGAGACTCGAACCGCATCACCGGAACCAGAG
124	32	GCGGATAAGTTACCAGAAAGTAAGCAGATAGC
125	32	TCACCGTACGAACGAGCGACCTGCTCCATGTT
126	32	CCTGGCCCTAGAGGCTGACGACGATAAAAACC
127	32	AATCGTCGCATGGAAAAGCCATTGCAACAGGA
128	30	TCACAAAAGAGCCACACCGACTTGAGCCAT
129	30	GACACCAGCCTTTATTTAACGTCAAAAATG
130	30	CCAAATCTAAAGACCAACGGCTACAGAGGC
131	30	CCCTGCCGCAAGCCGCCACCACCCTCATTT
132	30	GTTAAAGCTTCAAAAAGATTAAGAGGAAG
133	30	GGTTTTTCCACCAGATCGCCATTAAAAATA
134	30	TTTGATGTCATCAATTCCTGATTATCAGAT
135	30	CGTGGCATTTAGACTAAACAGGAGGCCGAT
136	30	AACCGATCAAAATCTGAGAAGAGTCAATAG
137	30	GCGTACTCCCTTATATGGTGGTTCCGAAAT
138	30	ATTTGCCATAGATATGCAGAACGCGCCTGT
139	30	CCATAAAGCTCATTTTACCTTATGCGATTT
140	30	GCTTGATTTGCGAAGAATAGAAAGGAACAA
141	30	TGGCATCGATTCCCGGAAGTTTCATTCCAT
142	30	AGTTTGAGATTAGATCTTTAGGAGCACTAA
143	30	TGGAAACGAGGCGAGAATACCAAGTTACAA
144	30	ACGCCAAATAATTATTAAATAAGAATAAAC

Table S12. Staple sequences for a FV pentagonal bipyramid of 42-bp edge length. The sequence is represented by colors; unpaired nucleotides with blue, and crossovers with orange, the 14-nt seed dsDNA domain with green, and the 4-nt dsDNA domain with red.

Staple ID	Length (bp)	Staple sequences
1	54	CCTTATTAGCGTTTGCCATCTTTTCATTCATCGGCATTTTTCATTATGCCACCC
2	54	AAACAGGGAAGCGCATTAGACGGGACCAGCCTTTACAGAGAACAGTTAGAGATA
3	54	CTAAAGTTTTGTCGTCTTTCCAGACAACAGCCCTCATAGTAAATCCGAGCGGAG
4	54	TCATTAAAGGTGAATTATCACCGTAGGGAAGGTAAATATTGAATCGTACCATTA
5	54	GTGAATAAGGCTTGCCCTGACGAGTAATCAACGTAACAAACTCAGAGCATTGTG
6	54	TTTGAAGCCTTAAATCAAGATTAGGCAGCGAACCTCCCGAGCCATATCGTCTTT
7	52	CTGAGTTTCGTCACCGTTAGTAAATGTCAACAGTTACCCATGTACCGTAACA
8	52	CTTTGAGGACTAAAAAGAATACACTACAAGCGCGAAGCAACGGCTACAGAGG
9	52	ATTATTCTGAAACACGAGAGGGTTGATACTCAGGATGCCTATTTCGGAACCT
10	52	AGCCTTTAATTGTACACGCATAACCGAAAGGCCGCAAAAAGGCTCCAAAAGG
11	52	AAATATGCAACTAAATTTCGCAAATGGGGCGCGAGGTAGCTCAACATGTTTT
12	52	TCAGAAGCAAAGCGAGCAAACTCCAACCTTTTGATTACCCTGACTATTATAG
13	52	ATCAGATATAGAAGTTGCTATTTTGCACGCTAACGCGCCCAATAGCAAGCAA
14	52	AATCCAAATAAGAAAGAATTAACTGAGCTAATATCGCCATATTATTTATCCC
15	52	ACATTATTACAGGTAAGAGCAACACTAACCAAAATAACGAACTAACGGAACA
16	52	ACCTTCATCAAGAGAAACACCAGAACTCAACTTTAGGCGCATAGGCTGGCTG
17	52	TTTACCAGCGCCAACACCGACTTGAGGTAGCACCAATAGAAAATTCATATGG
18	52	AGTAGCGACAGAATCATAATCAAAATCCCTCAGAGATAGCAGCACCGTAATC
19	52	TAATGCAGAACGCGTCGGCTGTCTTTGTACCGCACTAAACAACATGTTCAGC
20	52	GAAAAGTAAGCAGATATTACGCAGTAGTGGCAACAACCGAAGCCCTTTTTAA
21	52	TTGAGGCAGGTCAGAAGCGTCATACATAAGTTTTACCAGCATTGACAGGAGG
22	52	AGTCTCTGAATTTACCGTTCCAGTACCTCATTAAAGCCAGGACAGTGCCTTG
23	52	ACCAACCTAAAACGAAAGAGGCAAGAAAAATACGTAATGCAATACAACGGAG
24	52	CAGTACCAGGCGGATAAGTGCCGTTGAGGATTAGGATTAGTGTACCGCCACC
25	52	CCGACAATGACAACAACCATCGCCTCTAAACAGCTTGATATTGGATCGTCAC
26	52	CCAAAAGGAATTACGAGGCATAGTAGCATTCAACTAATGCAAGGCTTTTGCA
27	52	AGATTTAGTTTGACCATTAGATACAGGTTGATTCCCAATTCAGGTGGCATCA
28	52	AGAACTGGCATGATTAAGACTCCTTAAACGCAATAATAACCTGAAACGCAAA
29	52	AGCTTCAAAGCGAACCAGACCGGAGAGACTTCAAATATCGAACATTTTTGCG
30	52	GAGCATGTAGAAACCAATCAATAACCAAAAATAATATCCCTAGAACAAGCAA
31	51	GCTATATTTTCATAAGGTTTTTTTTGAACCGAACTGACCAGATACATAACG
32	51	ATCCTGAATCTAATTTGTTTTTTTCCAGTTACAAAATAAACAAGCAGAAAA
33	51	CAGAGGGTAAGAATTGATTTTTTTTGTTAAGCCCAATAAATCCTAATTTAC
34	51	AGAAGGAAAGAATAAGTTTTTTTTTTTATTTTGTCACAATCATTCATAAAT
35	51	GATATTCATTTCAGGGTTTTTTTTATAGCAAGCCCAATAGGATCCGACCTG
36	51	AGTACCTTTCTGGATAGTTTTTTTTCGTCCAATACTGCGGACGGAAATTAT
37	51	ACCAGACGAAGGACAGATTTTTTTTGAACGGTGTACAGACCAATCCACCAC
38	51	GCCAGCAAACGGAAACGTTTTTTTTCACCAATGAAACCATCGCCACCAGTC
39	50	TTTCCATTAATCGCCTTTTTTTTGATAAATTGTGTCGTAGCGTAACGAT
40	50	CCCCCAGCGCAGGCAAGTTTTTTTGCAAAGAGAGAATCCTTGCGGGAGGT
41	50	ATAAGTCCTATTTTCATTTTTTTTCGTAGGAATCATTACCGAGTTAACAA
42	50	GAACGCGAGATGTAATTTTTTTTTTAGGCAGAGGCATCCGATAGTTGCG
43	50	AGGCTTGCATAATAAGATTTTTTTGAATATAAAGTACCAATGGAAAGCGC
44	50	TTTTGCTAAAGAAAGGATTTTTTTACAACTAAAGGAATCGGGGTTTTGCT
45	50	ACCACCGGACGCCACCCTTTTTTTTCAGAGCCACCACCGGAATACCCAAA

46	50	TTGAGATGGTTATGCGATTTTTTTTTTTAAGAACTGGCCGGTCATAGCCC
47	49	TTCATTCCAATAGTAGTTTTTTTTAGCATTAACATCCCACTACGAAGGC
48	49	CTGTAGCATTTACTTATTTTTTTGCCGGAACGAGGCGCTGCGAACGAGT
49	49	AGATTTAGGTTGCCAGTTTTTTTAGGGGGTAATAGTACGTTTTAATTCG
50	49	GAGACTCCTGCCACCCTTTTTTTTCAGAACCGCCACCGCTGCTCATTCA
51	49	CAACCGATTGAATCCCTTTTTTTCCTCAAATGCTTTAAGAATAACATAA
52	47	GCTATCTTTATAAAACAGAGCCGCCATAAAGTGTTAGCAAACGTAGA
53	47	CAGGTCTTAAGAGGTATGTTTAGAAATTGCTCAGGTCAGGATTAGAG
54	47	GTTAATAAAGCGAGACTTTGAAAGCGATAAAATCATAACCCTCGTTT
55	47	AGCCGCCGACGGGGTCAAAAGGTACTGGTAATGGCTTTTGATGATAC
56	47	GACGACAATCATCGAAGAGCAAGAAAACCAACCTTATCATTCCAAGA
57	47	ACGAGGGTAACAAAGTAAATCATAATTATACAAACACTCATCTTTGA
58	47	ATGCCCCCGGTTTAGCGAATAATAATCACCGTATAAGTATAGCCCGG
59	47	TCTCCAAATTTTGCGTCGAGCCAGGGGAGTTATATATTCGGTCGCTG
60	47	ATAATGCTCTGAAAAGACGGTCAATCATTTGGTCAATAACCTGTTTA
61	35	AGGAGTGTAAAGTAATTTTTTTTTCTGTCCAGAC
62	35	AATAGGTGTATTTTTTCTTTTTTTTACGTTGAAAA
63	34	CAGACTGTATGGGAAGTTTTTTTTAAAAATCTAC
64	34	AAATACATACACCAGAATTTTTTTCCACCACCAG
65	34	ACGGGTATTAACAATGATTTTTTTAATAGCAATA
66	33	TTCGAGGTGCGAAAGATTTTTTTCAGCATCGGA
67	33	CACAAACAAGCCCGTATTTTTTTTAAACAGTTA
68	33	AAGAGGAAGGAGCTTATTTTTTTATTGCTGAAT
69	33	TCAAAAATGGACCATATTTTTTTAATCAAAAAT
70	32	ATTTGTATCAACGGGTCTTTTTCATGAGGAAG
71	32	CTCAGAACCCAAGAGAAAAGTATTAAGAGGCT
72	32	CCTCAGCAGAATTTCTGGTTTATCAGCTTGCT
73	32	ATTCTACTATATAACATACGGTGTCTGGAAGT
74	32	GATGGCTTACCCGAAATTGCATCAAAAAGATT
75	32	AAAGAAGTTAATACCAAAAGATTCATCAGTTG
76	32	GCCGTTTTTGAACAAGTGTTTATCAACAATAG
77	32	GACACCACGCCGAGGAGCCGAACAAAGTTACC
78	32	AGTAACAGTATAAATCGATTGGCCTTGATATT
79	30	CTCCATGTCCACAGGTACAAACTACAACGC
80	30	CGCCAACGCGTTTTTTATCCGGTATTCTAA
81	30	CGAGAATAAAATAGGATTTTTTGTTTAACG
82	30	CCTCATTTACCCAAATCTTGACAAGAACCG
83	30	ATTCATTGAGGGAGACAAAAGGGCGACATT
84	30	AGGACGTGCGCGTTAGTTTGCCTTTAGCGT
85	30	TGAGAATACAACTTAATTTTCTGTATGGGA
86	30	CCAGAGCCTTACCAACCCAGCTACAATTTT
87	30	ACCCACAATTGAGCACACCCTGAACAAAGT
88	30	AATTACCTTTAATTGAGTAGTAAATTGGGC
89	30	GCAAGGCATCACCACCATTTGGGAATTAGA
90	30	TCAGAACACCGCCTCACCGGAACCAGAGCC

Table S13. Staple sequences for the MV tetrahedron of 42-bp edge length. The sequence is represented by colors; unpaired nucleotides with blue, and crossovers with orange, the 14-nt seed dsDNA domain with green, and the 4-nt dsDNA domain with red.

Staple ID	Length (bp)	Staple sequences
1	59	CAAACGTTATAAACGCTGCGCGTAACCTGGCAAACTGCGCAACTGTTGTTTAATGGGAT
2	58	AGGAGCGGGTGCGCTGGCAAGTGTAGAATTGAGGAAGGTTATATATCTTTAGTGATAG
3	57	TAATGAATGTAAAGAGAACAATATTACCCGCCTGCCGGCCTCAGGAATTTTCGCACT
4	56	TTTTCACCAATTCGTCATCACGCAAATTAGTTAGAAGTCCACGCTGGTTTGCCTGC
5	56	TCACGACGGGAAGGGAATATCTGGTCAGTACCACACATCGGCAAAATCCCGCGGAT
6	54	GGGCGCCTGAAATTTGGATTATTTACATTGGCATTTTTATAATCTGCCACCGAG
7	54	AATGAAACAAACTAGCTAACTCACATTTTTTGCGTTGCGCTCACTCCTAGCAAT
8	53	CCCTAAGAAACCAGGCAATTTCGCCATTCGCCGGTGTAGTTTTTTTATGGGCG
9	53	TAAAAGAAAACAGGAGGCCGATTATTTTAGACAGGGAGCTTGACGGGCACCGC
10	53	CTGGCCTTTGAGAGAGTTGCACAACAGCTTTTTTTTGATTGCCCGTCCACTAT
11	53	ACGTCAAAGCATCACCAAAGGGAGCCCCCGATTTAAACGGTACGCCTCTGAGA
12	51	ACCCTTCTTAAGCGTAAGAATACGTCAGAAGATAAAACAGAGTGGTCAGTA
13	51	CATCACCTTCCTCAAATATCAAACCGCGCCGCTACAGGGCGCTGGTTGCTT
14	50	TTTCCTCACCGTTGGGGTACCGAGCTCGAGACTCTAGAGGATCCGCCCGC
15	49	TTAACACGCCAGCCATTGCAACATACGCTCATGGAAATACAGAGATAGA
16	49	TGACGAGTGATTAGTAATAACATTCCTGAGTAGAAGAACTAATCTAAAG
17	49	TAAAGAACAACCCGTCGGAGTGTTGAAAGGAAGGGAAGTAGCCGTAAAG
18	49	AGGTCGTGAGACGGGGCAAGCGTCAGAGCGGGAGCTGTCTGTCAATCAT
19	49	TGACCGGTAAAACGATTCCGAACCGCCGCGCTTAATCTCAATCCGATCG
20	48	CCGAAACCACCAGTTTTTTTAAGGAGATCTGGCCAATTCGAACAATAT
21	47	CCAGCAGGGGACGTTTTTTTACGACAGTTGCAAGGCGATTGCTGCAT
22	47	GGTGGCGGCCAGTTTTTTTTGCCAAGCTTGCATGCCCCAGAACGTGC
23	47	TAAAGTCGGCCATTTTTTTTACGCGCGGGGAGAGATTCCACTTGACGC
24	46	ATGCGCGAACGAGCACTAACATAGATTAGAGCCGTCAAAAAGCGAA
25	46	TGAACGGCGAAATTTTTTTTAACCGTCTACATTATCATTTGCGTATT
26	45	CACTAAATCGGTGGCGAGTTCCAGTTTGGAACAAGATTGAAAGCC
27	44	AGGTCACGTTATTCAGGTCAACAGTTGAAAGGCGGTCATCAAAA
28	43	GAATAGTTTCGAGATAGGGTTGATTCTCCTTTTTTTGTGGGAA
29	42	TACAAACTTCCTGTCATCTGCCAGTTTGCAGCTTTGAACGAA
30	42	TTTTGAAAAATACCCCGGCACCGCTTCTAACCGTGAGCCAGC
31	42	TGCCTAACGTGCCAAAGTTGGGTAACGCCGCCAGCAGCAGCA
32	42	GTGCGGGTTTCTTCGCTATTACAGGGTTTTTTTTTTCCCAG
33	42	GCTCACAGCGGTTTTGCGGAACAAAGAACGTTATTACATTCT
34	41	TTTCCATTTTTTTGTCGGGAAACCTGTTGAGTGATCGGCCT
35	41	CATCGTGGTGCCGAACATCGCCATTAATGGCTATTAGACTT
36	40	AGTTTGAGTAATACACGACCAGTAATTCTGAAAGTTATCC
37	40	GGGGATGTGCATAACAGTGCCACGCTAATATCCCTGGGG
38	40	GGTCATATTTGTTTCCTGTGAGGGTGGTTTTTTTTTTTC
39	40	GGCGAACGAACCCTCAAATCAAGTTTTTACGTGGACTCCA
40	37	AGTGGATTCACCAGTCCAGGGCGATGGCTTTACTACG
41	36	ACTTCTTCACGTATCAGGCGAAAATCTTTGTTTGAT
42	36	CCACCAGGGCACAGCAACTCGTATTAATTCCTTTGC
43	36	AGCGAGTATGGGGTCGAGGTGATAATACTTTGAGG
44	35	GGCCAACCTACATTACAACATACGAGCTTGAAGCA
45	25	ATTTAAACATTATTTTTTTAATGTG
46	23	TCAATCGAAAAGGGAATTTTAAA

47	23	TGCTGGTGAGAGCCTGGCGAAAG
48	23	TTTCATCGAAGTATTAGTCTTTA

Table S14. Staple sequences for the MV tetrahedron of 63-bp edge length. The sequence is represented by colors; unpaired nucleotides with blue, and crossovers with orange, the 14-nt seed dsDNA domain with green, and the 4-nt dsDNA domain with red.

Staple ID	Length (bp)	Staple sequences
1	61	CTTTGACCCTTAGCGATTATACGCCTTGATTTTTTTGTAACAGTGCCCGTTCAACACTCAT
2	61	ATAATGCTGTTGCTCAACATGTCAGTATGTTTTTTTTTAGCAAACGTAGATGTTGCTGAAT
3	60	CCACGGAGTATAGCTTAAACAGCTTGATAAGACTTGAATCAAGTTTGCCCTTGTCACAAT
4	60	CCGCCGCTCAAGAGGCTTTTGCGGGATCCTTGACACTGGCTGACCTTCAATGAGGTTGAG
5	57	TCCAGTATGTTACTTTTAATCATTGTGACCCTCAACACCGTCACCGATTTTGAGCCA
6	57	AAATTATGAATTAGTAGACTGGATAGCGCAACACTCAGTTGATTCCCATTTCTGCGA
7	56	TGGCATCTAGATTTATTCAACTAATGCAAGTCAGGTGTGTCGAAATCCTTGACCTG
8	56	CCGCCACCTTTAGCGAAGAGGAAGCCCGAACCGATAGAGGGTTGATATAAATAAGT
9	56	TCAGAGCTTTTCGGAAATCAGGTCTTTAAAACACCACTGACCAACTTTTTAAGAGG
10	55	ACCATTACAACCGAGCAAAGATATTACGTTTAAATGCGAGAGGCCCTTTAATTGC
11	55	AATCTCCCTTAGAGCTTAATATGGGATTTTTTTCACGCCACCCTCAGAAGAACCC
12	55	CGAAAGAAGAATACACTAAAAGAGTAATGTCACCCGAGGCTGAGACTCCCAGCAT
13	54	TTCATGAGGATCATTAAACGGGTAAAATACGATAGCCCTCATAGTTTTGCGTAA
14	54	GGTCAGTCAAGCGCAACAACATTTAATGCCACTACGAAGGCACCTAAACGAAAG
15	53	TCCTTTTGATTTCATTTTTGCGGATGGAAAAAAAAGGCTCCAAATTTTAATTG
16	53	AGGCAAACAGCATCGGAACGAGGGTGGCTACAGAGGCTTTGAGGAATGGAACC
17	52	TATCGGTCCAGACCGGAAGCAAATCAGGTCAGGATTAGAGAGTATTCGGAAA
18	51	CGCCAAAATCGAGGCATAGTAAGAGTCCAATACTGCGGAATCTATATTCAT
19	51	TTATAGTCTAAGCGGATTGCATCAAGACAACAACCATCGCCCTACCGATAT
20	50	TATTATTTTTGAAACATGAAAATGCCCCCTTTTTTTTGCCTATTATTTTC
21	49	TGAATCCATTACCTTATGCGATTTACTGGCTCATTATACCGATACATAA
22	49	ATTCGGTAAGCTGCTCATTCAGTTGGCTTGCCCTGACGAGCCCTGACTA
23	49	TTATTTCAGAGCCACCCGTCGAGTTGCGCCGACAATAAAGATTTCAGAC
24	48	ACGAGAATTCTACTTTTTTTTAATAGTAGTAGCACATATAAATCATAA
25	48	GAGTTTCGTCGACGTTAACAACTTTCAACAGAAAGGAACCTCAGAGCC
26	47	CACCCTAAAGGTGTTTTTTTGCAACATATAAAATCACCGTCTTGCTT
27	47	CTCCAAGCGTCATTTTTTTTACATGGCTTTTGAGATAAATACGTTGG
28	47	AAGTGCACCCTCATTTTTTTGAGCCGCCACCAGGCGGGGTGCTTGCA
29	47	ACAGAAACAAATTTTTTTTAAATCCTCATTAAAGAACCGAAGAACGA
30	47	AGGGATCAAACTACAACGCCTAAAGTTGGAGTGAGACTAAAGACTTT
31	47	TTTGGTCATTAAATTTTTTTGGTGAATTAAAATCACCGGATTACCGT
32	46	CGATCTGTAGCATTTTTTTTTCCACAGTGTTTAGCTATATTAACGG
33	45	CAATAGAAAAAGCGACACAAATATCGCGTTTGAATTTCCCGGAAT
34	45	GCAGGTCAGAGCATAGGAGAACCGGATATTCAAAGGCCAAGGATT
35	44	ACTGGTACGGAGATGTTAATAAAACGAATTCATCATCGCAAATG
36	44	CGCAGTCCGCAGACTTGAGATGGTTTAATCAGAAATTGCCATCT
37	42	CTTTCCAACCAGTAAGCAAGCCCAATAGCCGCCACTTGCGAA
38	42	ATCATACCGGTGTCACGACGATAAAAACTTGCCAGCACCATT
39	42	AGTACAAATAAGTTTTTTCATTTGGGGCATACATTGTTGAGA
40	42	GAAGAAAATACCACAGTTTGACCATTAGGCGAGCTGGAGTGT
41	42	TTTAGGAAATCTACTTGTATCATCGCCTTGATACAGAAAAGG
42	42	GGGAGTTATTACCCTGTACAGACCAGGCCGATTGGACCAGAG
43	42	TAAAGTAAGGCAAGTTGAGGGAGGGAAGCCAGTAGAGGGGGT
44	42	CCCTCGTAAATGTTAGCCAGCAAAATCAGTAAATACCAATAA
45	42	AATAGTATTACCAGTGGAAGTTTCATTCTTAACATTTGACGG
46	42	AACGAGGTCTGAATACCAGAGCCACCACTTAGCGTACGAGAA

47	42	GTAGTAAAAATCAATCATAGCCCCCTTACGGAACCTGGAAAG
48	42	TGACCATATTGGGCGGTCAATCATAAGGGCCAGAAGCCTCCC
49	42	TGTAGCGTTTTTTCATCGGCACGCCACCCTTTTTTTTCAGAA
50	42	AGGTGTAGAAACGCGGTTTACCAGCGCCGATAGCAAGCTTCA
51	42	TCGAGGTTAATTCGGCACCGTAATCAGTTTCATATAAAGACA
52	42	AGGATTAAACCACCCCTTGATATTCACATGAACGGAAATCAA
53	41	CGTCACTTTATGAAACCATCAAAGACATTTTTTTAAAGGGC
54	41	GACATTGCAAGGCTTGCAAAAGAAGTTCAAAATAATGCAAC
55	40	GTCAATAACCACTACAGGTAGAAAGACTAACGGGAAACAA
56	40	TTTCATAATCATATGCTTTAAACAGTTTTCAACTAGCCGG
57	39	ACCACCCTCTCAGAAAGGAACAACTTTTCAGCTTGTCGT
58	39	TAATAATTTGCTAAGTAAATGAATTTTCAACGTAACACT
59	36	AAGCGAATTATCAGACTCAGGAGGTTTTTGTACCGC
60	36	CGTAACACGCTGAGTTTGCTCAGTACTTTGGCGGAT
61	29	TGACAGAAACAGTTAGTATTAATCAGCAG
62	29	ATGTACATACATACATCAGAACCGTTGAA

Table S15. Staple sequences for the MV tetrahedron of 84-bp edge length. The sequence is represented by colors; unpaired nucleotides with blue, and crossovers with orange, the 14-nt seed dsDNA domain with green, and the 4-nt dsDNA domain with red.

Staple ID	Length (bp)	Staple sequences
1	60	CATCTTTCGTAGAACCTTATTACGCAGTGTAGCGCCTAAAGTTTTGTCGATTTATACCAA
2	59	AAACCAATCACACCACCTATAAGTATAGCCCACACAGGTTGATAAGAGGTCATTTTTGCG
3	59	ACCATTAGCAGTTTGCCAGACGTTAGTAAATTTCTTAAACAACAACCATCGTTCACGCA
4	59	GCAGATGCATTAGCTCAAATGCTTTAAATAGCAAAGAGCCACCACCGGAGTTACCAGAA
5	57	GGGAGGTACCAACGAAAAGGAATTACGAACGTTGGCTGGAAGTTTCATTTCATATAA
6	57	GCCCAATTGTTTAACTGACTATTATAGTCCACCCTACCACCCTCAGATTTCGCCACC
7	56	TGGCATCGATTCCCTCATTGTGAATTACCGGATATAAAGACAGCATCGTTACGAGG
8	56	GAAGCCCCAAAGTCAATGTTTAGACTGGAGGCGCATAATGCCACTACGTTGGCACC
9	56	AGTCCTGCTTAGAGATATCGCGTTTTAAAAGCCCGCCAATCCAAATATTTAAACGA
10	55	TTGCACGATAAAAACCAAAAGTGTACAACAGAGGCTTTGAGAGCGCCAGCCCAAT
11	55	CTCATCGAACCGCCCTCATTTTCAGGGACAGTTCAAAAACAGGGAAGCAGCCGA
12	54	TTTTTAGCAAGCTTTTTTTAAATCAGATATAGATTTATCAAAGACTTCTCATCA
13	51	TTTTAAGATCATTATACCAGTCAGGGGCATAGTAAGAGCAACTTAACCCTC
14	51	AATACTGCTTCATAAATATTCATTGCATGTACCGTAACACTGTTCACCAGT
15	50	GTTTACCGACTAAAAGGACAGATGAACGTAGCGAGAATTGAGTTGCTATT
16	50	ACAAAGAACAAGCAAATAACATAGAAAACGAGAATGCCACCACTCCCTCA
17	49	GTTTACCGCTGGCTGACCTTCATTTAATCTTGACAAGAACCTTATGCGA
18	49	ACAAACTGAAATCCGCGACCTGCTTTACTTAGCCGGAACGATAGCGTCC
19	49	GTATGGGATAAACAACTTTCAACATAAAGGAATTGCGAATTTTTTTCAC
20	49	GTTGAAATAATTGTATCGGTTTATTGCTTTCGAGGTGAATGAATTTTCT
21	49	GTATCACCTGGAGGTTTAGTACCGCAGAAGCAAAGCGGATTAAAAAGAT
22	49	TAAGAGGTTCGAGCTTCAAAGCGTACCGGAAGCAAACTCCGGAATAGGT
23	48	CAGTTAATTCTACTTTTTTTTAATAGTAGTAGCAACGGTGTGAAGAAA
24	47	GTAGCACATTCATTTTTTTTACCGATTGAGGGAGAGCAGCGTCATTAC
25	47	ATCACGAAACGCATTTTTTTATAATAACGGAATTAGCGTTCTGTAGC
26	47	GATGGAACAAGATTTTTTTAAAATAATATCCCACTCCTTTCAGGATT
27	47	TAACCCATTTGGTTTTTTTGAATTAGAGCCAGCGACAATGACAGCTT
28	45	GCGCGAAACATAACGATGTTTTCATCGGCATTAAGACTAATACAT
29	45	TATTAAGAGGGCGGATAGGAGGTTGAGGCAAATAAATCTGAATT
30	44	GGAAACCGAGCGGAACCGCCCAATAGGAACCAATCCCCACGGGA
31	44	ACCATTAAGCTATAATTAAAGGTGAATTTTGCAGGTAAGGCTTG
32	44	GAATTAATTGAACACCCTGAATTTTTAAGTTTTTTTAAAAGTAA
33	44	TGCCAGTGAACGCGGCAAAGACCTGTTTATAATGCTTATTACAG
34	43	CGGAATAAAATACGGACGGTCAATCATAATAGTAAGAGGGT
35	42	CAGAACTTCGCAAATTAATAAGTTTTAAAAAAAAGGAAACAC
36	42	CGGGGTCGATTGGCCATCGATAGCAGCCGGAGTGAGGATTAG
37	42	GTTAATGCCAGTAAGATATTCACAAACAGGTCAGATTTGCTC
38	42	GACGGAATTTTGCGCAAAGCTGCTCATTGCTTGAGTAGTTTG
39	42	ATCATACTTTTAAAAAACGAACTAACGGCATTCAACCTAATT
40	42	ACATAAATACACTAACGGAGATTTGTATAGACAGCCATAGCC
41	42	ACCAGTGTTAGCAAAGACCCCCAGCGAAGTTGCGCCAAAATC
42	42	TACCGTTCCCCCTGTCCTCAAGAGAAGGATTAGAAATAAACA
43	42	TTTACGATGGAAAGCTATTATTCTGAACTTTAATTGTCCTAA
44	42	CCCTTATACCCAAAACATATAAAAGAAAAAAACGATGATAAA
45	42	CCTGTTTGATACATGAGTAGTAAATTGGCAGTGAAGAGTTAA
46	42	AGGCCGCATTATTCTTTTCATTTGGGGCGTAGATTATGGTTT

47	42	CCAAATCACTTTAAAATTCTGCGAACGAGCGAGCTAAATATT
48	42	AATTTCAAACGTAAGGATCGTCACCCTCGGAAGGTGAAAAGG
49	42	ATTCCACCATCGCCAAGAGGCAAAAGAAGGTGGCAAGAACTG
50	42	ATTCTAATACAAAAATTTAGGAATACCAAACAACATGTAGCT
51	42	CAACATGAGGCAAGAGGCGTTTTAGCGATCCAGAGCTAATGC
52	42	AATCTACTAACGCCCTAACGAGCGTCTTACCTCCCCAATAA
53	42	AGATACAGTTAATATATGCAACTAAAGTTTAACATGACTTGC
54	42	AGTACCACTGAGACCCTATTTCGGAACCGCAGTCTCCTCATT
55	42	GCATGATTTTCGGTCCTCATAGTTAGCGAAGTACAAAACACT
56	42	AATAAGACCACAAGAGGCTTTTGCAAAATTGAAAGGACTTTT
57	42	ACCAACTGAAGTTTATCAGAGAGATAACGCAAGAATCATATG
58	42	TCATGAGAGAAAATACAATGAAATAGCACGCTAATTGCCAGA
59	42	AATTGAGATAGCTATTGTCACAATCAATGAAGTTTCGAACTG
60	42	GGGGGTAAGGGAACCCATTAAACGGGTAGTTTATTTCTTACC
61	42	TTCCTTACAGAGCCCAGAACCGCCACCCCTTTACCCGTCAAA
62	42	ATCAGGTTCAGAACAGAACCGCCACCCTTCATTCCTTACCGC
63	42	AATGAAAGGAATCAAAGAACGGGTATTACACCCTCCGCCACC
64	42	GAGCCGCAACCAAGTTATTTTCATCGTAATAGCAGATCAAAA
65	42	CTCAGAGACCATAACCTTTACAGAGAGAGCCGTTTTACCGCA
66	40	CAATGAAACCTTGCGTCATACATGGCTGCCCGTTAGAAAG
67	40	AGTGTACTGGGGTCACCGACTTGAGCGATATATCCAAAAG
68	40	CCCTGACGAGCTTCGGTCGCTGAGGCATCACCGTCAATAA
69	40	GTAGAAAGATAACTTAATTGCTGAATATCAACAATCCGGT
70	40	AAGATTAGTTAAAGACAAAAGGGCGAACGGCTGACCAGG
71	39	AAAGCCACATTGACAAGTGCCGTCGAGAACACATGAAAG
72	39	AGAGAGTGGGTTGAAGAGCCGCCGCCAGGAAGCATGTAG
73	39	GATACCGTCTTTCCTTTAGCGTCAGACTATAGCACCATT
74	36	CGCATAGAGACGACCCAGCTACAATTTTTATCCTGA
75	36	TTGTGTCACAACGCTGCCATCTTTTCTTTAATCAAA
76	36	GAACAACGTTTCAGACCGTAATCAGTTTTCGACAGA
77	35	GAGCCTTATCTCCAACGGGGTCAGTGTTTTTGAGT
78	34	GTTGAGTAAACAGCCATATTAAGGCTTATAGATA
79	28	ATCTTTTTGAAGCTTTTTTTCTTAAATC
80	28	ATCAAAGGCCGGATTTTTTTAACGTCAC
81	27	AACAGTTTTGATTTTTTTTGATACAGG
82	26	AGAACATAATCGGTTTTTTTCTGTCT
83	25	AACCTCGCAAAGTTTTTTTACACCA

Table S16. Staple sequences for the MV octahedron of 84-bp edge length. The sequence is represented by colors; unpaired nucleotides with blue, and crossovers with orange, the 14-nt seed dsDNA domain with green, and the 4-nt dsDNA domain with red.

Staple ID	Length (bp)	Staple sequences
1	60	CCGTGTTTTTTTTTGATAAATAAGTTACTAGAAAATTTTTTTTTAGCCTGTTTAGTGTAAA
2	60	ATAGCATTTTTTTTGCCTTTACAGATCAAGAAAACTTTTTTTTAAAATTAATTAAGCTTA
3	59	AGACTGCACCATTACCATTACAGCAAAATGAACGGTTTGACCAGGCGCATAGACCGTCA
4	59	GCCTAACACCGGAATCATAAGCGTTAAACCGAGTATTTTCTGTCCATCACGCTAATGGT
5	59	TTCTTAAGAAGAATCAGTATTAACACCTGGTCAGCGCTTTTGCGGGATACCCGATAGTT
6	59	AATAAGAAAATTCATATGGTGTAAAACGCCCGAAATTTAAATATCGCGTTTTAGGGTTA
7	59	GGGGTACAACCTAAATCCTTTGCCCGACAGATGAGGCCTCAGGAAGATCCTTAGACTGG
8	58	CCGACTTTATCTAAGTCGCTGATTTCAGGGAGTTGACAACATTTTTTTACCATCGCCC
9	58	GATTAATTTTTTTTGACGCTGAGACGCCAACATGTTTTTTTTAATTTAGGCATGAAA
10	58	TGCTGATTTTTTTTTGCAAATCCACAAATATATTTTTTTTTTAGTTAATTTACCGA
11	58	TTAACAAAGAGTCAAACCCGTCTTTTCCGTGGGTAGCCAGCTTTTTTTTTTCATCAAC
12	57	TCATCAACGTATTAAAACGAAAGTTTAAGAATACAGAAGTTTTTTTTTGCCAGAG
13	57	GTACCGCGCCTGTTTCGTGCCAGTTTTAATGAATAGCAAGCGTTTTTTTGTCCACGC
14	57	TTTTGCAAAACTAAAATTTAGAAGTATTAGGGCGACATAACAAAGCTTTATTCAGTG
15	57	TTATCAGCTAATATCCTACCGAACGAACCATGAAACCAATCAAGTTTTTTTAGCGTC
16	57	AACAAGAGTCTGCGCAGTTATATAACTATATATCATACATAAAGTGTTTCCTGGGGT
17	57	ATCAACAGAGGCGGCTCAAACTATTTTTGCTGGTTGCTTTCGTTTTTTTAGGTGAAT
18	57	TCCTCATTAATGTACCCCTGAATCTTACCATATAGAAGAGCCGCCATTTACCACCAC
19	57	TGAGCGCTGCTTTGTATGCAACTTTTCGGTGTCTGGGCGCGATTTTTTTGCTGAAAA
20	55	CCCGGGTTTCGAGCCAGTAATTTTTTGGCCACCCTCAGAACATGATACCCAGTGA
21	55	GAGGAAAGAAATAAAGAAATTCAATAGGCTTGCCCTGACGATAAGAGCACCATTA
22	55	TCGGGAGATAAAGGCTTTAATCATTTATTACCTTGATTTAGGTTTTTTTAATACC
23	55	GTTGGGTCGATCGGTTAACCTCCGGCTTTCTTACCACACAACATACGAGGTTGAG
24	55	ACTTTTTATCGCAAAAAGCGCCTTTCATTCAGGCCACTATTTTTTTTAAAGAAC
25	55	CAGTTGAATGCGATATTACGCAGTATGTTATCTTAATCAAAATCTTTAACCAGAG
26	55	TAAACAAGCCTAATGATAGCAAGTTTAGGAACCCAAGCCAGATTTTTTTATGGAA
27	55	GTCGAAACCCCAGCAATAGATAATACATGGAGGGATATTCATTACCCAAAAAAAC
28	55	GAACCTAATACTTCTGCCAGTTTTTGACGACGAATACTGCGTTTTTTTGAATCGT
29	53	GCTGGCAAGTGTTTTTTTTAGCGGTCACGCTTGAGGCCATAAGAATATAGAAA
30	52	TAAAGCACTATTTTTTTAATCGGAACCCTACAACGGCTGACCTAAAAAGCAT
31	51	ACGTAGTTTTTTTTAAAATACATACAAACAATAACGGTTTTTTTTATTCGC
32	51	ACGAGCTTTTTTTTGTCTTTCCAGACATGTTCAGCTATTTTTTTTATGCAG
33	51	GAAGATTTTTTTTTAAAACAGAGGTGTTGAAAGGAATTTTTTTTTTGAGGA
34	51	CAAACATTTTTTTTATTCGACAACTTATAATCCTGATTTTTTTTTGTTTG
35	50	GCCCGGAGTGCCTTCAAGGCAAAGATCATTTTTTATTTTTTTACCAATAG
36	50	AAATAAGAGAATGACACTCCAATTTTAATGGAAACATATTAATTAGGTCA
37	50	CAAAATCGCGACCTGAACCGGAAGGTAAATATTGACAGCCGTCGATTATA
38	50	GGCATAGGAAACACTTATTTTGTCACAATGCGTAGGATTTAGTTGATTAA
39	50	AAATGTACTACGTGAGTAATGCTAATTTTAAAAGTTTATCATCCAGCCAG
40	50	CAGAGCGGAATCATTACCGCGTTTTTAGAGCGGGATTTCAGGAGGCTGAC
41	50	TTCACAGTCGTCTTTACCGCCAACGCGAGGCGTTTTGCTATTTAGTACAA
42	50	GCTTTTGCGCCACCCAAATAAGAAACGATAAGAGATTTCTTTTAGGATC
43	50	CCACCAAATAATAAGAGCAAAAGAATTAAGAGAAGTTTGATTAGCGTTCT
44	50	TGTTGTCGCCAGGGTCAATTCCAGTATAAAGCCAACTACCTTTTGCGGGC
45	50	TTGATAGTGGCGAGAAATAACAACAGTGCCACGCTGATCAAACCTCAGCA

46	48	GCGTAAGAATGATAGCCATTGCAACAGGAAACAATCGTCAGTCACACG
47	47	AGCTTGCATGTTTTTTTCCTGCAGGTCGACTCTAGCAAGGAGTGTAC
48	47	TAGCGATCATTTAACTTTAATTGTTTTTTGATAAGAGGTCATGATGA
49	47	TCAGAAGCAATTTTTTTTAGCGGATTGCATCAAAAATGAACACTATCA
50	47	TCATAAGGGATTTTTTTACCGAACTGACCAACTTTGTTCACGTTGA
51	46	AACAAACAGAGAATTATCACCGTTTGGAGGTTTAGTACCTTTAACG
52	46	TTGAAATCATCTTCTACAGAGGTTTGGACTAAAGACTTTCGAGAAA
53	46	TCAAAAAGAGGCATTACCGAGCTTTTCGTAATCATGGTCGCCATAT
54	46	AAATCTCCAAATTTTTTTTAAAAAGGCTCCAAAGCGACAGATCGATA
55	46	TAACCCTCGTTTTTTTTTTACCAGACGACGATATCAACGTTCAACC
56	46	AATCAAAAGAATTTTTTTTTAGCCCGAGATAGGCCGGAAGTGCGTTA
57	45	TGGTAATAAGTTTTTTTTTTTAACGGGGTCAATAGGTGAACATAA
58	45	TAAACAACTTTTTTTTTTCAACAGTTTCAGCTTTCATACCGAAGC
59	45	TTGAGGCAGGTTTTTTTTTCAGACGATTGGCCACCCTCAGGCTTAT
60	45	GGACGTTAACGGAAGGAATTGCGAATAACGGCATTGTTACCAGAA
61	44	ACTACAATTAGCGTTTAGTAAATGAATTCTCAGAGCTCCCGACT
62	44	CGTTGGTATGCTTTCAAAAATCAGGTCTAGCGAACAATCAATAT
63	44	CTTTCCGACCGTCTCCCAAATCAAGTTTTCCATTACATTATCAT
64	44	GCGAAAGCTTGACGGGAAGAAAGCGAAAAGCAATAGCAGCAAAT
65	43	ACATTCAAATTTCAATGGCAACATATAAACAGTACCTCATTCC
66	43	AGCGCAGTTTTCAGGTTGCCAGTTACAAACCAGACGCGCGCGG
67	42	GATTAGTAAGGAAGGGGAAAGCCGGCGACGTCACCCCTCAAT
68	42	GAAGCAACATAAATAAACAGTTCAGAAAAATGGGATAATTTT
69	42	TGACCGTACTTCGCGTCTGGCCTTCCTGAACAAACGAAAACA
70	42	CCCTCAAGTAGATGCTGTAAATCGTCGCGTACATACAGACCG
71	42	GCAATAAAAATCTACGAAAGAGGACAGATCACCAGTGGAAAC
72	42	GCCTTAAGCATTCCACTGAGACTCCTCGAGTTAAGCTTTGAA
73	42	TAGTCTATGGAAATATCGTTAGAATCATTTTCATCGGGCTAT
74	42	AAAGGTGCACTAACAAGTACAACCCGATATATTCGAATATCT
75	42	CTTAATTAAAATCAGCCAGCTGGTGAGCGAGTAACATAGTGA
76	42	ATTTTTGAATTACGCCGCCAGAAAAGGGACATTACAGACAAT
77	42	AAGGAACCCTTATTGTAAGCAGATAGCCAAAAGAACCAGTCA
78	42	ATAAATCCTTAGAGCAATTACCTGAGCAGAAGCGCAAGTATA
79	42	AAAATACACCATCAATCAGGGCGATGGCCGCACTCATATTCC
80	42	CTTTAAACATTGGCATAGAACCCTTCTTAATCAGTAAGGAGC
81	42	TTTAGAGACAGCATGCTGAACCTCAAATAGAGCCACTTCTTT
82	42	ACGAACTGGGAAGAATAACGGAATACCCGAACAAATTCGGTC
83	42	ATAGCCCAACTAAACAACATTATTACAGCATTATACTGGCAT
84	42	CCTTTTTACTCCTTTTTAAGAACTGGCTGTAGAAAGAATAGA
85	42	GATTAAGAAGAAAAAGCGTTTGCCATCTGGAGTGAGATTCAT
86	42	GATACATACGAGTAATTTTCAGGTTTAAAATAAGTCAGAACG
87	42	ACCACGGCGTCAGATCCCAATTCTGCGATTCGCAAATTACGA
88	42	AGTAGTAAAAAGGAATGGTCAATAACCTAGTTGATTGAATAT
89	42	ATATAACGTTTAGCAGATACATAACGCCAATTGGGCAAAGAC
90	42	ACAGTAAAGAAACGCTTGAGATGGTTTACTAATGCTATATTT
91	42	ATTTATCGAGAATCATAGCTGTTTCCTGAAACGACAAGGGG
92	42	AAACAGGAAAGAAGATTTTTGCGGATGGATACAGGGAGTAAC
93	42	AGTGCCCTTGATATATTAGACGGGAGAATTCATTTCTTAATT
94	42	CGAATTATTAACTGTGCCGTCGAGAGGGGTATAAAACATCCA
95	42	GCTGAATAGCATTACAGTTAATGCCCCCGGATAAGAACACCC
96	42	ACCAGGCTGCCTATCTACTAATAGTAGTATAATGCGCAGAGG
97	42	TGAACAAAAATCGCTGTAGCTCAACATGATCAATTTTCGGAA
98	42	GATGTGCCTATTACTAGGTCTGAGAGACGCTCAACTTGTTAT
99	42	GAAATTTTTTTCATGAAAGTATTAAGAGGCATGGGATTTTGC

100	42	CTCATAGCGCCTGTAATCAAGATTAGTTAGCGAACCCGCCAC
101	42	CCTCAGACCAGACGAACGATCTAAAGTTCGTCACCTGCACCC
102	42	TTAGGAGAATTATCGCTGGCTGACCTTCCGAGGCGAGATTTG
103	42	GACGGGCGGGTGGTATATAAAGTACCGACCCAATCCTCAGAA
104	42	TATTTATCAAAAGGCGTATTGGGCGCCAAACAGCTATACATG
105	42	CCGCCACAAGCGTCGATTGCCCTTCACCCGGTTTGTAAAGTA
106	42	GGAGAGGGCCTGGCTTTACCGTTCCAGTCCTCAGAGCCATAT
107	42	ATTCTGTATAAACAGCCACCACCCTCATCTCTGAACCTGAGA
108	42	CTCTTCGTGCAAGGGTCACGACGTTGTATGTGAAAAGTAGGG
109	42	GCGAAAAGCACCGCAGAAGGAGCGGAATTGAGTAAAACGGGT
110	42	TATCATCCGAAACAAACTAATAGATTAGGGAAATTGTAATCT
111	42	CACCCGCGAGAAGTAATAATCGGCTGTCATATCCCATTGCGT
112	42	AAAAATATTTCCTTTACGCCAGAATCCTCGCGCTTGGTGGTT
113	42	TGCGCTCGTTTGATAATGCGCCGCTACAGGAACGGATCATTC
114	42	TTAGACAGGGCGCGCAGGCGAAAATCCTACTGCCCGAACAAG
115	42	CAAGAACAAGTCCTGCTTTCCAGTCGGGGCCCCAGTACTATG
116	42	GAGCTTTTTTTACGTATAACGTGCTTTCCCCTTGACAGGAGG
117	42	GCGAACTACGTGGCCTGGCCAACAGAGAGATTCACCTGAAAT
118	42	CCAAGCGGCCTGATTTACTTAGCCGGAAATCAAGAATTCATT
119	41	CATAAAGTGCATCTGAATAATGATAACCTTGCTTGGCGCAT
120	41	GGTGGCTTTTAAAAATACCAAGTTACAAGTCAGAGCTCAGT
121	41	TGGTTTAAACCTGTATCAACAATAGATGGGTATTAGGGATT
122	41	GAACGCAGAGTACCAATTTCATTTGAAAATCCTTGGCGGAT
123	41	GTGGACACCAGGCGACAAAGAAAAAGAAACCACCTTCTGGT
124	40	CTGATTAATATCAGAGATTTTTTTTGATAACCCACGAAAC
125	40	AACGCACTCATCGAGAATTTTTTTTCAAGCAAGCCGCCCA
126	40	ATGTGAGTGAGAAATTCGAGCTTCAATTACCCTTGAATCC
127	40	TTTGCGGAACCGTTCATGAGGAAGTTTTTGGGGTCAAAGG
128	40	TGCGGGAGGTCCCCGGAACCGCCTCCTTCTGTAGACAGCC
129	40	CCGGTATATTTTATGTAACACTGAGTTTTTAACAAATAAA
130	40	TACGAGCATGAATGAGTGAGCTAACTCGGCAAAACCACCA
131	40	GCAGCACTTAAAAAAGAACAATATTACCTTTTGTATCGGT
132	40	GAAAAATCTATTAAATTAACCGTTGTGGAGCGGCCCCGA
133	40	TACAAATAGGTTGGACTGTTGGGAAGGGAATCCAGTTTGG
134	40	GATTGAGTTGAGGACACTCATCTTTGACTCAGCGAGAGGC
135	39	GGAAACCGAAGTAGCGCGTTTTCATTAATTTTTAATAAA
136	39	ACCAGTAATCATACATTTTGACGCTAACGCTCTTAATGC
137	39	GGATTATGCCAGCCCTAAAACATCGCCACGGACCTGAAA
138	38	AGGTGAGCCATTTGGTTTTTTTTGAATTAGAGCGCAAG
139	38	GATTCCATATCAAAATTTTTTTTTTATTTGCACTTACC
140	37	CCAATCGTTTTTATAATCAGGCGCGTAATCCCTTATA
141	37	CACCTTCGGAACGAGGGTAGAAGGGAGGCGCTAGGGC
142	34	AGCTACATCTAAGACCCTCAGAGCCACCTTGATA
143	34	CAATATCGCCTGCATCACTTGCCTGAGTAACAGC
144	34	TGATTATACGTTATCACTACGAAGGCACATAGTA
145	34	CCCTTAGTTACCTTCAGGTCAGGATTAGCATCAA
146	31	AATGAATTTTTTTTATAGCAATAGCTAGCAA
147	31	ATAGCATTTTTTTTAGCAAATCAGAACGCTA
148	31	GCCGGATTTTTTTTAACGTCACCAACCAGCA
149	31	AGCGCCTTTTTTTTAAAGACAAAAGACTTTA
150	25	GCCGGAATCCAACGTCGAGGTGCCG
151	25	CGTAACCTATTCATGACTATTATAG
152	24	GCGCCGACAATAAAGGCTTGGCAA
153	24	ATAGCGTCCACAGTATCTGGCAAT

154	23	CCGAAATCACATTAATCCTAATT
155	21	TCATTTGGGAAGTTTTTACA
156	21	CCTATTAGGGTTTTGGGTAAT
157	21	GAGTTGCCGGCCAAACGACAA
158	21	GTTGCTTCGATTAAAACCAA
159	21	ACGCATAAGGCAGACGGTCAA
160	21	TGACAAGCTCCATGAAATTGT
161	21	ATTAAATGCGGGCCAGTGCCA
162	21	CCGCTCATTTCCCACGATTAA

Table S17. M13 scaffold sequences.

M13 scaffold sequence

(1-1000)

AATGCTACTACTATTAGTAGAATTGATGCCACCTTTTCAGCTCGCGCCCCAAATGAAAATATAGCTAAACAGGTTATTGACCATTTGCGAAATGTATCTA
ATGGTCAAACTAAATCTACTCGTTCGCAGAATTGGGAATCAACTGTTATATGGAATGAAACTTCCAGACACCGTACTTTAGTTGCATATTTAAAACATGT
TGAGCTACAGCATTATATTCAGCAATTAAGCTCTAAGCCATCCGCAAAAATGACCTCTTATCAAAAGGAGCAATTAAAGGTACTCTCTAATCCTGACCTG
TTGGAGTTTGCTTCCGGTCTGGTTCGCTTTGAAGCTCGAATTAAAACGCGATATTTGAAGTCTTTCGGGCTTCCTCTTAATCTTTTTGATGCAATCCGCT
TTGCTTCTGACTATAATAGTCAGGGTAAAGACCTGATTTTTGATTTATGGTCATTCTCGTTTTCTGAACTGTTTAAAGCATTTGAGGGGGATTCAATGAA
TATTTATGACGATTCCGCAGTATTGGACGCTATCCAGTCTAAACATTTTACTATTACCCCCTCTGGCAAAACTTCTTTTGCAAAAGCCTCTCGCTATTTT
GGTTTTTATCGTCGTCTGGTAAACGAGGGTTATGATAGTGTTGCTCTTACTATGCCTCGTAATTCCTTTTGGCGTTATGTATCTGCATTAGTTGAATGTG
GTATTCCTAAATCTCAACTGATGAATCTTTCTACCTGTAATAATGTTGTTCCGTTAGTTCGTTTTATTAACGTAGATTTTTCTTCCCAACGTCCTGACTG
GTATAATGAGCCAGTTCTTAAAATCGCATAAGGTAATTCACAATGATTAAAGTTGAAATTAAACCATCTCAAGCCCAATTTACTACTCGTTCTGGTGTTT
CTCGTCAGGGCAAGCCTTATTCACTGAATGAGCAGCTTTGTTACGTTGATTTGGGTAATGAATATCCGGTTCTTGTCAAGATTACTCTTGATGAAGGTCA

(1001 – 2000)

GCCAGCCTATGCGCCTGGTCTGTACACCGTTCATCTGTCCTCTTTCAAAGTTGGTCAGTTCGGTTCCCTTATGATTGACCGTCTGCGCCTCGTTCCGGCT
AAGTAACATGGAGCAGGTCGCGGATTTCGACACAATTTATCAGGCGATGATACAAATCTCCGTTGTACTTTGTTTCGCGCTTGGTATAATCGCTGGGGGT
CAAAGATGAGTGTTTTAGTGTATTCTTTTGCCTCTTTCGTTTTAGGTTGGTGCCTTCGTAGTGGCATTACGTATTTTACCCGTTTAATGGAAACTTCCTC
ATGAAAAAGTCTTTAGTCCTCAAAGCCTCTGTAGCCGTTGCTACCCTCGTTCCGATGCTGTCTTTCGCTGCTGAGGGTGACGATCCCGCAAAAGCGGCCT
TTAACTCCCTGCAAGCCTCAGCGACCGAATATATCGGTTATGCGTGGGCGATGGTTGTTGTCATTGTCGGCGCAACTATCGGTATCAAGCTGTTTAAGAA
ATTCACCTCGAAAGCAAGCTGATAAACCGATACAATTAAAGGCTCCTTTTGGAGCCTTTTTTTTGGAGATTTTCAACGTGAAAAAATTATTATTCGCAAT
TCCTTTAGTTGTTCCTTTCTATTCTCACTCCGCTGAAACTGTTGAAAGTTGTTTAGCAAAATCCCATACAGAAAATTCATTTACTAACGTCTGGAAAGAC
GACAAAACTTTAGATCGTTACGCTAACTATGAGGGCTGTCTGTGGAATGCTACAGGCGTTGTAGTTTGTACTGGTGACGAAACTCAGTGTTACGGTACAT
GGGTTCCTATTGGGCTTGCTATCCCTGAAAATGAGGGTGGTGGCTCTGAGGGTGGCGGTTCTGAGGGTGGCGGTTCTGAGGGTGGCGGTACTAAACCTCC
TGAGTACGGTGATACACCTATTCCGGGCTATACTTATATCAACCCTCTCGACGGCACTTATCCGCCTGGTACTGAGCAAAACCCCGCTAATCCTAATCCT

(2001 – 3000)

TCTCTTGAGGAGTCTCAGCCTCTTAATACTTTCATGTTTCAGAATAATAGGTTCCGAAATAGGCAGGGGGCATTAACTGTTTATACGGGCACTGTTACTC
AAGGCACTGACCCCGTTAAAACTTATTACCAGTACACTCCTGTATCATCAAAAGCCATGTATGACGCTTACTGGAACGGTAAATTCAGAGACTGCGCTTT
CCATTCTGGCTTTAATGAGGATTTATTTGTTTGTGAATATCAAGGCCAATCGTCTGACCTGCCTCAACCTCCTGTCAATGCTGGCGGCGGCTCTGGTGGT
GGTTCTGGTGGCGGCTCTGAGGGTGGTGGCTCTGAGGGTGGCGGTTCTGAGGGTGGCGGCTCTGAGGGAGGCGGTTCCGGTGGTGGCTCTGGTTCCGGTG
ATTTTGATTATGAAAAGATGGCAAACGCTAATAAGGGGGCTATGACCGAAAATGCCGATGAAAACGCGCTACAGTCTGACGCTAAAGGCAAACTTGATTC
TGTCGCTACTGATTACGGTGCTGCTATCGATGGTTTCATTGGTGACGTTTCCGGCCTTGCTAATGGTAATGGTGCTACTGGTGATTTTGCTGGCTCTAAT
TCCCAAATGGCTCAAGTCGGTGACGGTGATAATTCACCTTTAATGAATAATTTCCGTCAATATTTACCTTCCCTCCCTCAATCGGTTGAATGTCGCCCTT
TTGTCTTTGGCGCTGGTAAACCATATGAATTTTCTATTGATTGTGACAAAATAAACTTATTCCGTGGTGTCTTTGCGTTTCTTTTATATGTTGCCACCTT
TATGTATGTATTTTCTACGTTTGCTAACATACTGCGTAATAAGGAGTCTTAATCATGCCAGTTCTTTTGGGTATTCCGTTATTATTGCGTTTCCTCGGTT
TCCTTCTGGTAACTTTGTTCGGCTATCTGCTTACTTTTCTTAAAAAGGGCTTCGGTAAGATAGCTATTGCTATTTCATTGTTTCTTGCTCTTATTATTGG

(3001-4000)

GCTTAACTCAATTCTTGTGGGTTATCTCTCTGATATTAGCGCTCAATTACCCTCTGACTTTGTTCAGGGTGTTCAGTTAATTCTCCCGTCTAATGCGCTT
CCCTGTTTTTATGTTATTCTCTCTGTAAAGGCTGCTATTTTCATTTTTGACGTTAAACAAAAAATCGTTTCTTATTTGGATTGGGATAAATAATATGGCT
GTTTATTTTGTAACTGGCAAATTAGGCTCTGGAAAGACGCTCGTTAGCGTTGGTAAGATTCAGGATAAAATTGTAGCTGGGTGCAAAATAGCAACTAATC
TTGATTTAAGGCTTCAAAACCTCCCGCAAGTCGGGAGGTTCGCTAAAACGCCTCGCGTTCTTAGAATACCGGATAAGCCTTCTATATCTGATTTGCTTGC
TATTGGGCGCGGTAATGATTCCTACGATGAAAATAAAAACGGCTTGCTTGTTCTCGATGAGTGCGGTACTTGGTTTAATACCCGTTCTTGGAATGATAAG
GAAAGACAGCCGATTATTGATTGGTTTCTACATGCTCGTAAATTAGGATGGGATATTATTTTTCTTGTTCAGGACTTATCTATTGTTGATAAACAGGCGC
GTTCTGCATTAGCTGAACATGTTGTTTATTGTCGTCGTCTGGACAGAATTACTTTACCTTTTGTCGGTACTTTATATTCTCTTATTACTGGCTCGAAAAT
GCCTCTGCCTAAATTACATGTTGGCGTTGTTAAATATGGCGATTCTCAATTAAGCCCTACTGTTGAGCGTTGGCTTTATACTGGTAAGAATTTGTATAAC
GCATATGATACTAAACAGGCTTTTTCTAGTAATTATGATTCCGGTGTTTATTCTTATTTAACGCCTTATTTATCACACGGTCGGTATTTCAAACCATTAA
ATTTAGGTCAGAAGATGAAATTAACTAAAATATATTTGAAAAAGTTTTCTCGCGTTCTTTGTCTTGCGATTGGATTTGCATCAGCATTTACATATAGTTA

(4001-5000)

TATAACCCAACCTAAGCCGGAGGTTAAAAAGGTAGTCTCTCAGACCTATGATTTTGATAAATTCACTATTGACTCTTCTCAGCGTCTTAATCTAAGCTAT
CGCTATGTTTTCAAGGATTCTAAGGGAAAATTAATTAATAGCGACGATTTACAGAAGCAAGGTTATTCACTCACATATATTGATTTATGTACTGTTTCCA
TTAAAAAAGGTAATTCAAATGAAATTGTTAAATGTAATTAATTTTGTTTTCTTGATGTTTGTTTCATCATCTTCTTTTGCTCAGGTAATTGAAATGAATA
ATTCGCCTCTGCGCGATTTTGTAACTTGGTATTCAAAGCAATCAGGCGAATCCGTTATTGTTTCTCCCGATGTAAAAGGTACTGTTACTGTATATTCATC
TGACGTTAAACCTGAAAATCTACGCAATTTCTTTATTTCTGTTTTACGTGCAAATAATTTTGATATGGTAGGTTCTAACCCTTCCATTATTCAGAAGTAT
AATCCAAACAATCAGGATTATATTGATGAATTGCCATCATCTGATAATCAGGAATATGATGATAATTCCGCTCCTTCTGGTGGTTTCTTTGTTCCGCAAA
ATGATAATGTTACTCAAACTTTTAAAATTAATAACGTTCGGGCAAAGGATTTAATACGAGTTGTCGAATTGTTTGTAAAGTCTAATACTTCTAAATCCTC
AAATGTATTATCTATTGACGGCTCTAATCTATTAGTTGTTAGTGCTCCTAAAGATATTTTAGATAACCTTCCTCAATTCCTTTCAACTGTTGATTTGCCA
ACTGACCAGATATTGATTGAGGGTTTGATATTTGAGGTTCAGCAAGGTGATGCTTTAGATTTTTCATTTGCTGCTGGCTCTCAGCGTGGCACTGTTGCAG
GCGGTGTTAATACTGACCGCCTCACCTCTGTTTTATCTTCTGCTGGTGGTTCGTTCGGTATTTTTAATGGCGATGTTTTAGGGCTATCAGTTCGCGCATT

(5001-6000)

AAAGACTAATAGCCATTCAAAAATATTGTCTGTGCCACGTATTCTTACGCTTTCAGGTCAGAAGGGTTCTATCTCTGTTGGCCAGAATGTCCCTTTTATT
ACTGGTCGTGTGACTGGTGAATCTGCCAATGTAAATAATCCATTTCAGACGATTGAGCGTCAAAATGTAGGTATTTCCATGAGCGTTTTTCCTGTTGCAA
TGGCTGGCGGTAATATTGTTCTGGATATTACCAGCAAGGCCGATAGTTTGAGTTCTTCTACTCAGGCAAGTGATGTTATTACTAATCAAAGAAGTATTGC
TACAACGGTTAATTTGCGTGATGGACAGACTCTTTTACTCGGTGGCCTCACTGATTATAAAAACACTTCTCAGGATTCTGGCGTACCGTTCCTGTCTAAA
ATCCCTTTAATCGGCCTCCTGTTTAGCTCCCGCTCTGATTCTAACGAGGAAAGCACGTTATACGTGCTCGTCAAAGCAACCATAGTACGCGCCCTGTAGC
GGCGCATTAAGCGCGGCGGGTGTGGTGGTTACGCGCAGCGTGACCGCTACACTTGCCAGCGCCCTAGCGCCCGCTCCTTTCGCTTTCTTCCCTTCCTTTC
TCGCCACGTTCGCCGGCTTTCCCCGTCAAGCTCTAAATCGGGGGCTCCCTTTAGGGTTCCGATTTAGTGCTTTACGGCACCTCGACCCCAAAAAACTTGA
TTTGGGTGATGGTTCACGTAGTGGGCCATCGCCCTGATAGACGGTTTTTCGCCCTTTGACGTTGGAGTCCACGTTCTTTAATAGTGGACTCTTGTTCCAA
ACTGGAACAACACTCAACCCTATCTCGGGCTATTCTTTTGATTTATAAGGGATTTTGCCGATTTCGGAACCACCATCAAACAGGATTTTCGCCTGCTGGG
GCAAACCAGCGTGGACCGCTTGCTGCAACTCTCTCAGGGCCAGGCGGTGAAGGGCAATCAGCTGTTGCCCGTCTCACTGGTGAAAAGAAAAACCACCCTG

(6001-7000)
GCGCCCAATACGCAAACCGCCTCTCCCCGCGCGTTGGCCGATTCATTAATGCAGCTGGCACGACAGGTTTCCCGACTGGAAAGCGGGCAGTGAGCGCAAC
GCAATTAATGTGAGTTAGCTCACTCATTAGGCACCCCAGGCTTTACACTTTATGCTTCCGGCTCGTATGTTGTGTGGAATTGTGAGCGGATAACAATTTC
ACACAGGAAACAGCTATGACCATGATTACGAATTCGAGCTCGGTACCCGGGGATCCTCTAGAGTCGACCTGCAGGCATGCAAGCTTGGCACTGGCCGTCG
TTTTACAACGTCGTGACTGGGAAAACCCTGGCGTTACCCAACTTAATCGCCTTGCAGCACATCCCCCTTTCGCCAGCTGGCGTAATAGCGAAGAGGCCCG
CACCGATCGCCCTTCCCAACAGTTGCGCAGCCTGAATGGCGAATGGCGCTTTGCCTGGTTTCCGGCACCAGAAGCGGTGCCGGAAAGCTGGCTGGAGTGC
GATCTTCCTGAGGCCGATACTGTCGTCGTCCCCTCAAACTGGCAGATGCACGGTTACGATGCGCCCATCTACACCAACGTGACCTATCCCATTACGGTCA
ATCCGCCGTTTGTTCCCACGGAGAATCCGACGGGTTGTTACTCGCTCACATTTAATGTTGATGAAAGCTGGCTACAGGAAGGCCAGACGCGAATTATTTT
TGATGGCGTTCCTATTGGTTAAAAAATGAGCTGATTTAACAAAAATTTAATGCGAATTTTAACAAAATATTAACGTTTACAATTTAAATATTTGCTTATA
CAATCTTCCTGTTTTTGGGGCTTTTCTGATTATCAACCGGGGTACATATGATTGACATGCTAGTTTTACGATTACCGTTCATCGATTCTCTTGTTTGCTC
CAGACTCTCAGGCAATGACCTGATAGCCTTTGTAGATCTCTCAAAAATAGCTACCCTCTCCGGCATTAATTTATCAGCTAGAACGGTTGAATATCATATT

(7001-7249)
GATGGTGATTTGACTGTCTCCGGCCTTTCTCACCCTTTTGAATCTTTACCTACACATTACTCAGGCATTGCATTTAAAATATATGAGGGTTCTAAAAATT
TTTATCCTTGCGTTGAAATAAAGGCTTCTCCCGCAAAAGTATTACAGGGTCATAATGTTTTTGGTACAACCGATTTAGCTTTATGCTCTGAGGCTTTATT
GCTTAATTTTGCTAATTCTTTGCCTTGCCTGTATGATTTATTGGATGTT

Table S18. Data collection and processing for the cryo-EM imaging and 3D reconstructions.

	FV		MV			
	Tet84	**Oct84**	**Tet63**	**Tet84**	**Tet84***	**Oct84**
Microscope	Titan Krios	JEOL 3200	JEOL 3200	Titan Krios	Titan Krios	JEOL 3200
Voltage (kV)	300	300	300	300	300	300
Camera	Gatan K2 Summit	Gatan K2 Summit	Gatan K2 Summit	Gatan K2 Summit	Gatan K2 Summit	Gatan K2 Summit
Pixel size (Å)	1.77	2.4	2.4	1.77	1.77	2.4
Total dose (e-/Å2)	42.4	40.8	40.8	42.4	42.4	40.8
Number of micrographs	96	724	662	119	85	657
Number of final particles	1,669	3,308	2,511	1,092	586	5,705
Symmetry	Tetra-hedron	Octa-hedron	Tetra-hedron	Tetra-hedron	Tetra-hedron	Octa-hedron
Resolution (0.143 FSC, Å)	21	18	17.5	25	24	15.3

The Tet84* used the middle connection layer.